universität wien

DIPLOMARBEIT

Titel der Diplomarbeit

Near surface groundwater recharge modelling in the Cuvelai-Iishana Subbasin, Namibia

Verfasser

Harald Zandler

angestrebter akademischer Grad

Magister der Naturwissenschaften (Mag. rer. nat.)

Wien, 2011

Studienkennzahl lt. Studienblatt:	A 453
Studienrichtung lt. Studienblatt:	Theoretische und Angewandte Geographie
Betreuerin / Betreuer:	Univ.-Prof. Mag. Dr. Cyrus Samimi

Declaration of originality

I hereby declare that this diploma thesis was written by me and that I did not use any other sources and means than specified. This diploma thesis has not been submitted at any other university for acquiring an academic degree.

October 2011, Vienna

Signature

Acknowledgement

I want to thank Prof. Cyrus Samimi for the supervision and support of this diploma thesis at the University as well as for his contributions to a remarkable research stay in Namibia. Thanks to Manuel Mayr for his company during the stay at the African countryside and to the local people as well.

Furthermore, I thank Dr. Jenny Eisold for the connection of the thesis to the *CuveWaters* project. The Namibian Meteorological Service is kindly acknowledged for the provision of climatic data. I also want to thank Prof. Peter Udluft and Dipl.-Geol. Dipl.-Geogr. Armin Dünkeloh, both for the permission of using MODBIL and the latter for the supply of the software and for taking his time to answer my questions.

I would also like to thank Dipl.-Geogr. Martin Brandt for his help with some software issues during this thesis. Thanks also go to the laboratory team of the University. In addition, I want to thank all friends within the University and beyond for making the time of studying nice, enjoyable and interesting.

Above all, I want to express my sincere gratitude to my parents Gudrun and Walter, who always supported me. Without them, studying this way would not have been possible. Finally, I would like to acknowledge someone who explicitly did not want to be mentioned here, but I thank her anyway.

Contents

Abstract 6

Zusammenfassung 7

1. Introduction 8

1.1 Background 8

1.2 Objectives 9

2. The Research Area 10

2.1 Historical Outline and Population 11

2.2 Land Use 12

2.3 Geology 14

2.4 Soil 16

2.5 Climate 19

2.6 Hydrology 22

3. Theoretical Background – Groundwater Recharge in Semi-arid Areas 28

4. The Model 32

4.2 Calculation of Potential Evapotranspiration 34

4.3 Calculation of Actual Evapotranspiration 38

5. Derivation of Model Input Parameters 40

5.1 Land Use Classification 40

5.2 Climatic Data and Derivates 47

5.2.1 Climatic Data Comparison 48

5.2.2 Completion of the Meteorological Dataset 50

5.3 Methods Regarding Soil Sampling and Analysis 55

5.3.1 Laboratory Analysis 56

5.3.2 WRB Classification and Results 60

5.3.3 Pedo-transfer Functions and Derivation of Soil Hydraulic Properties 66

5.4 Derivation of Land Use Parameters 69

5.4.1 Factor for Macroporosity 71

5.4.2 Leaf Area Index 72

5.4.3 Interception Storage of Plants 74

5.4.4 Albedo 76

5.5 Topographic Data 77

6. Results 80

6.1 Temporal Variation of Recharge 85
6.2 Spatial Variation of Water Balance Components 87
6.3 Modelling Results Compared to Field Observations 93
7. Discussion 95
7.1 Sensitivity of Modelling Parameters and Uncertainties 98
7.2 Implications of the Modelling Results 105
8. Conclusions 108
9. References 110
10. Index of Figures 116
11. Index of Tables 119
12. Appendix 120

Abstract

The discontinuous perched aquifer is an important traditional source of freshwater supply in the *Cuvelai-Iishana Subbasin* of north-central Namibia. Therefore, the evaluation of near surface groundwater recharge is an important issue against the background of increasing population densities and intensified land use. This study investigates the spatial and temporal variation of water balance components with an existing model (MODBIL, UDLUFT and DÜNKELOH 2009) that has already been tested in other semi-arid regions in Namibia. The model is based on information about climate, topography, land cover, soil and associated hydrological properties. Field work during the end of the dry season 2010 provided the basis for modelling. Subsequent analysis and data processing involving laboratory and remote sensing techniques were utilised to compute regionally adapted input parameters. Results show high potential recharge rates with a mean annual amount of 241 mm in the comparably wet modelling period from 2003 to 2010. The spatial pattern is highly variable and determined by soil-vegetation units. Deep percolation is favoured by permeable sandy soils and shallow rooting depths which dominate the region. The water table is mostly found near the surface which results in a small threshold for infiltration. However, a number of reasons and processes suggest that modelled amounts are too high; thus, alterations of basic settings were conducted to test the implications of these uncertainties. Results show a maximum annual groundwater recharge decrease of 22% percent in the model run with a major change in boundary conditions (rooting depths) and of about 12% due to a parameter modification which is more likely to apply according to field observations (field capacity). Two other model runs, representing variations in relative humidity and vegetation factors, only showed minor influences of 2%. When these amounts are assigned to areas which are less prone to flooding and salinity, the estimated mean annual groundwater recharge ranges from 160 mm to 200 mm per year. Therefore, this study indicates that the aquifer in question has a large potential, but it also shows that occurring limitations and uncertainties require additional research and verification in the future.

Zusammenfassung

Der diskontinuierliche hängende Aquifer stellt eine wichtige traditionelle Quelle für die Süßwasserversorgung im *Cuvelai-Iishana Subbecken* in Nordnamibia dar. Vor dem Hintergrund zunehmender Bevölkerungsdichte und intensivierter Landnutzung ist die Abschätzung der oberflächennahen Grundwasserneubildung daher ein wichtiges Anliegen. Diese Arbeit untersucht die räumliche und zeitliche Variation von Wasserbilanzkomponenten mit einem bestehenden Modell (MODBIL, UDLUFT und DÜNKELOH 2009), welches bereits in anderen semi-ariden Regionen in Namibia getestet wurde. Das Modell basiert auf Informationen über Klima, Topographie, Landbedeckung, Boden und die damit verknüpften hydrologischen Eigenschaften. Geländearbeiten gegen Ende der Trockenzeit 2010 stellen die Grundlage der Modellierung dar. Nachfolgende Analysen und Datenverarbeitung, darunter Labormethoden und Fernerkundungstechniken, dienten der Bestimmung regional angepasster Eingangsparameter. Die Ergebnisse ergeben hohe potenzielle Neubildungsraten mit einer durchschnittlichen jährlichen Menge von 241 mm in der vergleichsweise niederschlagsreichen Modellierungsperiode 2003 bis 2010. Die räumliche Verteilung zeigt ein sehr unterschiedliches Muster und ist in erster Linie von Boden- und Vegetationseinheiten abhängig. Die Tiefenversickerung wird stark durch die regional dominierenden durchlässigen Sandböden und geringen Wurzeltiefen gefördert. Jedoch deuten einige Gründe und Prozesse auf zu hohe modellierte Raten hin und um die Konsequenzen dieser Unsicherheiten abzuschätzen, wurden einige Rahmenbedingungen variiert. Ergebnisse zeigen einen maximalen Rückgang der jährlichen Grundwasserneubildung von 22% bei tiefgreifenden Veränderungen (Wurzeltiefen) und 12% bei jener Parametermodifikation, welche auf Grund von Feldbeobachtungen als wahrscheinlicher angesehen wird (Feldkapazität). Zwei weitere Modellläufe, welche Variationen der relativen Luftfeuchtigkeit und Vegetationsfaktoren repräsentierten, zeigten nur geringe Einflüsse von 2%. Wenn diese Beträge auf jene Gebiete übertragen werden, welche weniger von Versalzung und Überflutung betroffen sind, dann bewegt sich die durchschnittliche jährliche Grundwasserneubildungsrate in einem Bereich von 160 mm bis 200 mm. Diese Studie deutet daher auf ein großes Potenzial des betreffenden Aquifers hin, sie zeigt aber auch, dass Unsicherheiten und Grenzen zusätzliche zukünftige Forschungsarbeit und Verifikation benötigen.

1. Introduction

1.1 Background

Currently the people of the Cuvelai-Iishana Subbasin in north-central Namibia face major challenges regarding sustainable water supply and its associated management. The main reason for this is the climatologic situation of the region, which is dominated by strong seasonal and annual variations of dry conditions with drought periods and wetter situations during the rainy season (MENDELSOHN et al. 2002). This situation can lead to extensive flooding events which happened just recently in March and April 2011. However, low precipitation and the high evaporation rates lead to prolonged periods of water shortage and increased salinity in many water bodies. This situation is aggravated by intensive land use, high population and livestock densities (KLUGE et al. 2008, MENDELSOHN et al. 2002). Therefore, access to water has been a very important issue for the region's life for centuries (NIEMANN 2002).

To meet the demands, regional water supply comes from different sources:
The Cuvelai system, a network of seasonally water filled channels, regionally referred to as "Oshana" (pl. "Iishana"), which mainly originate in Southern Angola and flow in the direction of the Etosha Pan, forms one important water source (FRENKEN 2005, KLUGE et al. 2006, 2008). Another important element for the provision of water to the northern regions is the Kunene River which is connected to central Owamboland via an extensive pipeline and channel system (KLUGE 2008, NIEMANN 2002).
Finally, groundwater forms an essential freshwater resource, whereby water from the uppermost discontinuous perched aquifer is traditionally utilised in rural areas using hand dug wells (CHENEY 1994).

Because of this complex situation and the associated limitations in water resources, the region is a central target area for the application of an Integrated Water Resources Management (IWRM), which became a very important political principle in Namibia (MAWRD 2000). The joint research project *CuveWaters*, which started in 2006, contributes to the implementation of the IWRM in the *Cuvelai-Etosha Basin* (EISOLD and BENZING 2010). The project is based upon a transdisciplinary

approach which involves scientists, practitioners and local stakeholders (KLUGE et al. 2008). One part of the project is the integration of results from different empirical studies to identify problems and increase the scientific knowledge of the region. This is the part where the presented diploma thesis is connected to and integrated in CuveWaters to improve the information about near surface groundwater recharge and natural interactions in the research area.

1.2 Objectives

As a profound knowledge of the groundwater system and associated processes is a prerequisite for the sustainable use and management of water resources, this thesis will address the hydrological interactions in the uppermost aquifer. Although some studies addressing groundwater recharge were conducted elsewhere in Namibia (e.g. WANKE et al. 2008), there exists no other study so far that deals with this issue in the region. Therefore, the main objective is the assessment of the water balance and the rate of near surface groundwater recharge in a small scale pilot area with an existing model (MODBIL, UDLUFT and DÜNKELOH 2009) that will be adjusted to the local hydrological conditions. The model is based on information about land cover and on topographic, meteorological and soil data assembled by various existing resources, own measurements during field work and subsequent analysis. Since detailed soil information is sparse, soil sampling and analysis are conducted to improve the respective environmental information. Another task is to relate these hydrological soil properties to vegetation units which are derived by supervised classification utilising RAPIDEYE (2011) satellite images. The final goal is a better view on the temporal and spatial distribution of hydrological processes like groundwater recharge, runoff and evapotranspiration (ET). Several maps of these parameters will be provided to illustrate them clearly for the research area. As the discontinuous perched aquifer is mostly fed by regional precipitation (MAWF 2006), observations in the following concentrate on local interactions, keeping in mind that processes elsewhere in the *Cuvelai* have a profound effect on the area's hydrology as well. In conclusion, the modelling results will be evaluated and occurring problems and uncertainties will be identified to evolve solutions for future studies.

2. The Research Area

The research area is situated in the center of the region generally known as Owambo or Owamboland between 15° 17' E to 15° 52' E longitude and 17° 45' S to 18° 12' S latitude with a total areal extend of 3,000 km² (Fig. 1). Owamboland, also called the "Four Os" because of its political regions Ohangwena, Oshikoto, Oshana and Omusati, is characterised by a diversified society, an eventful history and a significant environment dominated by hundreds of Oshanas (MENDELSOHN et al.

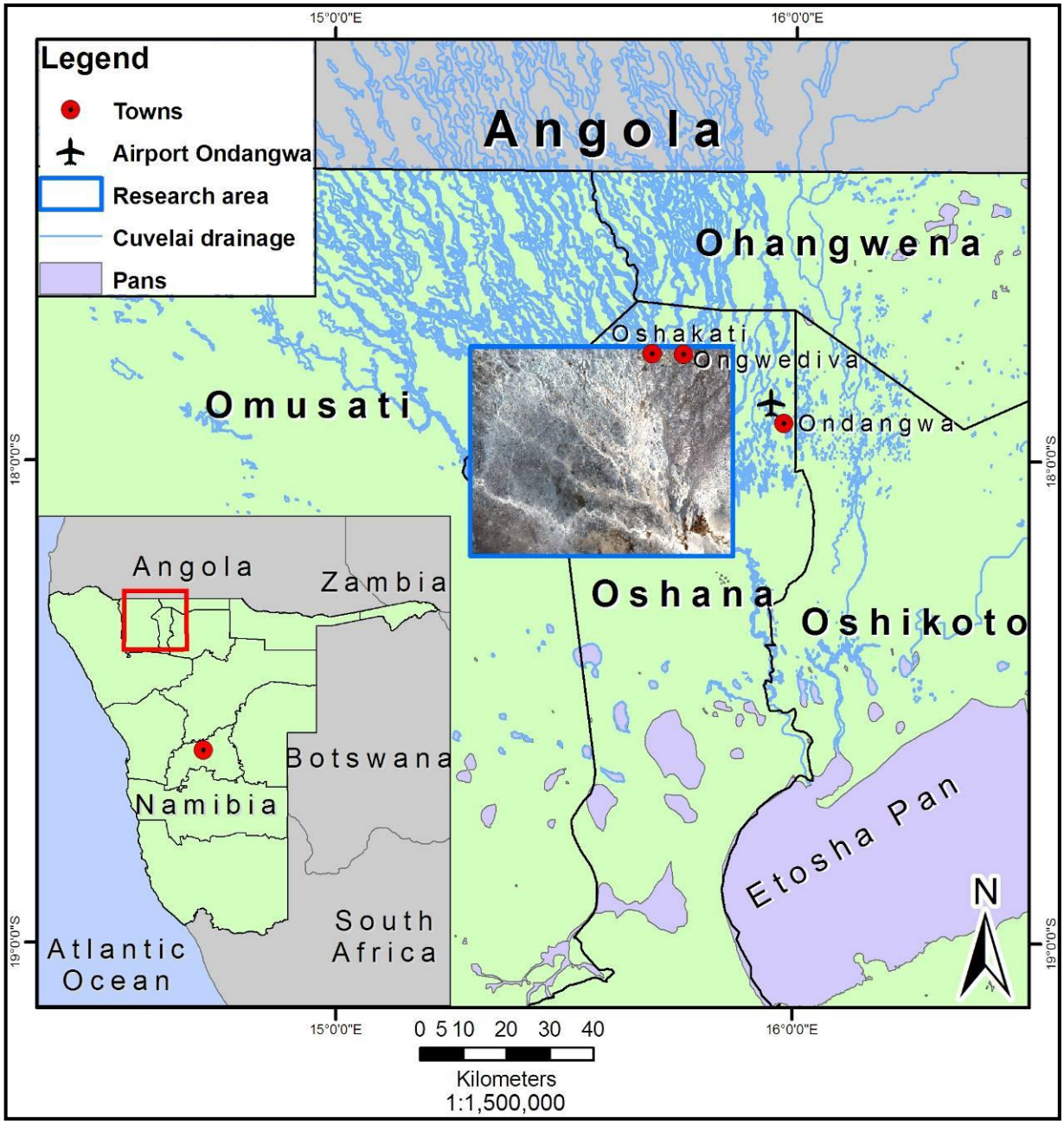

Figure 1: Central Owamboland with the research area highlighted by a blue rectangle and the satellite image. (Data source: MAWF 2000, RAPIDEYE 2011)

2000). Whenever the region is referred to in this thesis, mostly this area is meant. Large urban centres developed in recent decades, namely Oshakati, Ongwediva and Ondagwa, while the majority of the land around is still dominated by a multitude of homesteads, fields for small scale farming and grazing areas. The following chapter gives a short outline of the natural and cultural conditions of this interesting area.

2.1 Historical Outline and Population

The first Oshiwambo speaking people presumably arrived in the early 16th century and created Owambo kingdoms about a hundred years later (MENDELSOHN et al. 2002). The Cuvelai was preferable to other regions because of the availability of water, fish and cultivatable soil. In 1884, Namibia was declared a German protectorate and became a German colony in 1890 until it came under the rule of South Africa in 1915. During the 1960s the South West Africa People's Organisation (SWAPO) was formed to lead the struggle for independence which became an armed conflict in 1966 (MENDELSOHN et al. 2002). In the course of the war, the northern regions became the main combat zone with profound effects on demography, economy and environment (MENDELSOHN et al. 2000). Finally, Namibia became independent on March 21st, 1990 and since then development in the "Four Os" has increased substantially (MENDELSOHN et al. 2000).

Owing to the long history of settlement and more recent immigration from Angola, Oshiwambo speaking people are the overwhelming majority of the population. As stated before, high population densities can be found in the research area. These range from more than 300 people per km² in and around urban centres to about 10 to 40 in the northern parts (MENDELSOHN et al. 2000). Going to the southbound margins of the study area, densities drop below 10 inhabitants per km². Another distinctive attribute of the region is a high population growth rate of 2.8% per year from 1980 to 2000 with an expected average annual growth rate of about 2% until 2021 (MENDELSOHN et al. 2000). This trend may lead to increasing pressure on natural resources in the near future. Population growth is predicted to be higher in urban areas due to migration from rural neighbourhoods, as it has already taken place for the last 50 years. Nevertheless, the proportion of rural population in the "Four Os region" is still among the highest throughout Namibia (MENDELSOHN et al.

2002). The number of rural households is estimated to about 85,000, whereby almost all of these homesteads are encircled by small fields or grazing areas (MENDELSOHN et al. 2000).

2.2 Land Use

According to MENDELSOHN et al. (2000), about 53% of the Owambo population aged 15 and up (1996) do not earn any regular income and hence almost live exclusively from their agricultural products. Another big share of the people is directly or indirectly linked to farming activities. Obviously, this has profound effects on land use. Most of the region is either used for small scale farming or as grazing area which may raise concerns regarding sustainable development against the background of increased land requirements due to population growth. The majority of small scale farms consists of a zone used for crop cultivation often found just outside the residential area (Fig. 2), fenced off from a zone for livestock or woodland. The latter one serves as a source of lumber for fencing and building purposes. Cultivated areas are always erected on sandy soils at the highest part of the field where they are less prone to flooding. Although these sandy soils show bad nutrient supply and poor water holding capacities, lower areas in the study area are not suitable for growing crops. This is because of high salinity and a commonly found clayey layer, which leads to water-logging after rain events and the formation of a hard pan during dry conditions (see chapter 2.4). These circumstances make worthwhile tillage operations in the lowest parts of the field extremely ineffective or impossible.

When looking at the area's farming products, Mahangu, the Oshiwambo term for pearl millet (*Pennisetum glaucum*), presents itself as the most important crop of the region, given that about 90% of arable land is used for its cultivation (MENDELSOHN et al. 2000). This can be explained by its good drought resistance, low sensitivity to high temperatures and its adaption to poor water and nutrient conditions of the species (MENDELSOHN et al. 2000). Other arable crops of the region are cow-peas, beans, pumpkins, bambra nuts, peanuts or melons which are commonly grown as catch crops with mahangu (MENDELSOHN et al. 2000). Finally, sorghum is a widely cultivated plant which is frequently taken for beer production.

Small scale framing takes place without irrigation and is therefore highly dependant on the onset of the rainy season and the amount of precipitation each year. As a consequence, the timing of agricultural activities is adjusted to rainfall events and generally varies between growing periods. Usually, field preparation, ploughing and planting begins during November, December or January while harvesting is mostly done in May or throughout the following months (MENDELSOHN et al. 2000). Most farmers store their harvests instead of selling them in order to meet possible yield shortages in years with poor environmental conditions and crop shortfall. To do so, farming products, mostly mahangu, are stored up to three years in granaries equipped with plaited baskets, called *iighandi* (Fig. 2, MENDELSOHN et al. 2002).

Figure 2: Homestead with surrounding cropping area before cultivation and *iigandhi* granary for cereal storage (small picture upper right).

In addition to crop cultivation, animal husbandry plays a significant function in sustaining rural livelihoods. Accordingly, a great share of the research area is used as pasture and a big proportion of Namibia's livestock can be found in the entire region (MENDELSOHN et al. 2000). Important domestic animals are goats, poultry, donkeys, cattle, pigs and sheep. Apart from meat production, many animals also serve transportation or ploughing purposes. In addition, livestock, especially cattle, is

seen as an investment, so the number of cattle per household generally reflects the wealth and social status of a family. This may lead to high livestock densities even if the products are not needed for a family's subsistence. Overall, large discrepancies between very poor and rich households exist and those tend to increase (MENDELSOHN et al. 2000).

As these rural districts of the region are regarded as communal land, access to farming, settlement and grazing areas is managed via tribal authorities and therefore the competence lies with the local headmen (MENDELSOHN et al. 2000). Against the background of this rather complex situation and intensified utilisation of resources, land use regulations and steps to social equality may become a challenging task in the near future.

2.3 Geology

The local geology consists of several formations, but only one sequence, Namibia's youngest geological division, reaches the research area's surface (Fig. 3). The geological fundament is built by the Pre-Damara Basement, situated over 4,000 metres below ground level and formed about 2,600 to 1,700 million years ago (MENDELSOHN et al. 2000). After an erosional period that lasted until about 900 to 1000 million years ago, immense intercontinental rifting created deep valleys that were filled with sediments which became the sandstones of the Nosib Group. In course of the Rodinian land mass breakup, oceans were formed and the region itself became an extensive sea shelf, the foundation of the Owambo Basin, on which sediments of limestones and dolomites got deposited (MENDELSOHN et al. 2000). These sediments became the Otavi Group that was folded at the margins and subsided in the centre during the land mass collision leading to the formation of Gondwana (MENDELSOHN et al. 2000), thereby generating the Owambo Basin. Recurring erosion of surrounding mountains produced another layer of sedimentary rock in the basin, called Mulden Group, completing the rock units that were formed after the intercontinental rifting had begun, the Damara Sequence (MENDELSOHN et al. 2000). Another prolonged period of erosion was followed by the Dwyka glacial period; its tillites mark the beginning of the depositions cycle generating the Karoo sequence about 300 million years ago (CHENEY 1994, MENDELSOHN et al. 2000).

Approximately 20 million years later, a warmer climate led to ice meltdown and to the formation of shallow seas and lakes in the Basin that dried up and left shales, sandstone and organic material behind. Finally, extremely dry conditions led to the deposition of sands on top of those. During the fragmentation of Gondwana from around 180 to 70 million years ago, an enormous depression was created in the South African subcontinent, the Kalahari Basin, with a vast extent from the Northern Cape in South Africa to large regions in Botswana, Namibia, Zambia and Angola with branches up to the Congo River (MENDELSOHN et al. 2002). The Ovambo Basin presents itself as a small subdivision of this geological province. Sedimentation took place in arid to semi-arid conditions with alternating wet and dry phases; thus, different formations of the Kalahari sequence can be distinguished, namely the Ombalantu- (oldest), the Beiseb-, the Olukonda- and the Upper Andoni (youngest) Formation (HIPONDOKA 2005, MENDELSOHN et al. 2000).

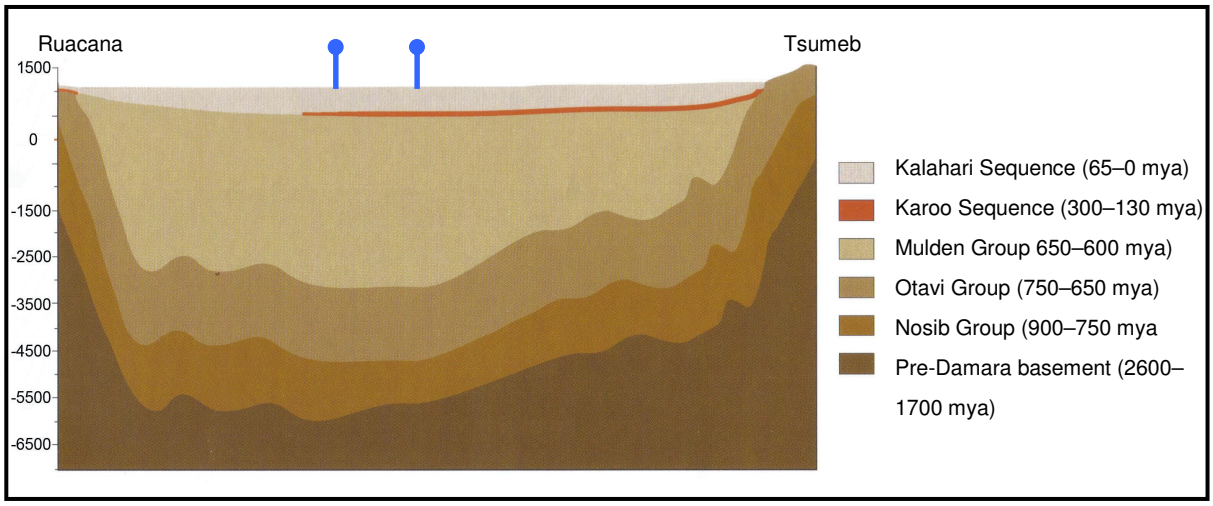

Figure 3: Geological profile from Ruacana to Tsumeb. Blue flags indicate approximate position of the research area (check marks by author, image source: MENDELSOHN et al. 2000)

Large rivers from the north and northwest flew into the Basin, creating extensive megafans and lakes that dried up later, leaving clay and salty layers behind (HIPONDOKA 2005, MENDELSOHN et al. 2000). The end of this sedimentation period was dominated by two large fluvial systems, namely the Kunene in the west and the Cubango in the east (MILLER et al. 2010). Later, the Cubango/Okavango river shifted eastward and got narrower and the Kunene River separated from the region about two million years ago due to bed erosion and changed its course towards the Atlantic Ocean (MILLER et al. 2010, MENDELSOHN et al. 2000). But the

early Kunene River also provided the basis for today's only remaining drainage system, the Cuvelai with its broad shallow Oshanas (MILLER et al. 2010). So for the last 70 million years, the research area has been filled with large amounts of sand and other deposits like clay and calcrete (MENDELSOHN et al. 2002) and these constitute the base material for the development of present soils.

2.4 Soil

The various soils occurring locally should be discussed in more detail because soils and their water characteristics play a significant role for recharge modelling. To begin with, there is no high resolution spatial data available for the whole research area. Provided information is restricted to a scale of 1:1,000,000 with some small parts mapped at 1:100,000 in the northern fringe (cf. COETZEE 2001) and is therefore insufficient for the desired modelling scale. The distribution of these soil units is not illustrated here, because they are so extensive and are presented in various publications (BATJES 2004, DIJKSHOORN and VAN ENGELEN 2003, MENDELSOHN et al. 2000, MENDELSOHN et al. 2002), albeit with different attributes sometimes. This chapter gives an overview of present soil types and their main properties. Results derived from soil analysis and assignment to vegetation units will be presented in detail in chapter 5.3.

As indicated, soil units clearly reflect the hydrological situation and hence an elevation gradient, which was already mentioned in the land use chapter. The highest parts of the research area, separating adjacent Oshanas, are covered by Arenosols (MENDELSOHN et al. 2000, RIGOURD and SAPPE 1999). These soils are typical for the quartzous Kalahari Sands and therefore represent the major soil type of the region (MENDELSOHN et al. 2002, MAWF 1999). Characteristic attributes of Arenosols are no or marginal soil development, coarse texture, hence high water permeability and low nutrient detention (FAO 2006).

In lower parts of the field, other soils can be found and the Cuvelai System, which is leading to annually or seasonally flooded areas, presents itself as determining factor of soil formation. The recurring cycle of flooding and evaporation as well as capillary rise of water leads to an accumulation of sodium and other water soluble salts. As a

consequence, saline or sodic soils develop, which are often found side by side in arid to semi-arid environments (FAO 2006).

Sodic soils often originate from saline soils in case of chlorine outwash. Enrichment in sodium leads to disproportionally high percentage of sodium ions on the exchange surfaces (BLUME et al. 2010). When these soils get wet, clay particles disperse and form an impermeable layer, a process that is amplified in regions with high rainfall variability (BLUME et al. 2010). As a result, this layer becomes very hard during the dry season and roots can hardly penetrate it. On the other hand, precipitation events cause water logging because infiltration is hampered by the clayey layer. Obviously, these circumstances make the mentioned soil a bad habitat for plants and agricultural activities, especially if the hard layer is near to the surface (BLUME et al. 2010, FAO 2005). Solonetz is a typical representation of these sodic soils.

Saline soils form if chlorine is present. The chlorine reacts with available sodium in large amounts, forming sodium chlorine, one of the crucial salts when speaking of salinization (other important salts are Na_2CO_3, Na_2SO_4, $CaCl_2$ etc., BLUME et al. 2010). When an accumulation of salts leads to the development of a salic horizon, then the soil is classified as Solonetz (FAO 2006). Salts lead to flocculation (in contrast to dispersion in sodic soils) and stabilisation of the soil. In extreme conditions, salt accumulation may lead to salcrete development. Another important consequence of high salinity is the reduction of plant available water due to a higher osmotic potential and some elements may have toxic effects (BLUME et al. 2010), making these soils only suitable for specialised salt tolerant plants.

Both of these processes, salinity and sodicity, play an important role in the research area. Therefore some sources specify the dominant soils in the research area as Solonchaks and Solonetz (BATJES 2004, DIJKSHOORN and VAN ENGELEN 2003, RIGOURD and SAPPE 1999). Naturally, also Solonchak-Solonetz transitions exist.

Finally, Vertisols are specified as an important subgroup (MAWF 1999, BATJES 2004) that is closely linked to hydrology. They usually occur in depressions at the lowest part of the field where alternating moisture conditions persist, for example due to repeated flooding and desiccation (FAO 2006). Another distinctive feature is their

very high clay content. Owing to the expansion of clay particles during wet periods and contraction throughout dry periods, these soils are characterised by intensive perturbation (BLUME et al. 2010). As a consequence, a polygon shaped pattern and shrinkage cracks, often referred to as slickensides, are distinctive features of Vertisols (FAO 2006). Generally, many soils of this category show a high proportion of organic matter but bad physical properties (BLUME et al. 2010). The latter comes from soil hardening during dry periods and water surplus in the rainy season. Together with high salinity in depressions and pans, this makes these soils unsuitable for cultivation.

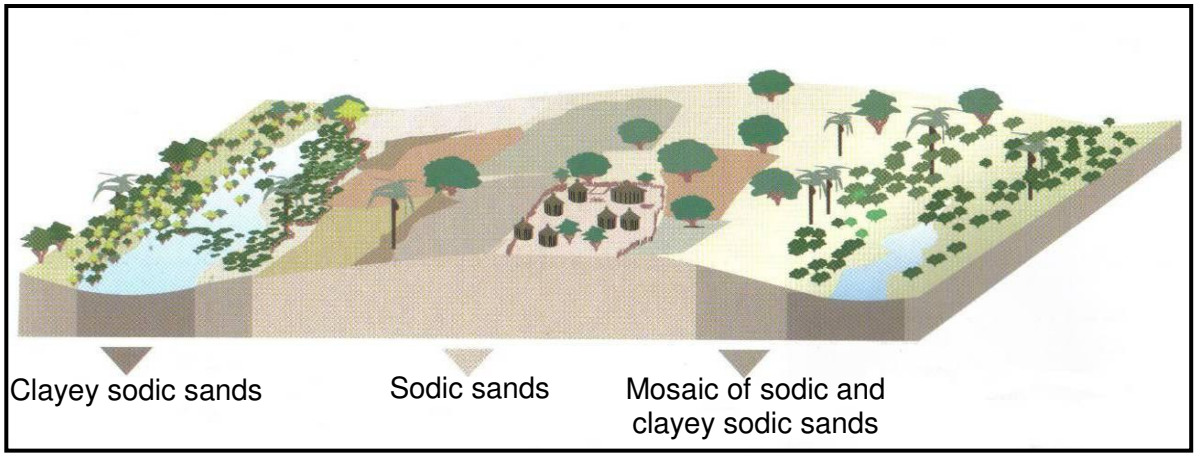

Figure 4: Characteristic pattern of soil and land use distribution in the research area (image source MENDELSOHN et al. 2000)

In summary, the allocation of soils and hence land use show a noticeable spatial pattern in the research area (Fig. 4). In good agreement with the information stated above, MENDELSOHN et al. (2000) outlines the succession of soils according to their relative position to the Oshanas. These Oshanas contain considerable amounts of clay and salt in opposition to higher, often populated areas which are dominated by a pure sandy texture and lower salinity. In the intermediate parts, a mixture of clayey and sandy soils can be found, both with a noticeable amount of salt (MENDELSOHN et al. 2000).

2.5 Climate

The climate of Northern Namibia can be classified as semi-arid and is dominated by the seasonal relocation of the Intertropical Convergence Zone (ITCZ), caused by the shift of the sun's zenith to the north during June and to the south in December. Therefore, the region is dominated by the subtropical high pressure zone in winter and the ITCZ low pressure system with associated precipitation in summer (Fig. 5).

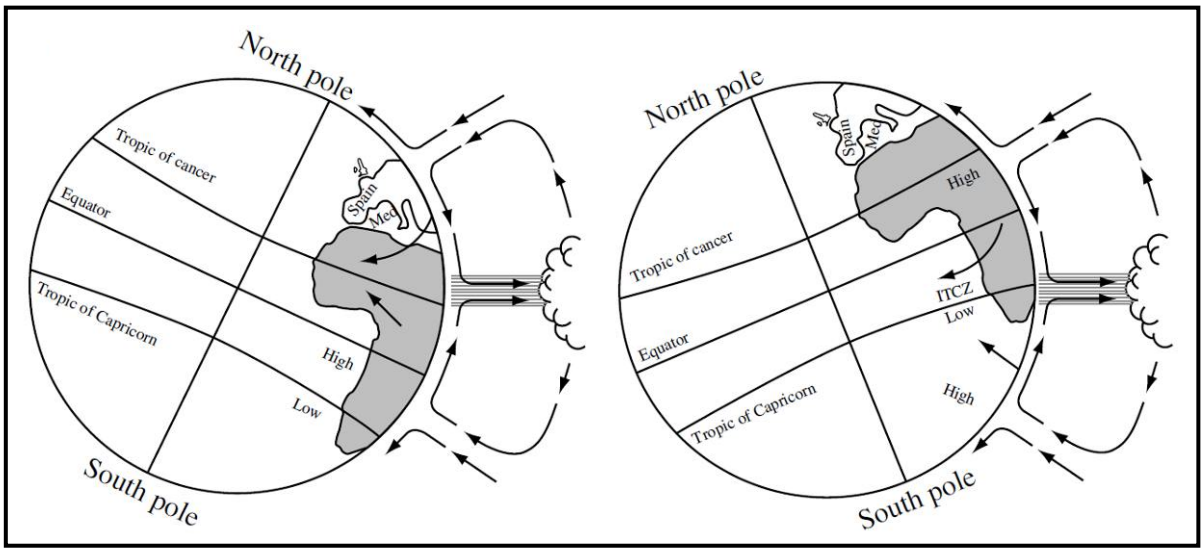

Figure 5: Simplified illustration of the ITCZ and its seasonal variation, left: June to August, right: November to February (image source: SHORROCKS 2007)

This situation in the transition zone between two pressure systems also leads to a high climatic variability. Minor shifts in the position of these systems produce either extraordinary dry or wet periods (MENDELSOHN et al. 2002).

To describe the climate of the region in more detail, averages from the climate station in Ondangwa, situated approximately 10 km outside the research area, are used. The long-term daily mean temperature ranges from about 17°C in winter to around 25°C during summer months (MENDELSOHN et al. 2000). September, October, November and December also show the highest mean maximum temperatures from 30°C to 35°C, while the average minimum temperatures of about 7°C to 8°C occur in June and July (MENDELSOHN et al. 2000). Another attribute of the regional climate are high evaporation rates of about 2,500 mm per year (MENDELSOHN et al. 2000).

Precipitation is probably the most crucial parameter for the region's life and should be discussed thouroughly. A reference period of 30 successive years is usually utilised to present climatological standard normals (WMO 2009). The period from 1960 to 1989 was chosen, because only a few years were missing (1960 – 1989 was taken instead of the standard period 1961 – 1990, because no data for the year 1990 was available). When looking at monthly means for this period, hardly any precipitation occurs from May to September, which clearly defines the dry season (Fig. 6).

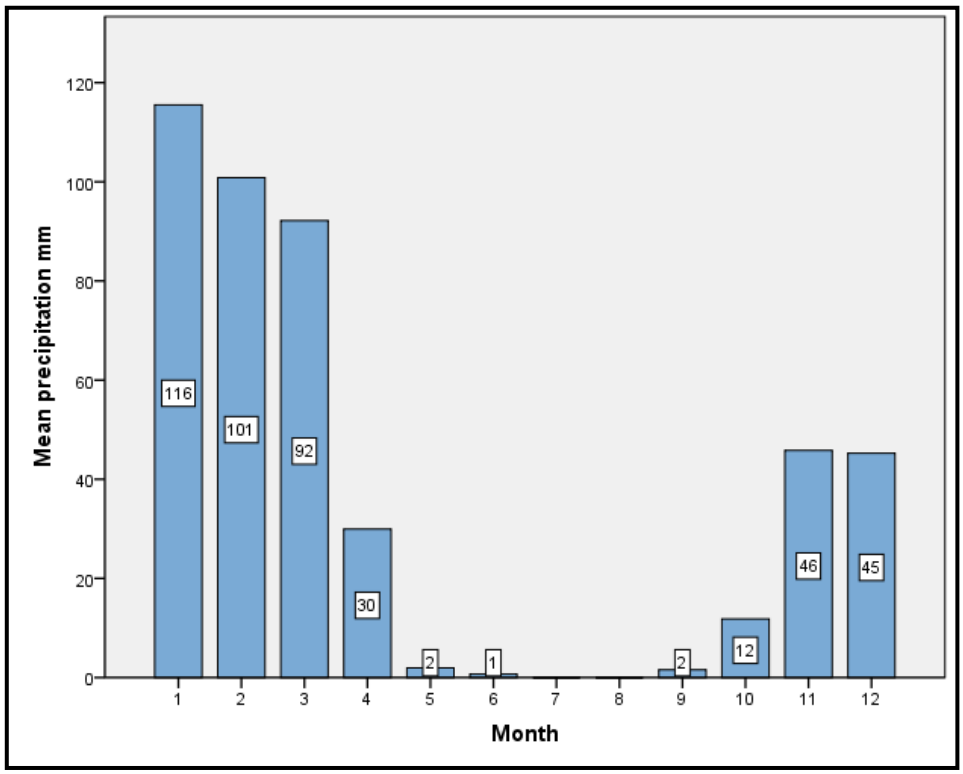

Figure 6: Monthly mean precipitation for the period 1960 – 1989 at Ondangwa (Nr. of years missing: 5 in Dec, 3 in Jan, Feb, Aug, Sep and Nov, 2 in Apr, 1 in March, May and Oct, data source NMS 2010)

With the onset of the rainy season, usually between October and late November, precipitation amounts increase gradually until January or February. Almost 70% of the total rainfall amount takes place from January to March and declines strongly afterwards. MENDELSOHN et al. (2000) states similar figures, but with highest precipitation amounts in February, lower values in November and higher ones in December. This discrepancy may be caused by a different reference period. On average, precipitation amounts were at about 450 mm per year from 1960 to 1989. As stated before, this puts the climate at the upper end of the semi-arid range from 200 mm to 500 mm as given by Lloyd (1986).

However, there are not only seasonal differences within a year, but there is also an extreme divergence when comparing rainfall amounts between several successive years. This can also be inferred from the distribution of monthly precipitation (Fig. 7).

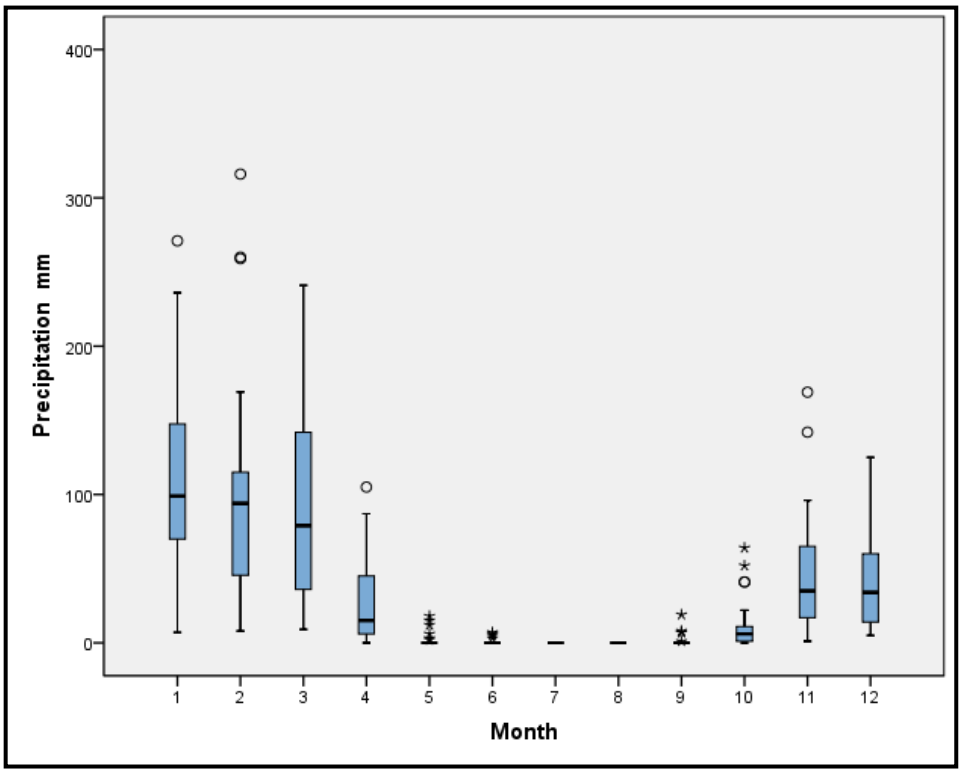

Figure 7: Box plot of monthly precipitation at Ondangwa 1960 – 1989. Showing median, minimum and maximum values, the blue box outlines the interval between the 25th and 75th percentiles. Circles designate outliers, asterisks extreme outliers (data source: NMS 2010)

The greatest fluctuations can be found during the wettest period, indicated by a large interquartile range. In March for example, a difference of 112 mm from the 25th to the 75th percentile can be found. With values of 80 mm and 76 mm, the fluctuations are quite high for January and March as well. Against a background of 450 mm average precipitation per year, these figures appear quite high. Thus a high variability of rainfall has to be expected in this environment, which may lead to flooding, droughts or well balanced conditions, affecting the people, agricultural activities and, lastly, groundwater recharge.

2.6 Hydrology

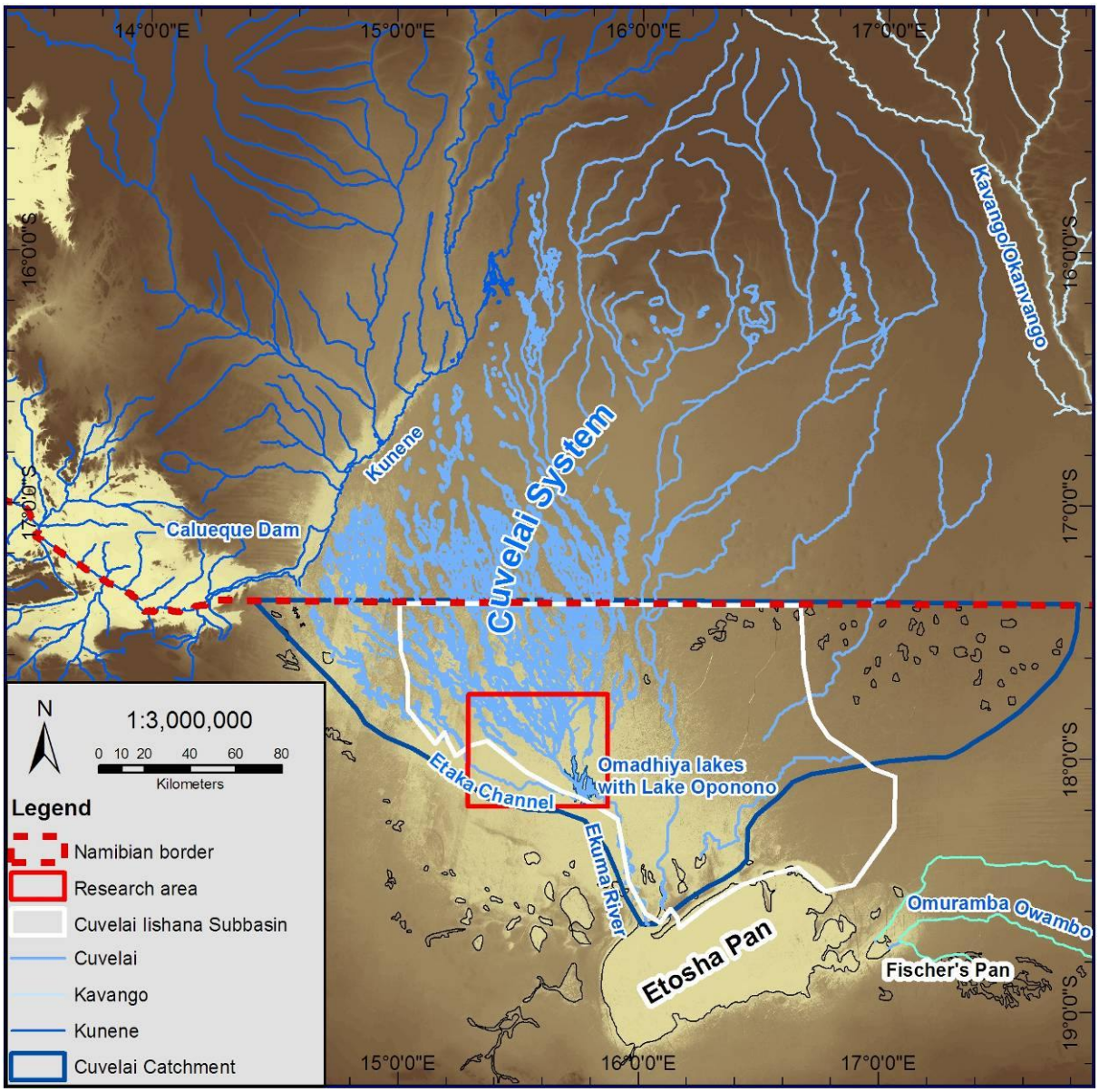

Figure 8: Cuvelai drainage system, Namibian part of its catchment and position of the Cuvelai Iishana-Subbasin (latter drawn according to KLUGE et al. 2006) Background: ASTER digital elevation model (data source: DEA 2002, NASA LP DAAC 2009, MAWF 2000)

The study area is situated in the Cuvelai catchment and most of it is part of the *Cuvelai-Iishana Subbasin* (Fig. 8), which in turn is a subset of the *Cuvelai-Etosha Basin*. Basin boundaries originate from results compiled by the IWRM basin demarcation project and are based on a number of criteria; among which are physiographic parameters, water supply and demand, political and cultural districts, infrastructure and population distribution (MAWF 2006). In all of these basins, groundwater and overland flow is directed southwards towards the Etosha Pan.

When looking at the area's surface hydrology, the Cuvelai drainage system, a large inland delta, is the most striking feature of the region. Its northern branches, emerging at about 15° southern latitude, reach deep into the rain-laden Angolan highlands and the longest channels stretch over 400 km before the whole system ends in the north-western part of the Etosha Pan. The drainage area extends over more than 70,000 km², whereby 50,000 km² of those are located in Angola (MENDELSOHN et al. 2000). According to MILLER et al. (2010), the Cuvelai system comprises two parts: on the one hand, an eastern active part which is partly fed by Angolan rivers and local rainfall; on the other hand a western part that doesn't receive water from Angola and is just fed by regional precipitation. This differentiation is also visible in figure 9, were the eastern part of the catchment is more affected by flooding caused by water inflow from the north.

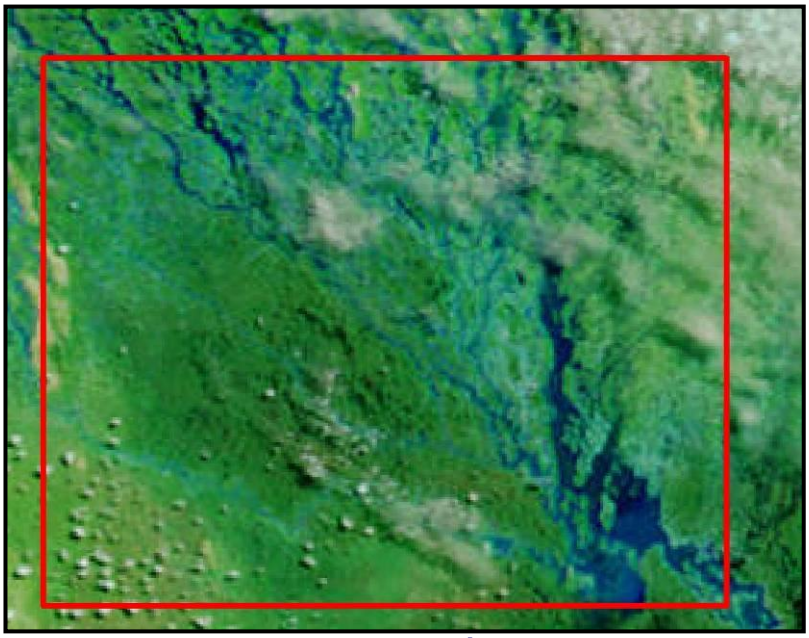

Figure 9: MODIS image from 20th March 2011 showing a large flood (*efundja*) in the research area (outlined by red rectangle; image source: NASA 2011)

The whole catchment is characterised by an exceptionally erratic discharge pattern, as rainfall is highly variable and it plays an important role where exactly precipitation happens. In average years, the Iishana in the research start filling up with the beginning of the wet season and approximately in February, Angolan waters reach the region where they trigger slow outflow towards the Etosha Pan (HIPONDOKA

2005). This surface runoff in the Oshanas persists until May (HIPONDOKA 2005). When there is extensive rainfall over the entire catchment, then a large flood occurs, locally known as "*efundja*" (MENDELSOHN et al. 2000). MENDELSOHN et al. (2000) state that in a mean period of 20 years, about eight extensive floods occur, three of which are major floods, the *efundjas*. One of those events just happened in the wet season 2011 and led to the flooding of large parts of the region with severe damage to crops and infrastructure (Fig. 9, NASA 2011).

But large floods are also of great importance to the region. They replenish groundwater resources and bring new fish into the Oshanas (MENDELSOHN et al. 2000). As there is a very smooth elevation gradient in the region (averaging 1:5,300 according to HIPONDOKA 2005), flow velocities are usually very slow and much of the water gets captured in the Iishana at the end of the rainy season where most of it evaporates before the next rainy season.

As to groundwater resources of the Cuvelai-Etosha Basin, there exist different aquifers, but not all of them are usable for drinking purposes. In the geological formations below the Kalahari sequence, mostly brackish aquitards were discovered in the Karoo and the Mulden Group, although some sources assume the existence of freshwater in the Damara sequence aquifers deep below the research area (MAWF 2006). The freshwater aquifer in the Otavi Group is very important for the Tsumeb area (CHRISTELIS and STUCKMEIER 2011) but up to date, the use of these water sources is restricted to the southern part of the Cuvelai-Etosha Basin and therefore outside the research area.

Most information about groundwater in the region of interest is connected to the Kalahari sequence with its alternating sediment layers. No data about aquifers is available in the lowermost of these, the Ombalantu formation. Conditions regarding the Beiseb Formation are similar: CHENEY (1994) states that its geological attributes and extent would make this layer a possible freshwater source, but only brackish water has been discovered so far. In the above lying Olukonda Formation, the so-called *"Very Deep Aquifer"* can be found which is tapped in Northeast Oshikoto and East Ohangwena (CHRISTELIS and STUCKMEIER 2011, MAWF 2006). In the northern parts, the aquifer is characterised by a relatively good water quality whereby

salinity gradually increases southwards, which indicates recharge in Angola (CHRISTELIS and STUCKMEIER 2011).

Several aquifers can be found in the younger Andoni Formation (Fig. 10). On the base of these sediments, investigations found some freshwater aquifers outside the research area but no information is available for the situation within (CHENEY 1994, CHRISTELIS and STUCKMEIER 2011). Overall, water quality in the deeper parts of the formation varies substantially and most water may be regarded as highly saline because of the salty remains of former paleolakes (cf. MENDELSOHN et al. 2000).

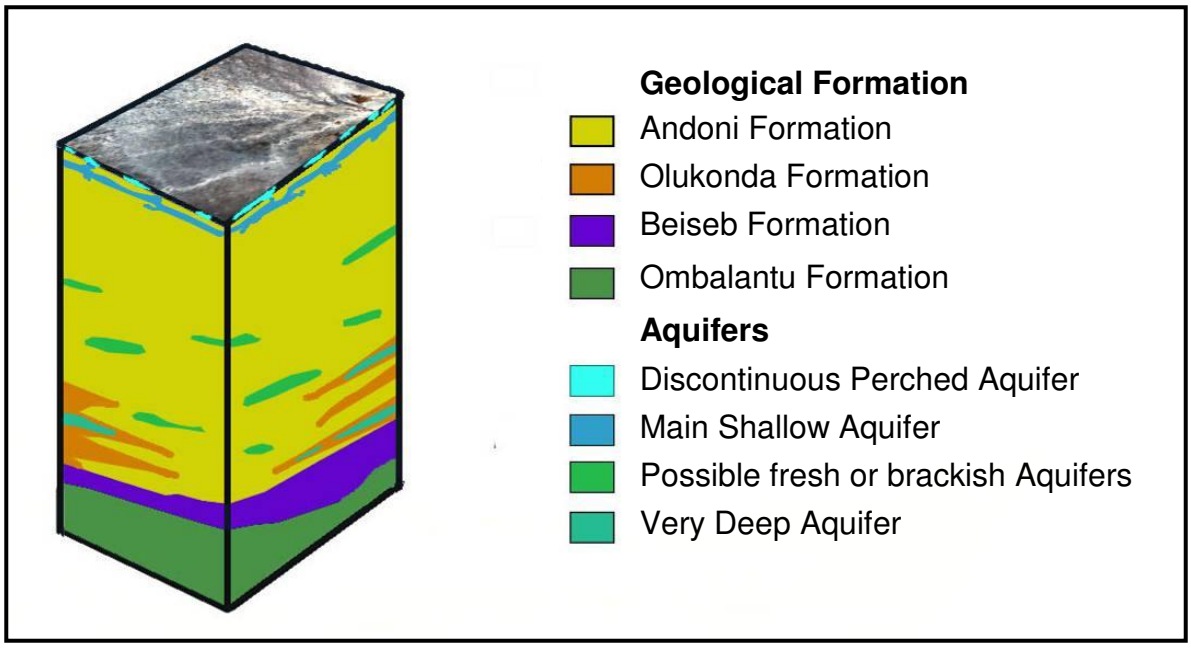

Figure 10: Simplified schematic illustration of the geological formations of the Kalahari Sequence and existing or assumed aquifers (drawn according to information given in CHRISTELIS and STUCKMEIER 2011, HIPONDOKA 2005, MAWF 2006, satellite image source: RAPIDEYE 2011)

The most prominent aquifer which principally extends over the whole Cuvelai-Iishana Subbasin is the so-called "*Main Shallow Aquifer*". In contrast to the formerly mentioned, this aquifer is unconfined. Also called "*Oshana aquifer*" in some references (MAWF 2006), it presents itself as an alluvial multi-layer aquifer, with permeable, water rich sandstone layers interbedded with less permeable, often cemented clayey aquitards (MAWF 2006, CHRISTELIS and STUCKMEIER 2011). The position of this aquifer mostly ranges from 6 m to 80 m below the surface and the various wells tapping it, usually called "*oondungu"*, just reach the uppermost

section of it (CHRISTELIS and STUCKMEIER 2011, MENDELSOHN et al. 2000). Water quality is mostly saline and increasingly so towards the centre of the region with values generally above 5,000 mg/l, sometimes peaking to more than 20,000 mg/l (CHENEY 1994). Therefore, the water can be regarded as saline to hyper saline and is often nonpotable. In some parts of the research area, it is not even usable for watering livestock. Recharge mostly occurs through flooding events in the Cuvelai, triggered by Angolan rainfall. Then temporal fresh water lenses may form on top of the denser salt water (MAWF 2006).

Figure 11: Shallow hand dug well (*omithima*), not fenced off and therefore used for livestock watering

Finally, the "*Discontinuous Perched Aquifer*" is the uppermost and lies in recent deposits. It presents itself as the main traditional and still important water source of the rural population of the region (CHENEY 1994) and is also the main focus of the study's recharge modelling. The aquifer either lies on top of an impermeable clayey layer or just above the denser saline "Main Shallow Aquifer" (CHENEY 1994). As its name indicates, the aquifer does not consist of big connected parts but of many small portions of water (MAWF 2006). This leads to the fact that it will not produce high yields and freshwater resources may become depleted or saline during the dry

season. However, the “Discontinuous Perched Aquifer” can be found in many places all over the research area and because it contains fresh water, it serves as the simplest accessible water resource. It is mostly used via shallow hand dug wells (Fig. 11) called “*omithima*” (MENDELSOHN et al. 2000), which are often also exploited by livestock if not fenced off. The “Discontinuous Perched Aquifer” is mostly recharged by infiltration water originating from local precipitation (MAWF 2006, CHRISTELIS and STUCKMEIER 2011) but may also be partly replenished by flooding (MENDELSOHN et al. 2000). Therefore, this aquifer is totally dependent on seasonal conditions and momentary recharge. This study now aims at a better understanding of the pattern and quantity of the replenishment of this aquifer.

3. Theoretical Background – Groundwater Recharge in Semi-arid Areas

Generally, groundwater recharge is defined as the amount of water reaching the water table, thereby contributing to the groundwater reservoir (DE VRIES and SIMMERS 2002). This simple definition introduces a complex hydrological subject, which is associated with a couple of problems and uncertainties and involves several scientists, especially in Southern Africa (XU and BEEKMAN 2003). To give an overview, figure 12 illustrates an abstract impression of determining parameters.

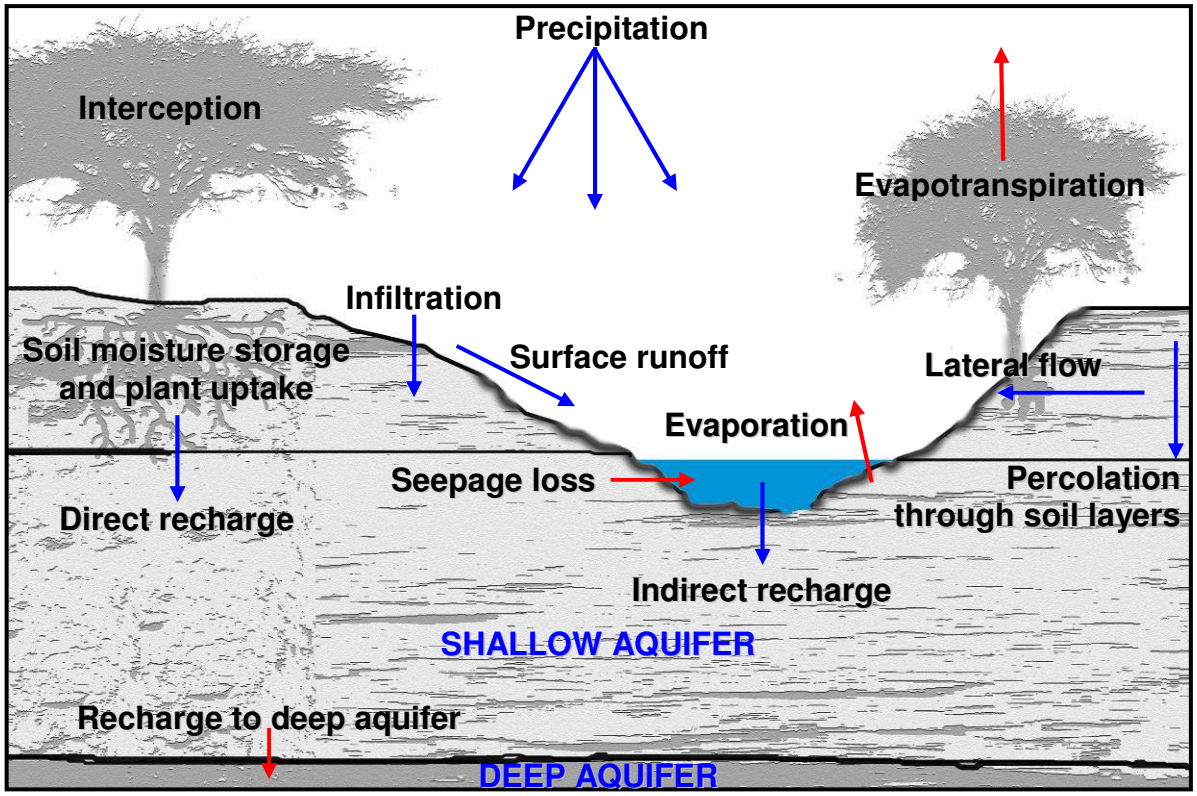

Figure 12: Simplified scheme of groundwater recharge in semi-arid areas.

Naturally, precipitation presents itself as one of the most important input variables, whereby not only its amount, but also its intensity, duration and spatial distribution are essential, especially in an arid to semi-arid environment. This becomes apparent when looking at another crucial factor, namely potential evapotranspiration (ETpot), which on average is considerably higher than precipitation in those areas (DE VRIES and SIMMERS 2002). Also other near surface conditions are important for recharge characteristics, like infiltration rate and its determining influence on how effective

precipitation is partitioned, if it either percolates rapidly, thus escaping evaporation or if it fills depressions and riverbeds. This may also lead to recharge later on, infiltrated water may in turn get dammed at deeper impermeable layers and contribute to lower areas as lateral flow. Furthermore, attributes of vegetation, soil conditions, storage and their horizontal structures influence groundwater recharge. Beyond that, the circumstances in the aquifer or the aquifers themselves and associated exchange flows affect the process. Finally, surface or subsurface influx into a region may play a decisive role, which becomes clear in regard to the Cuvelai.

According to the various ways groundwater may be recharged, three mechanisms of recharge are conceptually distinguished (LERNER 1990 in DE VRIES and SIMMERS 2002):

- Direct recharge through vertical infiltration of precipitation water.
- Indirect recharge from rivers and surface streams.
- Localised recharge from (temporal) water accumulation in surface depressions, pans or joints.

These different processes imply that the methods for recharge estimation have to be chosen according to the dominant mechanism. Naturally, a coexistence of those can be found in most hydrological systems, which is also true for the research area. This makes a quantification of the various parameters more complex and may lead to an incomplete view with only a single approach. However, a complete investigation of all recharge processes lies outside the scope of this thesis. Therefore, this study focuses on the estimation of direct recharge which is also the main water source of the discontinuous perched aquifer as given by MAWF (2006) and CHRISTELIS and STUCKMEIER (2011). According to KÜLLS (2000), analysing the vertical moisture flow or water balance methods, e. g. in a model are suitable approaches for assessing recharge if direct recharge is the dominant mechanism. This should not detract from the importance of other recharge mechanisms, especially indirect recharge through flooding which may also contribute to the aquifer in question and is the main water source for the main shallow aquifer. Furthermore, localised recharge certainly plays another role in this undulating landscape with its numerous pans and depressions. The latter may be hampered by an often found clayey layer in those

areas with parallel sealing through sodicity. The indirect and localised recharge processes generally gain in significance the more arid an environment is. Direct recharge may become an uncommon occurrence below mean precipitation rates of about 250 mm because of the high thresholds posed by the moisture deficit of deep surface horizons (Lloyd 1986). According to that, a completely different approach is necessary and different methods are needed for the assessment of recharge stemming from these indirect or localised mechanisms (KÜLLS 2000).

The limiting factors of a hydrological system are also important issues. If climate and soil conditions supply a greater amount of water than the saturated zone can store or conduct, which may lead to overland flow and a shallow water table, then the geological situation controls the recharge rate (SANFORD 2002). When the saturated zone has a hydraulic conductivity that is able to transmit more water or store a larger amount than the climate and soil can provide, then the surface factors are the limiting and controlling factors of groundwater recharge (SANFORD 2002). The first of these two situations is often associated with a humid climate or low topographic relief where the geologic framework is the main control variable, while the latter is typical for more arid climates or areas with high topographic relief (SANFORD 2002). Again, natural systems may be controlled by both of these limiting factors or they may vary temporarily, which adds complexity to assessing the recharge.

As the discontinuous perched aquifer is shallow, another process may be relevant which may introduce additional uncertainties in recharge assessment. Initial recharge may alter the water table and some water may become surface water where it evaporates. Thereby, net recharge is lower than the anticipated amount gained from percolating water. Furthermore, plants adapted to arid conditions may be able to extract water from great depths (DE VRIES and SIMMERS 2002). Therefore, DE VRIES and SIMMERS (2002) recommend the application of the term potential recharge for the amount of water that passes the root zone and actual recharge for the amount of water that reaches the water table in fact and is stored there more permanently.

In summary, groundwater recharge in semi-arid areas is extremely variable, both spatially and temporally; its estimation, therefore, is exceptionally dependant on the spatial and temporal boundary demarcations in a study. Due to this fact, a range of methods exist to estimate recharge and some of the most important ones should be addressed shortly. Tracer techniques are widely used for this purpose, among them tracers like tritium, bromide and colour, which are actively deployed on the surface to track their distribution in time (SCANLON et al. 2002). Furthermore, historical tracers (^{3}H und ^{36}Cl) set free by nuclear weapons or testing in the past may be applied for long term recharge estimation (SCANLON et al. 2002). One of the most widely applied natural tracer methods is the utilisation of the chloride mass balance method, which is seen as a very promising approach (XU and BEEKMAN 2003). It is based on the difference in chloride concentrations of precipitation, surface pore water and groundwater and assumes mass conservation between atmospheric input and its subsurface flux, which makes it unsuitable for areas with mixing or capillary rise of saline groundwater (XU and BEEKMAN 2003). Several other methods exist, which mostly involve water balance approaches with gauging data or the relation of water table fluctuations with recharge, or soil water balancing utilising moisture measurements (SCANLON et al. 2002). However, the majority of these techniques is not suitable for the research area, either because the environmental conditions are unfavourable for its application or because the required data are not available or too costly or time consuming to obtain.

Finally, numerical modelling of recharge by water penetrating the root zone is a widely used approach, whereby a number of different models exist (SCANLON et al. 2002). Because these models estimate recharge from meteorological input parameters, data with a high temporal resolution are a prerequisite to capture extreme events which may be crucial for the water balance (KÜLLS 2000).

4. The Model

The software for the model and associated information was kindly provided by Armin Dünkeloh. If not stated otherwise, the main source for the following chapter is therefore DÜNKELOH ARMIN (personal communication 2011).

4.1 Model Scheme and Processing Steps

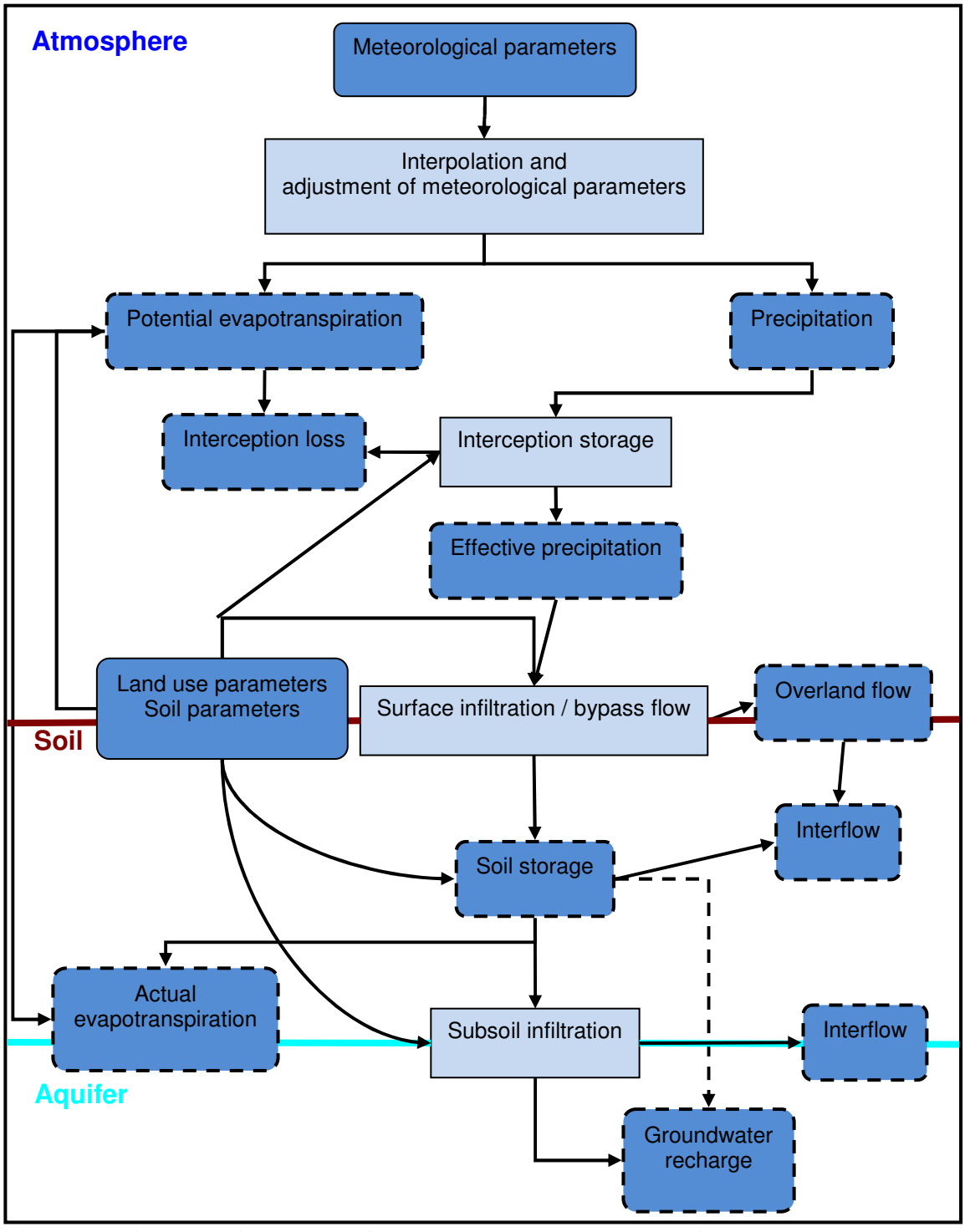

Figure 13: Abstract flowchart of the water balance model MODBIL

The assessment of the water balance should be achieved utilising the latest MODBIL version available (V49, UDLUFT and DÜNKELOH 2009). MODBIL is a raster based, process oriented, water balance model that consists of several physically based modelling steps and solves all involved equations for every single grid cell. To meet the demands of high temporal resolution, MODBIL processes the water balance on a daily time scale. The model consists of three major sections, namely the atmosphere, the soil column and the aquifer. A simplified scheme of the different levels is illustrated in figure 13.

Primarily, meteorological input parameters are interpolated. Required data are precipitation, minimum and maximum (mean) temperature, minimum and maximum (mean) relative humidity and wind speed. To improve the modelling and if data is available, also rainfall intensity, sunshine duration or global radiation could be included. The interpolation of the parameters is based on topographic information, like exposition and elevation, whereby a digital elevation model is needed. Potential evapotranspiration (ETpot) is then calculated according to meteorological and land use parameters. MODBIL provides different approaches in estimating ETpot (Penman-Monteith, Penman-Monteith FAO and HAUDE), the approach used in this study is discussed in the next chapter. Dependant on land use parameters, precipitation is then partitioned into an interception amount and effective precipitation that passes the canopy reaching the soil. Interception storage is then reduced in relation to ETpot.

Effective precipitation reaching the surface is then separated in an infiltrating part, bypass flow through macropores and overland flow. This step depends on soil cover (e.g. sealed surfaces), soil hydraulic properties and soil saturation. If the infiltration capacity of the soil is exceeded by effective precipitation, overland flow occurs. Due to soil hydraulic conductivity, percolating water is then proportioned into interflow and soil moisture storage which is dependent on effective field capacity. The latter refers to the amount retained against gravity in the root zone and which is available for plant consumption (called PAW herein, TAW in ALLEN et al. 1998). Water content below wilting point is assumed to be the minimum quantity always present in the soil. The amount of water stored in the soil is reduced by actual evapotranspiration (ETact) taking water stress into account, whereby MODBIL allows the use of different

approaches for its determination (e.g. ALLEN FAO, RENGER et al. 1974). If an area has water access, e.g. due to a high water table or capillary rise, areas with secondary ET (ETsec) may be defined which leads to higher ETact even in cases when no precipitation happens.

When the soil moisture exceeds effective field capacity due to additional infiltration water, deep percolation occurs. This amount, together with bypass flow, may be regarded as potential groundwater recharge if no further geological conditions have a limiting influence. Under these circumstances, undisturbed flow to the water table takes place because water below the root zone is unavailable for ET (without capillary rise). The process is represented by the dashed line in figure 13.

If the hydraulic conductivity of the subsoil is a limiting factor and the terrain is sloped, then interflow generates and the final groundwater amount passing the subsurface layer is reduced.

4.2 Calculation of Potential Evapotranspiration

ETpot is calculated according to the original Penman-Monteith equation. It combines the physically based evaporation process driven by meteorological parameters with factors that represent resistance by plants, leaves, soil surface and friction (ALLEN et al. 1998). This approach is preferred in this thesis because the application of the reference crop in the FAO Penman-Monteith equation may not resemble the research area well enough and the derivation of a basal crop coefficient may be erroneous (see discussion in chapter 5.4.2). Another reason is that calculations are applicable to all climate regions (in contrast to the HAUDE approach which has to be calibrated according to the region). The utilised method is described explicitly by ALLEN et al. (1998), which is the reference for all of the following equations:

$$\lambda ET = (\Delta^* (R_n - G) + p_a * c_p * (e_s - e_a) / r_a) \ / \ \Delta + \gamma (1 + (r_s / r_a))$$

where

λET = evaporative latent heat flux ($MJ/m^2/day$)

Δ = slope of saturation vapour pressure-temperature relationship ($MJ/m^2/day$)

R_n = net radiation ($MJ/m^2/day$)

G = soil heat flux (MJ/m²/day) may be ignored for daily time steps = 0

p_a = mean air density at constant pressure (kg/m³)

c_p= specific heat of air (MJ/kg/°C)

e_s = saturation vapour pressure (kPa)

e_a= actual vapour pressure (kPa)

(e_s - e_a) = saturation vapour pressure deficit (kPa)

r_a = aerodynamic resistance (s/m)

γ = psychrometric constant (kPa/°C)

r_s = (bulk) surface resistance (s/m)

$$\Delta = (4098*(0.6108*2.7183^{(17.27*T/T+237.3)})) / (T+237.3)^2$$

p_a (considering ideal gas law) = P/ (1.01(T+273)*R)

$c_p = (\gamma\varepsilon\lambda)/P$

$\gamma = c_p*P/\varepsilon*\lambda$

where

T = air temperature (°C)

R = specific gas constant = 0.287 kJ/kg/K

ε = molecular weight of water vapour / dry air = 0.622

λ = latent heat of vaporization, taken as 2.45 (MJ/kg),

P = atmospheric pressure (kPA)

(Bulk) surface resistance (r_s) abstractly describes stromatal, cuticular and soil vapour flow resistance; its value is taken from literature. Heat and water vapour transfer are controlled by aerodynamic resistance (*r_a*):

$$r_a = (\ln((zm-d)/zom))* \ln((zh-d)/zoh))/ k^2uz$$

where

zm = wind measurement height (m) = 2m

zh = relative humidity measurement (m) = 2m

*d = zero plane displacement height (m) = 2/3 * plant height*

*zom = roughness length governing momentum transfer (m) = 0.123 * plant height*

*zoh = roughness length governing heat and vapour momentum transfer = 0.1*zom*

k = von Kraman's constant = 0.41

u = wind speed (m/s)

Net radiation is another important input parameter, which is given as:

$$Rn = Rns - Rnl$$

where

Rns = incoming net shortwave radiation (MJ/m²/day)

Rnl = outgoing net longwave radiation (MJ/m²/day)

As there is no measured radiation data available from the research area, radiation is calculated in MODBIL according to ALLEN et al. (1998):
Outgoing longwave radiation is therein calculated using the Stefan-Boltzman law with correction factors for humidity and cloudiness.

$$Rnl = s * (Tmax^4 + Tmin^4/2) * (0.34 - 0.14 * \sqrt{ea}) * (1.35 * (Rs / Rso) - 0.35)$$

where

s = Stefan-Boltzmann constant (4.903 10^{-9} $MJK^{-4}/m^2/day$)

Tmax = maximum absolute temperature during 24h in Kelvin

Tmin = minimum absolute temperature during 24h in Kelvin

Rs/Rso = relative shortwave radiation (limited ≤1)

Rs = solar radiation (MJ/m²/day)

Rso = clear sky radiation (MJ/m²/day)

Solar radiation is calculated from extraterrestrial radiation, an adjustment coefficient and from daily temperature differences which represent cloud conditions. This is based on high amplitudes if the sky is clear because of high incoming radiation during the day and high outgoing radiation during nights, whereby a dense cloud cover reflects incoming radiation and may hamper strong heating. During night time, the same clouds reflect outgoing radiation back to the surface resulting in a low daily temperature range (ALLEN et al. 1998).

$$Rs = Ra * krs \sqrt{(Tmax - Tmin)}$$

The clear sky radiation is the fraction of extraterrestrial radiation that reaches the surface without a cloud cover.

$$Rso = (0.75 + 2 * l0^{-5} z) * Ra$$

where

Ra = extraterrestrial radiation (MJ/m²/day)

Krs = adjustment coefficient, recommended values by ALLEN et al. (1998): 0.16 for interior regions which are not influenced by large water area, 0.19 for coast or region where air is influenced by large water body

Tmax = maximum temperature (°C)

Tmin = minimum temperature (°C)

z = elevation above sea level (m)

Extraterrestrial radiation is the incoming solar radiation at the top of the atmosphere and is controlled by the angular derivation from the normal of the sun's incidence. Therefore, it can be calculated from latitude and the day of the year.

$$Ra = (23*(60)/\pi) * Gsc*dr*(\omega s * \sin(\varphi)*\sin(\delta)+\cos(\delta)*\sin(\omega s)$$

where

Gsc = solar constant 0.0820 (MJ/ m²/min)

*dr = inverse relative distance from earth to sun = 1 + 0.033 cos((2*π/365)* number of day a year)*

*ωs = sunset hour angle = arccos (-tan (φ) * tan (δ))*

φ = latitude (rad)

δ = solar decimation (rad) = 0.409 sin((2*π/365)* nr. of day in the year -1.39)*

The net solar shortwave radiation is global radiation minus the reflected portion, called albedo.

$$Rns = (1- A) * Rs$$

where

A = dimensionless albedo (see chapter 5.4.4.)

4.3 Calculation of Actual Evapotranspiration

ETpot represents the maximum possible amount that can be evaporated without restrictions resulting from the soil and water stress therein. Therefore, a water stress coefficient has to be applied to represent the reduction of ET when the soil water supply is limited, whereby three approaches are available in MODBIL (UDLUFT and DÜNKELOH 2009): either a simple factor from the ratio of actual soil water to field capacity (FC) or a more sophisticated approach by RENGER et al. (1974) and another approach by ALLEN et al. (1998) which may be utilised if a vegetation specific water stress coefficient is favoured. The third approach will be applied in this thesis, so the ETact is derived as

*ETact = rc * ETpot*

where

ETact = actual evapotranspiration
rc = water stress coefficient
ETpot = potential evapotranspiration
(*UDLUFT and DÜNKELOH 2009*)

The water stress coefficient is dependant on a threshold where water stress begins. The threshold in turn is calculated using the plant specific factor p, which is the mean fraction of plant available water (PAW) that can be absorbed without water stress, referred to as readily available water (RAW, ALLEN et al. 1998):

Wt = PAW - RAW = (1-p)(PAW)*

where

Wt = soil moisture threshold where water stress begins
p = factor p, ranging from 0 to 1 (ALLEN et al. 1998)
*PAW = plant available water = (water content at field capacity minus water content at wilting point) * rooting depth*
*RAW = readily available water = PAW * p*

If the available water in the soil is above this threshold, then the coefficient is 1 and if water content is below wilting point, it is 0 and no ET takes place from the soil. When

the soil water content is above the wilting point but below the threshold value, then rc reduces plant available water (Fig. 14.).

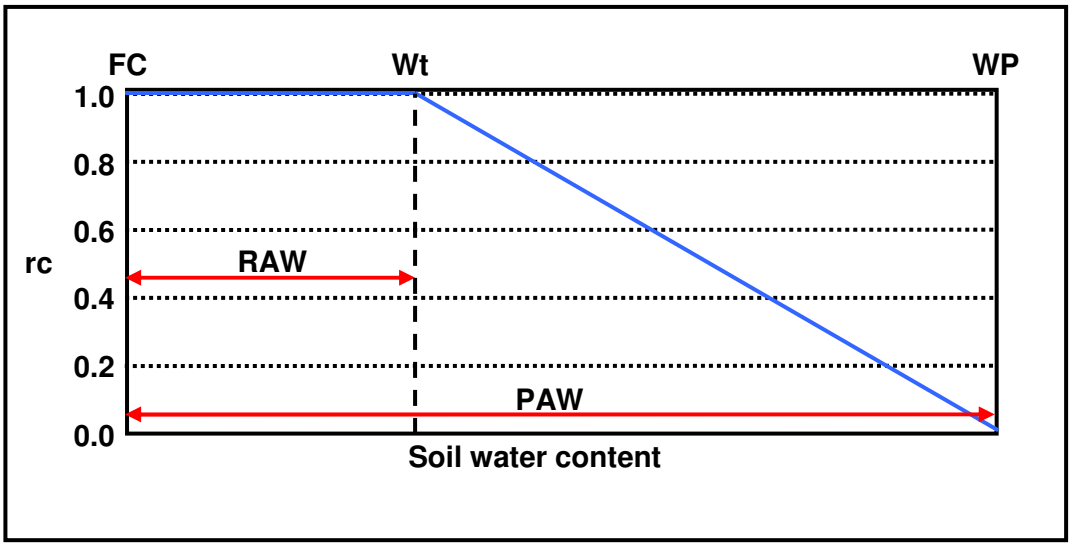

Figure 14: Relationship of water content and water stress coefficient. Blue line = soil water content, rc = water stress coefficient, FC = water content at field capacity, Wt = soil moisture where water stress begins, WP = water content at wilting point, PAW = plant available water, RAW = readily available water (redrawn according to ALLEN et al. 1998)

The coefficient is calculated as (ALLEN et al. 1998):

$$rc = PAWact / Wt$$

where

PAWact = plant available water content at current time interval

Wt = soil moisture threshold where water stress begins

5. Derivation of Model Input Parameters

The model is based on climatic data and on spatially resolved information of vegetation parameters and soil hydraulic properties which are all handled using land use categories. Field work was carried out at the end of the dry season from 12th October to 17th November. To relate information derived from field work to an areal extent, a remote sensing approach was pursued. To do so, test plots with a minimum area of 30 x 30 m were defined in the field and mapped using Trimble's Juno handheld GPS device equipped with ArcPad from ESRI. Overall, more than 100 test sites were defined in the field with 16 different categories. They were reduced during the classification process. These plots should represent the regional pattern of vegetation, whereby plant species determination was carried out by MAYR (2011). Since vegetation is strongly connected to soil and topographic position, especially on a local scale (MENDELSOHN et al. 2000, WANKE et al. 2008), soil samples were taken according to vegetation units. Therefore, test plots should represent both vegetation and soil and ought to be transferred to the whole research area with a supervised classification method using spectral information of RAPIDEYE satellite image, acquired on 9th November 2010 (RAPIDEYE 2011). The derived soil vegetation units serve as a basis for assigning several modelling parameters. Their determination, climatic data processing and assignment of soil properties will be discussed in the following chapter.

Data processing was implemented with several software products: GRASS GIS 6.4.1 was used for the land use classification, R 2.10.1 served for raster based time series analysis (e.g. MODIS-LAI/TRMM data), ArcGIS 10 was applied for visualisation and analysis of spatial data and PASW Statistics 18 was used for statistical analysis.

5.1 Land Use Classification

The derivation of the region's land use classes from remote sensing data is also the main focus of another diploma thesis at the Department of Geoecology at the University of Vienna (MAYR 2011). As the final results of this thesis have not been available yet for including in the modelling, a relatively simple approach is

implemented in this thesis. The more sophisticated method developed in the mentioned thesis will be applied when available.

Reflectance values for each pixel were calculated by MAYR (2011) for the blue, green, red, red edge and NIR bands of the RAPIDEYE product. These values, together with the mapped, categorised test plots served as a basis for classification. The supervised classification was implemented with the sequential maximum a posteriori (SMAP) modul in GRASS GIS (2010). The method incorporates two steps: in the first step the spectral signature for each class designated by the test plot is generated; based on this, the second step creates segments of the image using a Gaussian mixture distribution model at various scales, whereby the coarser resolution guides the finer scale classifications (GRASS 2007). This results in a classification with larger continuous areas in comparison to the standard maximum likelihood method which classifies every pixel separately.

In the course of the classification, some originally mapped test plots and categories had to be abandoned because their spectral information was not well distinguishable from other areas. Finally, 14 different classes were used for land cover demarcation. GRASS (2010) calculates Kappa values, which compare classification results with the categories defined in the first step, and computes conformity parameters. The Kappa coefficient is generally defined as *"coefficient … representing the proportion of agreement obtained after removing the proportion of agreement that could be expected to occur by chance"* (FOODY 1992, p. 1459). These values are taken as estimate for the classification accuracy for each category. As all test areas are used for classification and for computing kappa values, this is a simplified method for accuracy testing. A more significant way may be the use of split samples, one for building categories and another for the evaluation of the results. The latter approach is not applied in this thesis. Values are shown in table 1.

Class	Commission	Omission	Kappa
Woodland	12.50	29.06	0.87
Shrubland	39.20	21.07	0.60
Mopane shrubland	16.68	13.35	0.83
Grassland	35.65	5.55	0.64
Acacia pond mosaic	34.79	5.77	0.65
Shrub savannah	8.63	39.51	0.91
Seasonally flooded grassland high	14.70	15.47	0.85
Seasonally flooded grassland low	31.19	16.81	0.69
Grassland tufts	32.56	4.17	0.67
Halophytic vegetation	11.09	3.76	0.89
Oshana bright	0.85	3.29	0.99
Oshana dark	16.23	16.99	0.83
Water	0.70	0.74	0.99
Agricultural land	7.13	6.15	0.93

Table 1: Accuracy assessment values for the supervised classification. Commission: percentage of pixels classified as the class in question in test plots of other classes by pixels of respective class. Omission: percentage of pixels classified different to total number of pixels in the category's test plot. Kappa: coefficient of agreement (0 = no agreement, 1 = complete agreement)

Best accuracy values were computed for classes without vegetation and clearly differentiated surfaces like *Water, Oshana dark* and *Oshana bright*. Areas with greener vegetation, like *Mopane shrubland* and *Woodland,* showed good agreement as well, which may be caused by increased contrast to the spectral information of dry plants that dominate other classes. The *Seasonally flooded grassland* areas show different rates of agreement, whereby *Grassland* has a relatively high Kappa factor which may result from denser vegetation, different soil parameters and associated colour compared to adjacent sandy areas. Finally, values for *Halophytic* and *Agricultural areas* also indicate reasonable classification results. This may be explained by comparably high reflection rates due to salt or bright sediment deposits at former sites. Farming activities may in turn lead to a more uniform surface pattern and hence homogenously spectral information which leads to high accuracy values for agricultural land. A number of classes, especially those with dry vegetation, were connected with increased inaccuracy and therefore partly confused with other classes. This may be the result of a more heterogeneous spectral range caused by fuzzy transitions between the areas. Another class that was not captured very well

were the *Acacia pond mosaic* sites, which generally show small areal extent and contain green acacias and little water bodies which may result in a mix up with other categories (e.g. water or woodland). The class was not abandoned however, because it is characterised by soil hydraulic properties different from many other areas; moreover it may represent hand dug well sites.

Visual inspection of the classification showed mostly reasonable results, especially in the central area, although some uncertainties derive from a confusion of *Acacia pond mosaic* sites with *Woodland*, *Oshana dark* or *Water* areas. Inaccurate output was detected particularly in the southernmost parts of the research area, which results from the fact that nearly all test plots were mapped in the greater Iipopo and Omulunga regions (triangles in figure 15) which are characterised by dryer grassland or shrubland vegetation with occasionally occurring patches of green vegetation. Green areas were mainly found in the vicinity of homesteads or in *Acacia pond mosaic sites* (access to water table). In the south-western areas, greener and woodier vegetation may be found which was mostly classified as the *Acacia pond mosaic* category to an extent that seems immoderately large. But as no test plots were mapped in this area, ground truthing is not possible in these areas; thus the classification results are highly uncertain there. Another argument for the extensive classification of the *Acacia pond mosaic* category may be different soil properties and hence different spectral information of the area. This is inferred from information given in MENDELSOHN et al. (2000), who state finer soil texture in the south-western corner of the research area. A further issue is related to the southernmost central areas (south of the *Etaka Channel*) of the classification. In the RGB image, some darker areas are visible here which were classified as *the Oshana dark* category, but visual inspection showed that no Oshanas are present in that region. As examination of the satellite image indicates grassland areas and this is the predominant vegetation in the region, these areas were changed manually after the classification. The same had to be done with some areas just north of the *Etaka Channel*. *Grassland* areas and *Seasonally flooded grassland high* areas, which are both characterised by a dense grass cover, were also confused in some of the central areas and, where possible, wrong classification results were corrected by visual inspection. Therefore, some uncertainties and errors may still be present in the current classification, but the general vegetation and soil distribution seems to be

captured well and the final results (Fig. 15) show good agreement with generalised vegetation units delimited by the MAWF (2000).

The original classification was performed in a resolution of 5 m according to the RAPIDEYE images. The result was resampled (majority) to a 30 m land use raster that was used for modelling. This was mainly done to reduce processing time and because a 30 m resolution seems sufficient for the modelling scale.

Example images and short explanations of classified soil-vegetation units are illustrated in figure 16. Detailed information and species composition is outlined by MAYR (2011). Built up areas were mapped separately and are not part of the modelling.

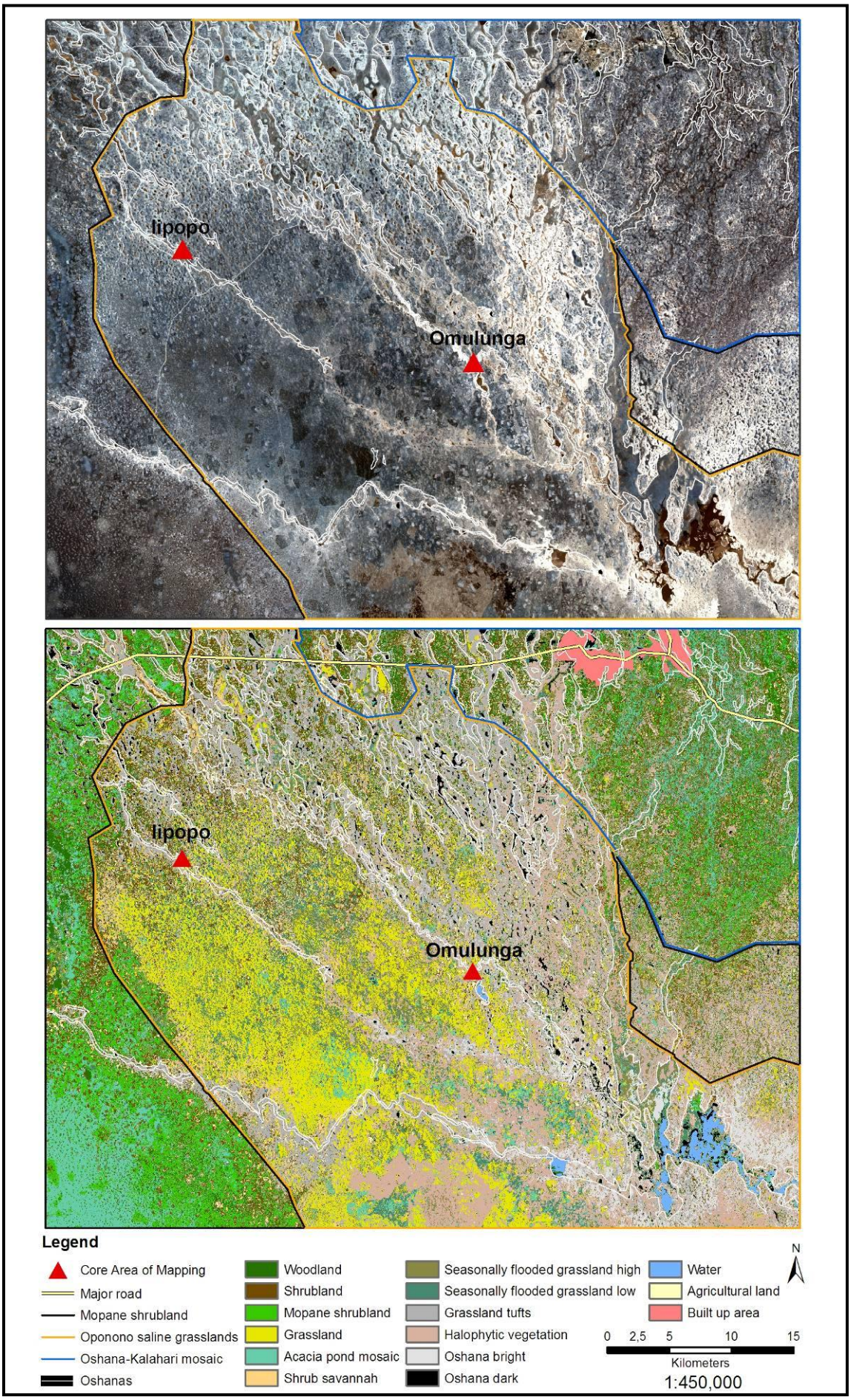

Figure 15: RAPIDEYE (2011) RGB image (above), derived land use/cover classes and outlines of general vegetation units as given by MAWF (2000) for comparison.

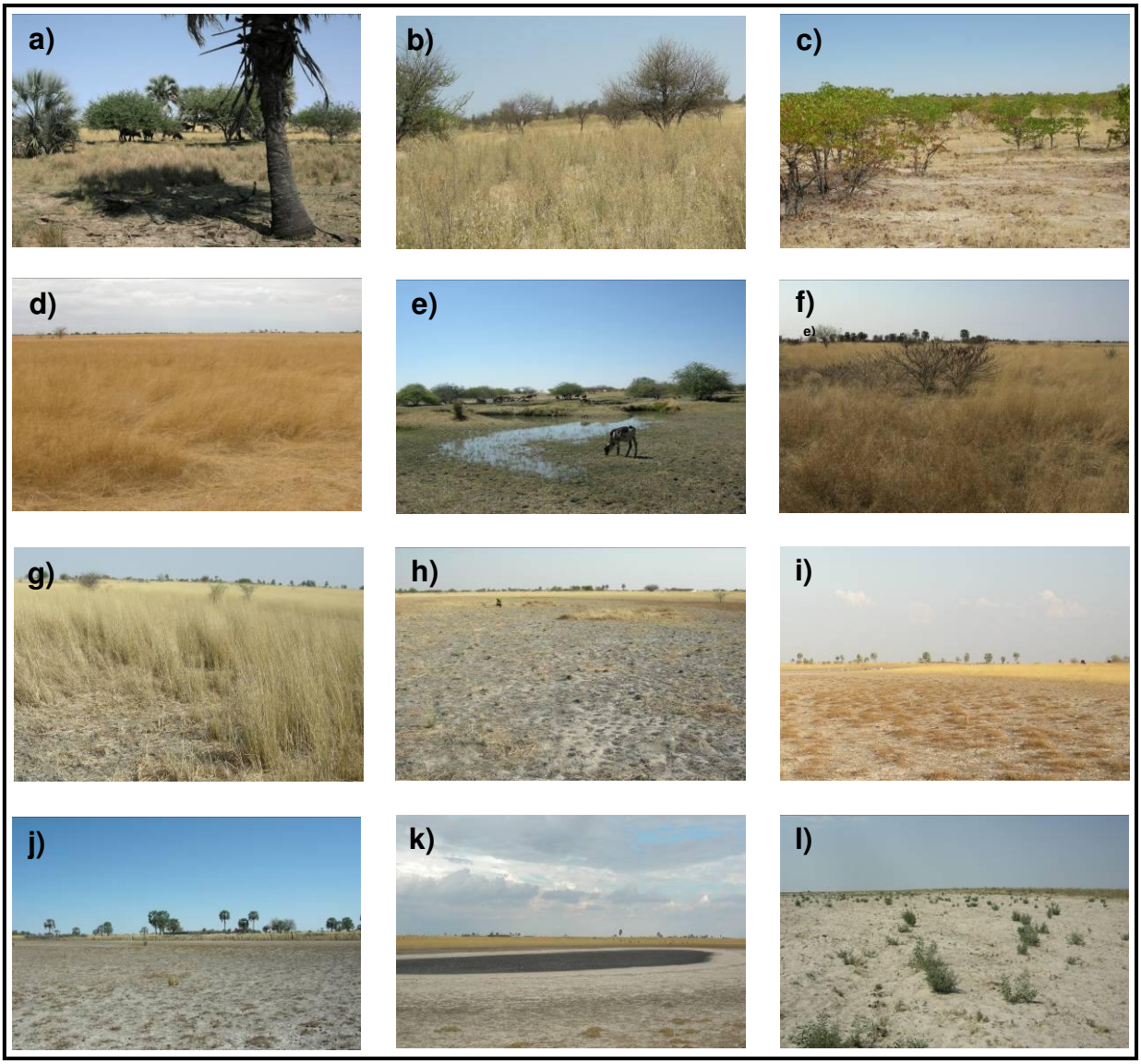

Figure 16: Overview of classified soil-vegetation units: a) *Woodland*: trees higher than 5m mostly in small patches near homesteads, highest relative elevation; b) *Shrubland*: usually 30 – 40% shrubs lower than 5m, highest relative elevation; c) *Mopane shrubland*: 30 – 40% mopane shrubs, higher relative elevation; d) *Grassland*: tall and dense grass without shrubs, highest relative elevation; a) – d) all with vegetation cover of >50%; e) *Acacia pond mosaic*: largely green grass and acacia vegetation next to small water areas, the latter are often hand dug wells tapping the discontinuous perched aquifer, lower relative elevation; f) *Shrub savannah*: grassland with patchy cover and some small shrubs (about 10%), higher relative elevation; g) *Seasonally flooded grassland high*: relatively dense and tall grass in oval to round depressions with darker soils that are characterised by a hard layer, low relative elevation; h) *Seasonally flooded grassland low*: same as g) but short grass with lower areal coverage and no or just occasionally developed hard layer; i) *Grassland tufts*: clustered vegetation besides considerable proportions of bare soil with a characteristic hard layer at some depth; low relative elevation; j) *Halophytic vegetation*: salt tolerant plants growing in clusters, salty depositions at the surface or at some depth, infrequent hard layers on margins, just above the lowest parts in the field; k) *Oshana dark* and adjacent *Oshana bright* areas: the former is situated at the lowermost part of the field with the latter directly above, often water filled (especially in the southeastern parts) or moist even at the end of the dry season, no vegetation; l) *Agricultural* land: cropland before cultivation, highest relative elevation; areal cover for all units is derived from MAYR (2011).

5.2 Climatic Data and Derivates

MODBIL requires a number of meteorological parameters on a daily basis. Essential input data comprise precipitation, maximum temperature, minimum temperature (or mean temperature), minimum relative humidity and maximum relative humidity (or mean relative humidity). If available, rainfall intensity, wind speed, sunshine duration and global radiation could also be utilised to improve the water balance model.

Several different climatic datasets are available in the vicinity of the research area. The nearest official climate station which is operated by the Namibia Meteorological Service (NMS) is located in Ondangwa (NMS 2010) and will serve as main data source for modelling groundwater recharge because it provides the longest existing time series for the region. Unfortunately, this dataset contains some series of missing values and MODBIL does not allow climatic data gaps. To resolve this issue, one approach was to use other datasets to complete missing values via linear regression when proposed preconditions mentioned in ALLEN et al. (1999) were fulfilled. These supplementary data were taken from the Global Surface Summary of the Day dataset (GSOD, NCDC 2011) and originate from two different sites at or nearby the airport of Ondangwa. When no other data was available, gaps had to be determined via interpolation of neighbouring values. The statistical operations are discussed in Chapter 5.2.2.

Finally, measurements of temperature and relative humidity were conducted by the author from 14th October to 17th November by using a “Hobo” micro station (location: Iipopo-triangle in fig. 15). The climate station was erected at a grassland site, which is considered as a representative site for the research area. Although the data covers only a very small time period, it is used to compare climatic conditions in the field with the data from Ondangwa which is approximately 60 km apart.

5.2.1 Climatic Data Comparison

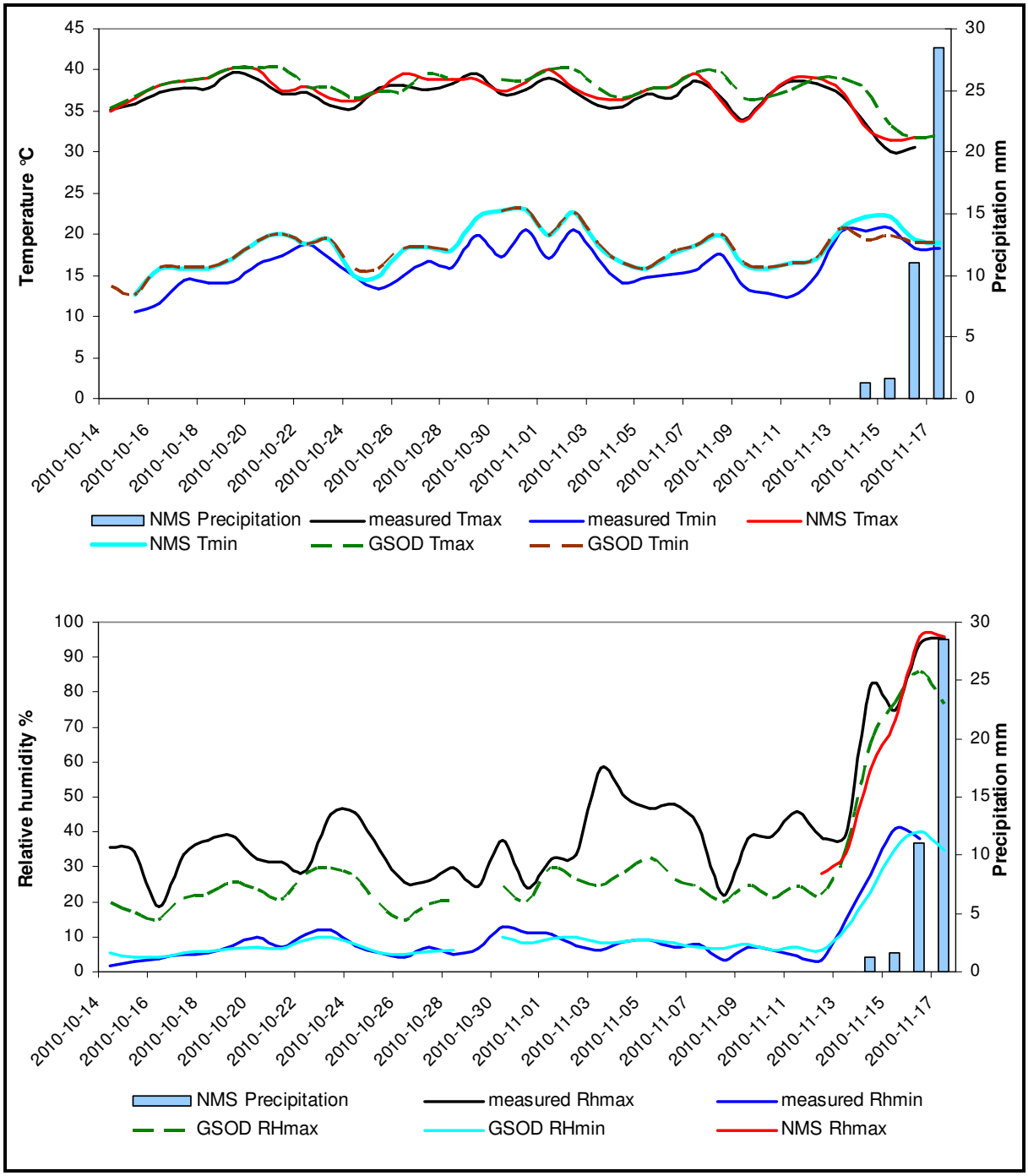

Figure 17: Climate time series comparison of field measured, NMS- and GSOD (station nr. 680060) data. Above: precipitation, maximum and minimum temperatures, below: precipitation, maximum and minimum relative humidity (data source: NMS 2010, NCDC 2011)

Climate measurements taken by the author showed a good agreement with available long term data (Fig. 17). Greatest conformity was observed between measured and GSOD minimum relative humidity with a correlation coefficient (Pearson product

moment correlation) of 0.972, although the latter had to be calculated from dew point data (see next chapter). Comparison of observed and NMS maximum temperatures showed similar values (correlation coefficient 0.966), which indicates very good correlation, whereby the GSOD data did not match that well (correlation coefficient 0.847). Overall, both maximum temperatures and minimum relative humidity data show great affinity in variation and range. Unfortunately, the NMS dataset lacked minimum relative humidity values in the measurement period and therefore no evaluation was possible.

When looking at minimum temperatures, it is visible that GSOD and NMS have nearly identical values but the agreement with the measured data is not perfect, leading to 2°C lower average minimum temperatures in the field. Nevertheless, the time series still shows reasonable conformity (correlation coefficient: 0.906 NMS/ 0.860 GSOD) and the difference may derive from a different heat capacity of the respective microclimate. Regarding maximum relative humidity, nearly no data was available from the NMS station, but present data indicates good agreement. When comparing field data with available GSOD values, then correlation seems relatively high (correlation coefficient 0.919), but field measured mean values are about 10% higher on average. All correlations stated show a significance level of <0.01.

The first precipitation event was observed in the field on 14th November. Although rainfall is spatially variable even over short distances, the NMS station detected rainfall simultaneously. This can also be inferred from the contemporaneous rise of all humidity values with the onset of precipitation. Maximum temperatures showed a significant decrease in the same period. This indicates that precipitation data from Ondangwa may also be representative for the location of the climate station.

In summary, comparison of field measured data and data from other sources leads to the conclusion that only minor differences exist and correlation is generally high. The application of data from Ondangwa for modelling is therefore seen as appropriate. However, the measured time series is short and contains only the beginning of the rainy season. Therefore, the applicability for comparison is limited and a longer time series covering the entire precipitation period would lead to increased confidence and some possibilities of data adaption to field conditions.

5.2.2 Completion of the Meteorological Dataset

The daily meteorological parameters precipitation (mm), temperature (°C) and relative humidity (%) are available for the period from 2003 to 2010 with some data gaps. Precipitation data, also from Ondangwa but at a slightly different site, is also available for a period from 1913 to the beginning of 1993 but incorporates several major gaps especially at the start and the end of the series. Therefore, this data availability defines the feasible modelling period from 2003 to 2010. Periods and quantity of missing data are outlined in appendix 1.

To complete missing values in the NMS series (2010), regression analyses were performed whenever appropriate data from the GSOD (NCDC 2011) dataset was available. According to ALLEN et al. (1998), several conditions should be met for the substitution of missing data with a neighbouring dataset. These are a high R^2 (over or equal 0.7) and a value of the regression coefficient b between 0.7 and 1.3 (ALLEN et al. 1998). Moreover, the datasets should be homogenous, which can be assessed via visual interpretation of the scatter plot of the regression.

Values for the first three months of the time series (until 20 March 2003) were missing in all datasets. Therefore these values had to be completed using mean values of similar months that showed no significant increasing or decreasing trend. This was the case in the years from 2004 to 2007.

Temperature

Regarding the comparison of temperature data between the NMS- and GSOD series, all the above mentioned conditions applied, which indicates good circumstances for deriving missing data from the supplementary dataset (Tab. 2, Fig. 18). Better results and agreement were derived regarding the longer GSOD record from the station with the WMO number 680060. Therefore, this record was preferred for data substitution when possible. All values stated were at a <0.01 significance level.

Parameter	WMO Station Nr.	Regression equation	R - Square
Tmax			
	680060	Treg = 1.467 + 0.930 * Tgsod	0.834
	680130	Treg = 6.725 + 0.816 * Tgsod	0.739
Tmin			
	680060	Treg = 0.081 + 0.991 * Tgsod	0.975
	680130	Treg = 1.012 + 0.894 * Tgsod	0.769

Table 2: Regression terms for substitution of missing temperature values in the NMS data set, whereat Treg – calculated temperature, Tgsod – temperature of GSOD station

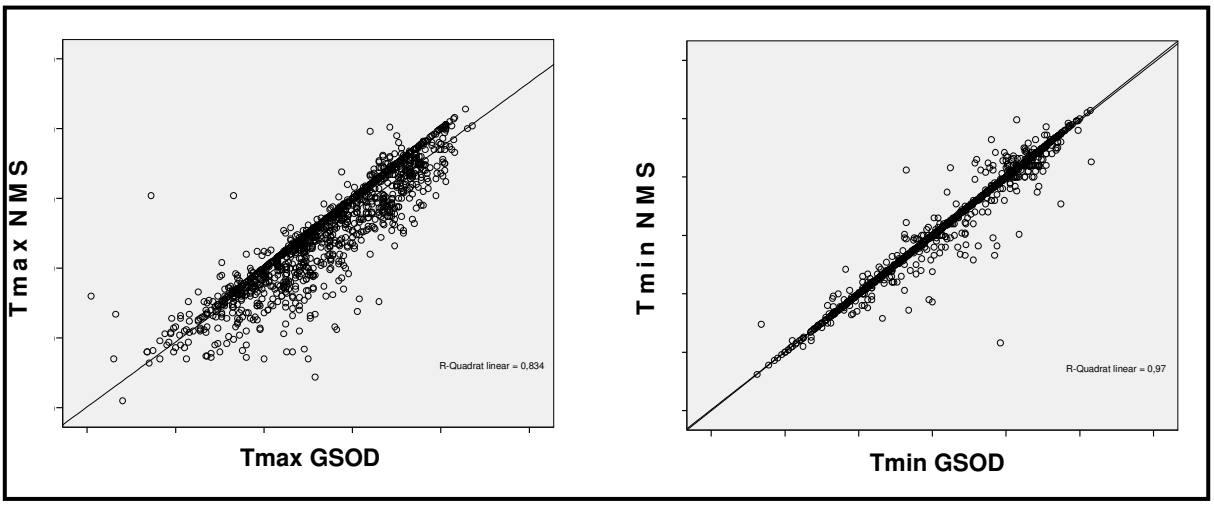

Figure 18: Scatter plots with regression line of maximum temperature (left) and minimum temperature (right) between the NMS- (Y- axis) and the GSOD (X – axis, station 680060) datasets. Homogeneity is assumed when the derivations of the regression line are in about the same range for all values.

Cross validation was performed to test the regression analysis. Two noticeable outliers in the NMS maximum temperature set (both 12°C in contrast to comparable days in the range of 25°C to 28°C) were corrected using arithmetic means of neighbouring days. Still existing, smaller gaps after data completion using GSOD data were filled via calculation of mean values from adjacent existing data. This operation was assumed to be an acceptable solution because the variance of temperature values of successive days is small and most missing values just cover a few (1-4) days.

Relative Humidity

The completion of the relative humidity dataset was connected with some complications. First of all, the NMS humidity time series contained the largest quantity of gaps of all climatic variables. Secondly, the GSOD data for substitution just contained the mean daily dew point temperature and no minimum or maximum values. To get the corresponding maximum and minimum relative humidity values, the following formulas given in ALLEN et al. (1998) were used:

$$es\ (T) = 0.6108 * 2.7183^{(17.27*T/T+237.3)}$$

$$ea = 0.6108 * 2.7183^{(17.27*Tdew/Tdew+237.3)}$$

$$RH_{max} = 100 * ea / es(T_{min})$$

$$RH_{min} = 100 * ea / es(T_{max})$$

where

es (T) = saturation vapour pressure at air temperature T (kPa)

ea = actual vapour pressure (kPa)

T = air temperature (°C)

RH_{max} *= maximum relative humidity*

RH_{min} *= minimum relative humidity*

$es(T_{min})$*= saturation vapour pressure at minimum temperature*

$es(T_{max})$*= saturation vapour pressure at maximum temperature*

This approach leads to reasonable values when the absolute moisture content in the air does not change during the day but introduces errors when moist or dry air is advected over short time periods. But as no other data is available for relative humidity, these uncertainties have to be taken into account. Finally, statistical analyses showed that the circumstances for linear regression were not ideal for the dataset. R^2 for the whole series was at about 0.5 and therefore below the suggested value for data substitution (ALLEN et al. 1998). This was caused by increasing differences in the middle and at the end of the time series. However, the first three years led to good results and an R^2 well above the recommended value. In spite of the mentioned problems and uncertainties which have to be considered, the approach of data derivation via linear regression was also pursued for the relative humidity dataset, as it is one of the most straightforward solutions for data substitution.

Parameter	WMO Station No.	Regression equation	R-Square
Rhmax			
2003 - 2005	680060	RHreg = -0.683 + 0.897 * RHgsod	0.829
2006	680130	RHreg = 24.228 + 0.799 * RHgsod	0.381
2007 - 2010	680060	RHreg = 36.129 + 0.751 * RHgsod	0.58
Rhmin			
2003 - 2005	680060	RHreg = -1.254 + 1.074 * RHgsod	0.814
2003 - 2005	680130	RHreg = -2.838 + 0.862 * RHgsod	0.927
2006	680130	RHreg = 12.013 + 0.625 * RHgsod	0.498
2007 - 2010	680060	RHreg = 24.189 + 1.050 * RHgsod	0.562
2007 - 2010	680130	RHreg = 35.142 + 0.792 * RHgsod	0.509

Table 3: Regression terms for substitution of relative humidity in the NMS data set, with RHreg – calculated relative humidity, RHgsod – relative humidity GSOD station

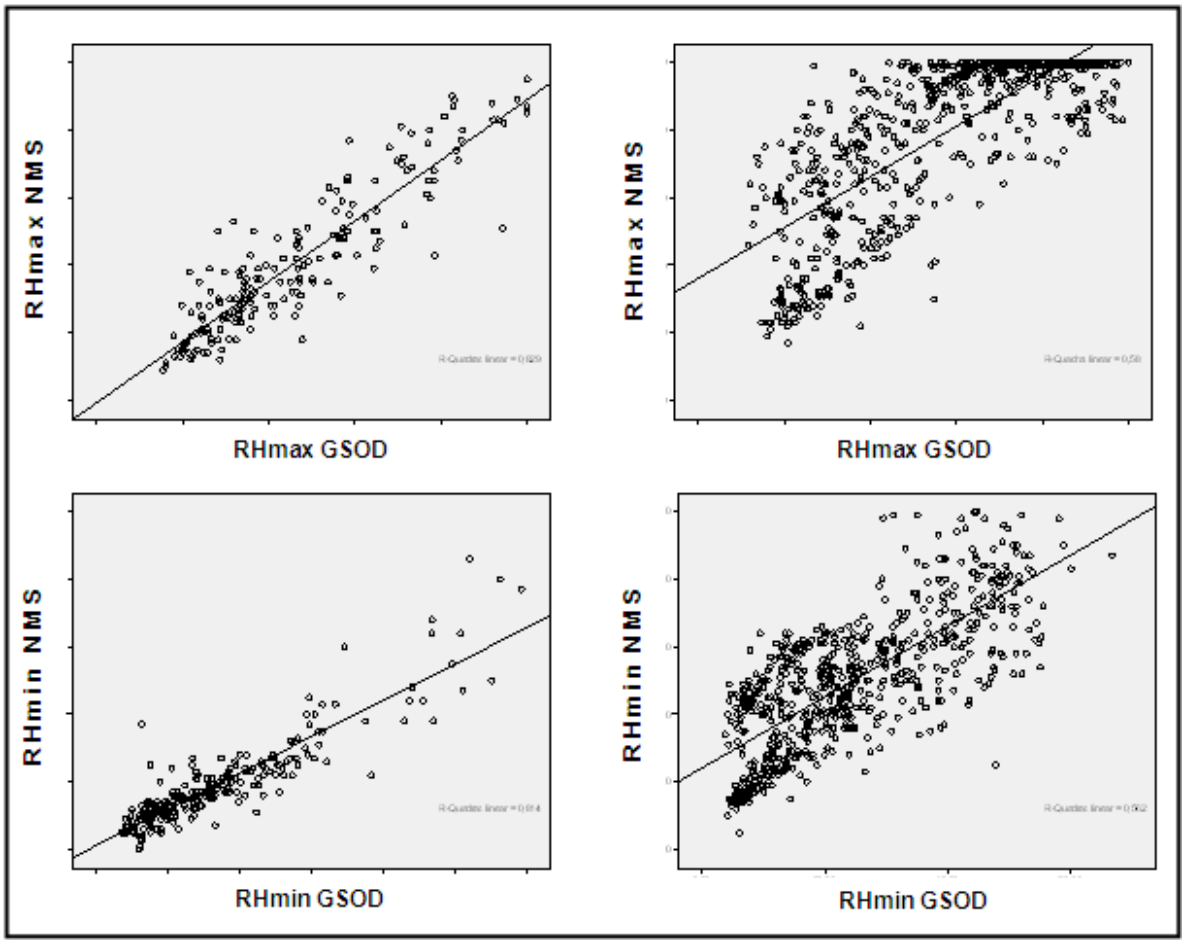

Figure 19: Scatter plots with regression line of maximum (top) and minimum (bottom) relative humidity 2003 - 2005 (left) and 2007 - 2010 (right) between the NMS (Y- axis) and the GSOD (X – axis) datasets.

To keep errors between the years at a minimum and R^2 at a maximum, the data series was divided into different time periods, namely 2003 to 2005, 2006, which lead to a very low R^2 but was just used for the derivation of a few values, and 2007 to 2010. The latter also had an R^2 below the recommended value, but as no other data was available, this inconvenience had to be accepted. Scatter plots of the regression are illustrated in figure 19, regression terms are outlined in table 3. All values stated were significance level of <0.01. The remaining gaps after data completion had to be computed via arithmetic means of neighbouring days. Just as with temperature data, these gaps were small in most cases. In summary, it has to be mentioned that the relative humidity dataset is connected to a set of uncertainties and problems due to the bad data availability. Therefore, the effect of relative humidity changes on modelling results should be evaluated. This was implemented in the performance of a model run with 10% decreased relative humidity values to compare the results with the basic model.

Precipitation

The NMS precipitation dataset for the period 2003 to 2010 contained the smallest amount of data gaps and some of them can be set to a value of zero because they occur during the dry season (May to September) when no rainfall happens. The only remaining data gap which includes March and April 2005 had to be substituted by mean values from the period of the time series that showed no significant trend (2003/2004 – 2007). This is not a very good solution, but there is no other dataset available that leads to comparable results. Initially, the TRMM 3B42 V6 (2010) rainfall estimates should either serve as a data source or as missing data substitution. To evaluate the data, daily mean rainfall values were calculated for the region from 17°45’ S to 18°15’ S and 15°15’ E to 16° E, which covers a little bit more than the research area. Results showed a good agreement with the NMS dataset in the timing of precipitation events, but the quantity of rainfall was considerably less. Yearly mean precipitation amounts of the TRMM data were over 160 mm lower on average. Because of this relatively large inconsistence the usage of the dataset was abandoned. Comparison of TRMM- and NMS precipitation datasets is illustrated in appendix 4.

Not only the amount of precipitation, but also its intensity is important for modelling. It was set to 5 mm per hour. This is the standard value of the model when no other data is available (DÜNKELOH ARMIN 2011, personal communication), which is the case for the research area. Besides, the value fits to the rainfall intensity estimated by rather short field observations. This estimate is derived from the strongest precipitation event with a duration of approximately 6 hours (17th November), which resulted in a total amount of 29 mm according to the records from the NMS station.

Wind Speed

The NMS wind speed dataset showed the largest quantity of data gaps of all climatic variables. Substitution with GSOD would still lead to a significant amount of missing data. Therefore, wind speed was generally set to a value of 2 m/s, which means light to moderate wind according to ALLEN et al. (1998). This is not a very sophisticated approach, but it is a generally recommended value if no other data is available (ALLEN et al. 1998) and analysis of existing data shows that the value comes close to measured data with mean values ranging from 1.27 to 2.10 m/s whereby most are above 1.7 m/s.

5.3 Methods Regarding Soil Sampling and Analysis

MODBIL requires information about the saturated hydraulic conductivity and effective field capacity (=PAW) of every soil-vegetation unit. However, the determination of soil hydraulic properties in the laboratory is labour intensive and time consuming, and a number of different techniques have been developed to estimate them from other soil properties. These methods are generally known as pedo-transfer functions (PTFs, BLUME et al. 2010) and are a widely used method in water balance modelling (e.g. WANKE et al. 2008). Therefore, this approach was also pursued in this thesis and it is based on analysis outlined in the following section.

In addition to qualitative assessment of relief and soil components (e.g. texture, organic content, hydrology) in the field, two representative soil samples per test plot were taken using metal cylinders with a volume of 100 cm³ to evaluate bulk density. These samples were mixed, weighed and homogenized to analyse some chosen samples in the laboratory. These were selected according to their representativeness

for specific soil vegetation units after field work, when an overview of typical soils and their properties was established due to the qualitative assessment. All samples were taken in depth ranging from 10 cm to 15 cm. On the one hand, this depth was chosen because it is well within the root zone of grasses (KNOOP and WALKER 1985, WILLIAMS and ALBERTSON 2004) which cover extensive parts of the area, on the other hand it was chosen for practical reasons. Furthermore, soil moisture for all soil vegetation units was measured by a ThetaProbe soil moisture sensor from UMS to derive the remaining water content at the end of the dry season and to compare the results of PTFs with field conditions.

5.3.1 Laboratory Analysis

The laboratory analysis comprised those soil properties relevant for estimation of soil water characteristics using PTFs. These include texture, salinity, organic matter and bulk density (SAXTON and RAWLS 2006, DONATELLI and ACUTIS 2001). Air dried bulk density was determined with all soil samples after field work, as this simple analysis can be carried out without laboratory equipment and remaining water content was subtracted after the oven drying of representative samples.

The first step of laboratory analysis should resolve the question if there are considerable differences of soil properties in all mapped units or if their hydrologically important characteristics vary more due to relative elevation as indicated by qualitative analysis in the field. Therefore, laboratory analyses were conducted with 2 samples per test unit. More samples were tested for determination of electrical conductivity, because of its higher variation. Results showed that there were only small differences in texture within soil-vegetation units (appendix 6) and so the number of samples for additional analysis (clay and silt fractions) was reduced. Sample locations are presented in appendix 5.

Electrical Conductivity

Electrical conductivity is a widely used index for concentration of ionized solutes (RHOADES et al. 1999) and is analysed to determine salinity which influences the osmotic potential of the soils (BLUME et al. 2010). Therefore, this parameter is used in some PTFs to estimate the wilting point (SAXTON and RAWLS 2007).

A widely used standard method for salinity assessment is the determination of electrical conductivity in saturated soil paste extracts (RHOADES et al. 1999). Consequently, this value is also used in PTFs (SAXTON and RAWLS 2007). However, another approach was necessary for this study because of the large amount of soil needed for the method (200 – 400 g, RHOADES et al. 1999) which was not available. Therefore the fixed-extraction ratio method was chosen according to the Austrian standard ÖNORM L 1092 2005 03 01. An advantage of this technique is its easier reproducibility compared to the saturated paste method (SONMEZ et al. 2008). However, although this is a convenient method if the amount of soil sample is limited, the higher water-soil ratio may lead to relatively higher salt content compared to the standard method (US SALINITY LABORATORY STAFF 1954).
Hence, electrical conductivity was measured according to the following procedure: 100 ml distilled water were added to 10 g of air dried soil and hand shaken. Afterwards the mixture was left to rest overnight and again shaken for 1 hour. Finally, the solution was filtered through a micropore filter and measured. As the international standard is the electrical conductivity at 25° (RHOADES et al. 1999), results were adjusted using the generally accepted temperature-coefficient (ft) of RHOADES et al. (1999):

$$ft = 1 - 0.20346\,(T) + 0.03822\,(T^2) - 0.00555\,(T^3)$$

where

T = [temperature in degrees Celsius - 25] /10

*Electrical conductivity at 25°C = conductivity at measured temperature * ft*

(RHOADES et al. 1999, p. 6)

Finally, the electrical conductivity values derived by the fixed extraction ratio method had to be converted to corresponding values for saturated soil paste extracts for comparison reasons and for their use in PTFs of SAXTON and RAWLS (2007). As electrical conductivity decreases approximately twofold with a likewise increase in soil to water ratio (SONMEZ et al. 2008), the values for a 1:5 ratio can be estimated

by multiplying the 1:10 values by two. To derive saturated past conductivity values from measured data, the following regression equations without intercept presented by SONMETZ et al. (2008) were utilised:

Sandy soils	$ECe=7.98\ EC_{1:5}$
Loamy soils	$ECe=7.62\ EC_{1:5}$
Clayey soils	$ECe=7.19\ EC_{1:5}$

Where

ECe = electrical conductivity of saturated paste extract, $EC_{1:5}$ *= value for 1:5 water ratio* (SONMEZ et al. 2008)

Organic Matter

Organic matter was analysed using the combustion method that follows the Austrian standard ÖNORM L 1079 1999 04 01. This approach is based on the assumption that all carbon loss is organic origin and inorganic components are negligible, which is the case for the soils of the research area, as no sample showed a reaction to the hydrochloric acid (HCl) test. Furthermore, dissociation of inorganic carbonates should not occur below temperatures of 650°C (BLUME et al. 2010). Another inaccuracy may result from the loss of structural water in the clay fraction, which affects a minor part of the samples. To deal with that issue, a correction factor was tested. HOWARD (1964) states a 2% weight error for fine textured soils. This factor was applied for clay soil (e.g. Oshana dark). However, comparison of measured water content and water content derived from PTFs (where organic matter is one input variable) was in better agreement without the correction factor. Therefore, it is likely that most of the structural water is lost during oven drying so this approach was abandoned.

The analysis was carried out with 20 g oven dried soil (105°C) which was burnt in a muffle furnace at 550°C for 4 hours, cooled in a desiccator and then weighed. Organic matter was finally calculated as loss by combustion using the following formula:

$$CL = (m_b - m_c) * 100 / (m_b - m_a)$$

where

CL = combustion loss as % mass

m_a = mass of sample vessel

m_b = mass of sample vessel and oven dried sample (105 °C)

m_a = mass of sample vessel and combusted sample (550 °C)

(according to ÖNORM L 1079)

Texture

Because of the strong correlation between texture and water holding capacities of soil, texture is the most important property of PTFs to estimate the soil hydraulic properties (SAXTON and RAWLS 2006, DONATELLI and ACUTIS 2001, BLUME et al. 2010). Determinations of texture classes encompass two methods: the sand fraction was analysed using wet sieving technique. Silt and clay fractions were obtained via the Köhn pipette method (modified ÖNORM L 1061-2) which is based on sedimentation times of solid particles. Soil samples were treated with sodiumphyrophosphate $Na_4P_2O_7*10H_2O$ to disperse aggregates and with hydrogen peroxide H_2O_2 to remove organics.

There are various classification systems for soil texture. As analyses were carried out at the laboratory of the University of Vienna, the Austrian/German system was chosen because of the availability of appropriate laboratory equipment (e.g. sieves). Therefore, particle size distributions of sand comprise coarse sand (630 µm – 2000 µm), medium sand (630 µm – 200 µm) and fine sand (200 µm – 63 µm). Particle sizes of the silt fraction cover coarse silt (63 µm – 20 µm), medium silt (20 µm – 6 µm) and fine silt (6 µm – 2 µm). The clay fraction contains particle sizes below 2 µm. Fractions above 2 mm were virtually nonexistent. Since many PTFs use the international FAO/USDA (SAXTON and RAWLS, 1986, 2006, 2007) classification system, interpolation was applied assuming log-normal distribution of the particle sizes following the method by DONATELLI and ACUTIS (2001).

5.3.2 WRB Classification and Results

Laboratory and field results were used for soil classification according to the World Reference Base (WRB, FAO 2006) and assigned to each vegetation unit (Tab. 4, map: appendix 5). Due to differences in soil parameters, some additional demarcation had to be made within the groups. All higher parts of the field, e.g. *Woodland, Shrub savannah, Shrubland, Mopane shrubland, Grassland* as well as *Agricultural* areas can be classified as Arenosols (cf. RIGOURD and SAPPE 1999). Symptomatic features are a high hydraulic conductivity, a low organic matter and the lowest electrical conductivity which implies nearly no salinity. This in turn may be a consequence of dissolved solids which were washed out in these permeable soils.

The soils of lower areas differ more, especially due to hydrology and therefore salt content. Soils on *Seasonally flooded grassland low* sites had an increased electrical conductivity and slightly lighter texture as areas above and may also be identified as Arensols, with a tendency to sodicity whereby some may be in a transitional stage to Solonetz. The soils at grassland tuft sites show a high electrical conductivity in the hard layer with lower values at the softer surface horizon (mostly above 10 - 5 cm, measured, not included in mean). Furthermore, prepared soil solutions for conductivity measurements showed a distinctive cloudiness, which is a good indicator for sodicity (FAO 2005). A natric horizon, characterised by a darker colour and a texture of loamy sand or finer compared to much coarser particle sizes in the overlying horizon (FAO 2006), could be clearly distinguished in these soils. The natric horizon mostly appeared at about 10 cm depth. Usually these soils also showed a light coloured albic horizon on top of those. In summary, Solonetz presents itself as the predominant soil on *Grassland tuft* areas, which is prone to water logging because of the dispersion of clay particles (Fig. 20, see chapter 2.4). In addition to the natric horizon, salic horizons may also be found in some depth. If the soils are saltier and connected to a shallow water table, also sodic Solonchaks or Solonetz-Solonchak transitions may be found, but always with a clayey hard pan (cf. BATJES 2004, RIGOURD and SAPPE 1999). Seasonally flooded areas with high grass could also be described as Solonetz, because they also showed a hard natric horizon, usually finer in texture (mostly clay) and without a coarser horizon above.

Furthermore, electrical conductivity and therefore salinity was much lower, which may be an explanation for increased plant growth on these units. On areas designated as *Acacia pond mosaic*, soils were similar but with increased organic matter and clay content in account with a lower silt fraction. Vegetation soil units that lie just above the lowest parts of the field (*Halophytic vegetation, Oshana bright*) and are moistened frequently by flood water or groundwater show a distinctive salic horizon, with a layer of soluble salts on the surface or subsurface and very high conductivity values of 15 dS/m or more or 8 dS/m or more if pH is over 8,5 (FAO 2006). On areas where the salic horizon was below 10 – 15 cm – which was true for many *Halophytic vegetation* units (Fig. 21) – conductivity values were much lower (leading to a mean value of about 6 ds/m) because of the soil sampling depth, but a salic horizon was present. The mentioned soils had the highest conductivity values and only salt adapted plants are able to grow here. Regarding *Oshana bright* units, extreme surface salinity and repeated flooding lead to an environment where no plants are able to grow.

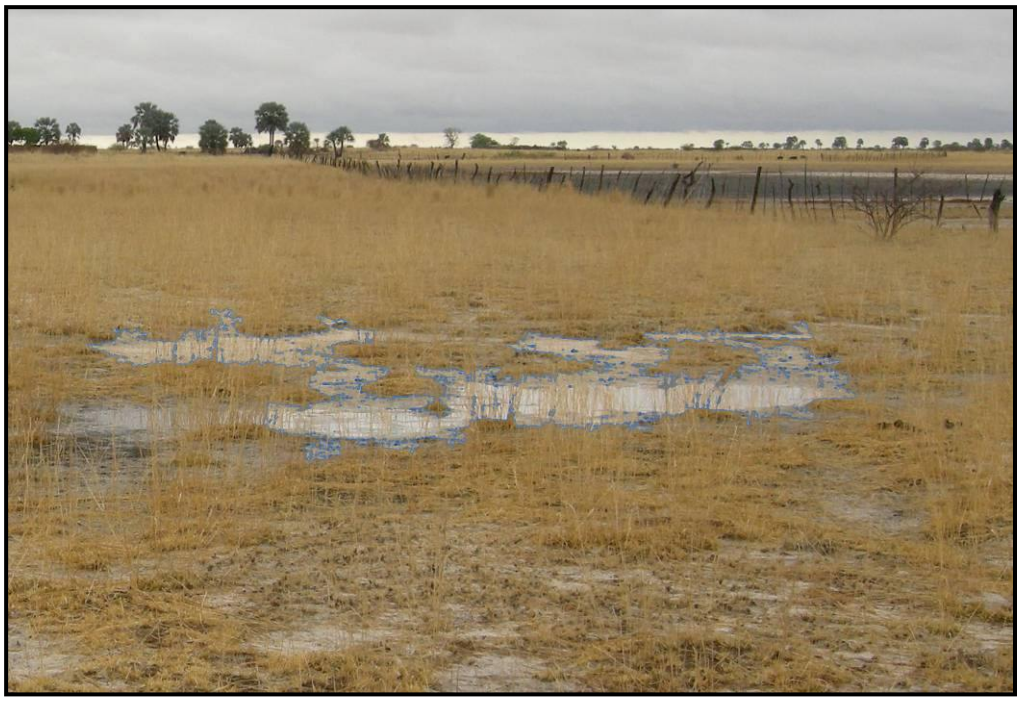

Figure 20: Water logging on *Grassland tuft* area after first precipitation event in November 2010, highlighted by light blue outline

Some of the *Halophytic vegetation* sites also show aspects of sodicity with tendencies to hardening at higher peripheral areas of the vegetation unit. This may be due to lower water table in some years, followed by desalination with

simultaneous chlorine outwash and enrichment in sodium ions, which would mean a transition to sodic Solonchak or Solonetz (BLUME et al. 2010).

Finally, the lowermost part of the field, which is mostly occupied by *Oshana dark*, can be classified as Vertisol. This can be concluded from noticeable cracks resulting from shrinking (Fig. 22) and a very high clay content which is typical of these soils (clay content ≥30% with thickness ≥15cm, FAO 2006, BLUME et al. 2010). Another attribute of these soils with regular moisture supply is a high electrical conductivity and therefore, high salinity. Finally, a hard, relatively impermeable layer is found on top of most dark Oshanas. Water areas are also classified as Vertisols, as remaining surface water is only found in *Oshana dark* at the end of the dry season.

Figure 21: Excavation on *Halophytic vegetation* site. The salic horizon can be found about 40cm below the surface (upper margin indicated by white lines)

The soil classification contributes to the definition of some model parameters. Some processes that are induced by sodicity like water logging through dispersed particles are not fully captured by texture or hydraulic properties derived by PTFs. Therefore, these effects have to be simulated otherwise. MODBIL allows a definition of sealed surfaces which is taken in this thesis to represent impermeable sodic layers. The units affected most strongly by this phenomenon are *Grassland tuft* areas and

Vertisols; their sealed surfaces are set to a value of 50% to represent their water retaining properties. This is based on the assessment of the mean additional water cover of respective areas after the first precipitation events. Acacia pond mosaic sites revealed the same tendency, but a lower value of 30% was set because the effect was not as pronounced and present vegetation may increase permeability. *Seasonally flooded grassland high* areas showed hard sodic layers as well but the characteristically dense vegetation may decrease water logging, so sealed surfaces were defined to cover 25%. *Halophytic* and a *Seasonally flooded grassland low* units showed only patchy developed impermeable layers. To take this into account, a value of 10% of sealed surfaces was estimated.

Figure 22: A typical Vertisol in one of the *Oshana dark* areas. On the fringe of those, *bright Oshana* units can be found. They show a clearly visible white salic horizon on the surface which identifies the soil as Solonchak.

Laboratory derived soil parameters are summarized in table 4. Single samples and results are listed in appendix 7. There is some generalised information of soil properties available in BATJES (2004), which is used for comparison. Two of the reference profiles given there are situated in the northern part of the research area, namely a Pelli-Calci-Vertisol NA-OWA-15 and a Calci-Sodic-Solonchak NA-OWA-22. The latter is situated in the transition of the *Halophytic vegetation* to the *Grassland*

tuft class according to the supervised classification results and therefore in accordance with assigned WRB groups for respective units. When comparing the analysed textures, there is a better conformity between *Grassland tufts* and the profile which shows similarities to Solonetz, as indicated by the sodic qualifier. Electrical conductivities are very different, though and much higher in BATJES (2004), even when compared to vegetation units with Solonchak soils. Textures of the latter show a better match of results for a profile outside the research area (NA-OWA-27); other values (organic carbon, bulk densities) are in a sensible range too.

The reference profile for the Vertisol lies just outside of a classified *Oshana dark* area and shows a reasonable match as well. Lower clay values may be due to the profiles location at the rim of the Oshana. However, it has to be mentioned that no calcic-conditions were observed on the author's own soil analysis, because there was neither a calcic horizon present nor a positive reaction to the HCl-test in any of the samples. As these were taken in shallow depths, a calcic horizon may be present in deeper layers anyhow. All other soil parameters in BATJES (2004) are derived from profiles located some distance outside the research area. In spite of this, mostly similar values are recognised.

Vegetation Units / Profile #	Soil (WRB)	Sand %	Silt %	Clay %	Corg mass %	Bulk density	EC ds/m
Woodland Shrub savannah Shrubland Mopane shrubl. Grassland Agricultural land	Arenosol I	92	4	4	0.34	1.54	0.5
Seasonally flooded grassland low	Arenosol II	86	6	8	0.72	1.68	1.1
Grassland tufts	Solonetz I	82	6	13	0.82	1.55	4.8
Seasonally flooded grassland high	Solonetz II	66	12	21	1.56	1.43	1.1
Acacia pond mosaic	Solonetz III	66	3	31	2.64	1.41	1.5
Halophytic vegetation	Solonchak I	91	3	6	0.16	1.54	6
Oshana bright	Solonchak II	90	6	4	0.32	1.53	19.5
Oshana dark	Vertisol	49	7	44	2.3	1.3	4.6
NA-NAM-445*	Arenosol	94	4	2	0.17	1.5	0.1
NA-OWA-22*	Solonchak I	81	7	12	0.31	1.51	149
NA-OWA-27*	Solonchak II	92	1	7	0.26	1.54	128.9
NA-OWA-118*	Solonetz	89	5	6	0.24	1.4	7.5
NA-OWA-15*	Vertisol	58	11	31	0.34	1.26	6.4

Table 4: WRB classification of vegetation units and assignment of averaged soil properties. Profiles labelled with asterisks in the lower section show values given in BATJES (2004) for comparison.

5.3.3 Pedo-transfer Functions and Derivation of Soil Hydraulic Properties

A large number of PTFs exist and different methods may lead to variable results and accuracy in soil hydraulic property determination. Evaluation of PTFs is discussed in several papers (e.g. BUCCIGROSSI et al. 2010, GIVI et al. 2004, TIETJE and HENNINGS 1996) with different conclusions and the selection of a PTF that is most compatible to the soils of the research area lies outside the scope of this study. Two different approaches will be applied and evaluated by comparing them to soil moisture measurements carried out in the field. One approach is the method developed by SAXTON et al. (1986, extended by SAXTON and RAWLS 2006) which is also used by similar other studies (WANKE et al. 2008) and shows good results in saline soils (ABBASI et al. 2011). Another method is suggested by GIVI et al. (2004), who rate the "British Soil Survey" as one of the most appropriate methods in their study. It has to be mentioned, however, that PTFs may be susceptible to errors, although some sources suggest that better results may be derived in sandy soils (TIETJE and HENNINGS 1996), which is the predominant texture in the research area.

Evaluation of results from PTFs confirmed this statement. The basis for the validation is the assumption that the moisture content before the onset of the rainy season is equal to the moisture content at the wilting point because the soil dried out for several months and plants consumed all extractable water. Moisture content at FC is not applicable for a complete evaluation, because only a few measurements were made after the precipitation events and many soils may either be oversaturated or have not reached FC under these circumstances. Therefore, the calculated water content at the wilting point (WP) was compared to the residual moisture content before rainfall, excluding areas that were influenced by standing water. Values were determined with the software products of DONATELLI and ACUTIS (2001) for the "British Soil Survey Topsoil" method and the "Hydraulic Properties Calculator" from SAXTON and RAWLS (2007). Arenosols showed a very good agreement with results derived from using the method of SAXTON and RAWLS (2006) with a difference of only 0.5 mm/m. The "British Soil Survey Topsoil" method overestimated the WP by a value of 57.5 mm/m compared to measurements. Vertisols showed reasonable

results as well, with a calculated water content at WP of 281 mm/m (by SAXTON and RAWLS 2006 method) and a measured value of 299 mm/m, but this value is not a robust mean, because only a few dark Oshanas were dry at the sampling depth. The "British Soil Survey Topsoil" method showed a WP of 250 mm/m. The other soils showed increasing derivations from calculated values, generally with a much higher WP. This was especially true for the "British Soil Survey Topsoil" method, which was abandoned for this reason and because of the large differences in the Arenosols.

Measured residual moisture values and soil hydraulic properties calculated by the technique of SAXTON and RAWLS (2006) are illustrated in table 5. As mentioned, some soil-vegetation units had much lower moisture content at the end of the rainy season as given by the calculated WP. Since WP is a reference value that is valid for most cultivated plants, it may be much lower for a vegetation which is well adapted to the semi-arid environment (e.g. halophytes) and which, therefore, is able to extract water at high soil moisture tensions as well (BLUME et al. 2010). On clayey or salty soils where the differences are greatest, only these adapted plants are able to grow, which may be one explanation for the results. However, possible errors either in the PTFs or in soil water measurements cannot be excluded. Many clayey soils developed a very hard layer making the insertion of the soil moisture probe extremely difficult (affects the connection to the soil matrix) and sometimes impossible. The greatest discrepancy occurred in *Seasonally flooded grassland high* areas , followed by *Acacia pond mosaic* sites and strongly salt affected soils. Obviously, halophytes extract more water than ordinarily expected, as outlined above. *Oshana bright* areas even show a WP higher than the FC due to the salt content, which is not possible.

The mentioned disagreement between calculated and measured values is also noticeable in other studies (WANKE et al. 2008), often with greater discrepancies than those discussed here. But as the effective field capacity or PAW (FC minus WP multiplied by rooting depth) is an important modelling parameter, calculated uncertainties in the WP cannot be accepted. Therefore, this thesis follows the approach by WANKE et al. (2008), which determines PAW as calculated FC minus measured residual water content. This method is reasonable because measurements represent maximal depletion of the water storage capacity in the soil before the rainy season and so these measurements define its lower range.

Vegetation Units	FC mm/m	WP mm/m	Moisture meas. mm/m	PAW calc. mm/m	PAW meas. mm/m	Ks m/s
Woodland Shrub savannah Shrubland Mopane shrubl. Grassland Agricultural land	63	23	23	40	41	3.57E-05
Seasonally flooded grassland low	84	62	29	22	55	1.48E-05
Grassland tufts	144	95	63	49	81	1.27E-05
Seasonally flooded grassland high	243	147	31	96	212	7.19E-06
Acacia pond mosaic	315	214	173	101	142	2.29E-06
Halophytic vegetation	72	63	23	9	49	2.81E-05
Oshana bright	69	>69	23	0	47	2.45E-05
Oshana dark	399	281	299	118	100	8.75E-07

Table 5: Soil water characteristics calculated with the software by SAXTON and RAWLS (2007) and mean measured moisture content previous to the first precipitation event (=Moisture meas.). Plant available water is derived by two different methods for comparison: calculated FC – calculated WP (PAW calc.) and FC – Moisture meas. (PAW meas.). The latter is used for modelling. (FC = field capacity, WP = calculated wilting point, Ks = saturated hydraulic conductivity)

The previous discussion shows that the values derived by PTFs are connected with some uncertainties that have to be taken into account, especially as some parameters cannot be verified without intensive laboratory analysis (e.g. hydraulic conductivity). However, comparison of field measured parameters with calculated results leads to the assumption that some soils are represented very well as far as the WP is concerned. Given that better agreement was determined in sandy soils

which cover the greater part of the research area, the applied method appears acceptable.

As far as FC is concerned, the results of PTFs had to be used for modelling and moisture measurements after the precipitation events had been used to assess an approximate error range. Water logging soils were excluded because they represent oversaturated conditions due to standing water or cause extremely variable results. On sandy soils, measurements which were conducted about 3-5 hours after the strongest rainfall showed mean soil water content of 99 mm/m (mean of 7 sites). This indicates an increased storage amount of about 30-40 mm compared to calculated FCs. This implies that PTFs may not represent FC values sufficiently, but as stated before, moisture measurements after precipitation are scarce and connected to uncertainties as well, especially on soils with water logging properties or access to the water table. To evaluate the effect of this inaccuracy, one model run with additional 30 mm effective FC will be conducted. Results of moisture measurements for individual plots are listed in appendix 8.

5.4 Derivation of Land Use Parameters

Several important parameters for each land use class/vegetation-soil unit have to be established for a model run. These encompass interception storage, proportion of areal vegetation cover, ETsec, percentage of sealed surfaces, effective rooting depth, crop coefficient for ET (kc, kcb in ALLEN et al. 1998), factors for hydraulic conductivity adjustment (not applied), macroporosity, fraction of soil water usable by plants before water stress (factor p in ALLEN et al. 1998), albedo, effective vegetation height, leaf area index and (bulk) surface resistance (UDLUFT and DÜNKELOH 2009). Obviously, some parameters are only needed if a related modelling approach is pursued (e.g. original Penman-Monteith or FAO Penman-Monteith equation).

Areal vegetation cover for each test area was determined in the field by MAYR (2011) and respective means were assigned to each land use class. For *Agricultural land*, monthly cover values were assessed because field derived values are related to the season before cultivation. A maximum cover of 50% was estimated for

January, February and March and 20% for other months based on illustrations in MENDELSOHN et al. (2000). A factor for ETsec was set for units which had water access until the end of the dry season. This was set to a value of 1 for *Water* areas, which means that evaporation is not limited and equals ETpot. *Acacia pond mosaic sites* contained some water areas and the vegetation mostly has access to water the whole year. Therefore, a value of 0.5 was assumed in order to take this into account.

Effective rooting depth, the vertical zone where the majority of roots can be found, is a very important modelling parameter because it defines the soil column where water can be extracted by plants. The parameter was determined in the field for shallow rooting vegetation units (like grasses) and estimated from different literature sources for deeper reaching plants. Soil profiles revealed that most roots occur within 30 cm in grassy vegetation, which is in good agreement with other studies (KNOOP and WALKER 1985, SHORROKS 2007, WILLIAMS and ALBERTSON 2004). For areas with woody vegetation and several Acacia species, rooting depths were set according to information given in KNOOP and WALKER (1985), SKARPE (1996) and SHORROCKS (2007) to a range of 50 cm to 150 cm. Depth for *Mopane* areas was set at 60 cm as stated in BURKE (2006). Regarding *Agricultural land*, rooting depths of 40 cm were assigned as it is the average for millet (ALLEN et al. 1998). To assess the weight of this parameter, one model run will be conducted with 30 cm increased effective rooting depths. As this is an excessive amplification for many areas, large alterations for modelling can be expected.

Factor p was assigned to the average value of 0.5 (ALLEN et al. 1998) for all vegetation units in the basic model run. As p factors are only given for agricultural crops in the respective reference, they may vary for the vegetation of the research area. To evaluate the effects of changed factors on the water balance, one model run was conducted with an increased value of 0.6 for vegetation with grassland (as given for pasture in ALLEN et al. 1998) and 0.7 for *Halophytic vegetation* because they are generally adapted to decreased water availability and may therefore show a higher threshold before suffering moisture stress.

Effective vegetation height or zero plane displacement height was calculated as two-thirds of the average plant height according to ALLEN et al. (1998). Plant height is

estimated from field observations. The value of (bulk) surface resistance was set to 100 as a typical value for savannah vegetation (ALLEN et al. 1996). There is another method to compute surface resistance from LAI, but this approach does not work properly with LAI values below 1.

5.4.1 Factor for Macroporosity

A part of the water originating from precipitation or flooding runs past soil water stored in micropores along cracks and cavities in the soil and is therefore called macropore – or preferential flow (BLUME et al. 2010). Thus, this quantity is an important part of the infiltration process. MODBIL deals with the aspect via calculating bypass flow depending on a specific factor for macroporosity (DÜNKELOH Armin 2011, personal communication). The macroporosity factor is difficult to obtain and depends on many influencing variables like root densities and depths, agricultural practices, rate of soil compaction and other natural conditions (BRAUN 2002). BRAUN (2002) states high factors of about 10 for forested areas and average factors of 5 for other areas. A factor of 1 implies no macroporosity. As there is no basic straightforward way to determine the factor, it has to be assessed on conditions that can be observed in the field and the lab. Hence, factors applied were 5 for sandy soils containing shrubby vegetation (roots), 3 for sandy grasslands and no macroporosity for sodic soils with hard pans (*Tufts, Seasonally flooded*, water logged areas), because dispersed clay particles block larger pores in sodic soils when wet (BLUME et al. 2010). Granted that sodic or clayey soils also develop cracks when dry which would lead to increased macroporosity, but they close with increasing moisture. Furthermore, almost all Oshanas on Vertisols had a wet subsurface, hence there were no cracks there. However, resulting from mentioned difficulties in the determination of macroporosity, modelling of macropore flow is connected with several problems and uncertainties (DÜNKELOH Armin 2011, personal communication).

5.4.2 Leaf Area Index

The leaf area index (LAI) is a dimensionless representation of the one-sided leaf area per unit ground area (ALLEN et al. 1998) and may present a basis for several modelling steps. If the FAO Penman-Monteith equation (ALLEN et al. 1998) is used to compute ETpot, LAI is incorporated into a series of formulas to estimate the basal crop coefficient kcb or LAI could be taken to estimate surface resistance from active LAI (ALLEN et al. 1998). In this thesis, both of these approaches were not followed because the low LAI (mostly <1) would lead to unnaturally high surface resistance values (as it is the divisor in respective formula) and to extremely low kcb values, which is problematic as this factor is an extremely important parameter in the FAO-Penman-Monteith method. By using the original Penman-Monteith approach, determination of kcb is not necessary, which may result in lower uncertainties for the determination of ETpot. But the LAI is utilised to estimate interception which is an important component of the water balance calculation (see next section). Therefore, LAI values had to be determined for the whole year.

LAI was measured in the field by MAYR (2011) using the LI-COR Biosciences "LAI 2200" device. As vegetation growth did not start at the time of the measurements, they represent the minimum LAI in the dry season. To estimate the seasonal LAI variation during the whole year, measured data were compared to remote sensing data of the MODIS MOD15A2-LAI product (NASA LP DAAC 2011). Monthly values were computed using a factor derived from the MODIS 2010 raster time series of the research area (NASA LP DAAC 2011). The factor was calculated as averaged MODIS LAI value for respective month divided by mean MODIS values in November. MODIS values are averaged over eight day periods which means that November consists of measurements from 25th October to 25th November, which is mostly simultaneous to the time of field work. The procedure is connected with some problems that mainly originate from the coarse resolution of the MODIS product (1000m) in contrast to the more differentiated vegetation units that were classified (30m). Additionally, some problems may derive from dense cloud cover during the wet season, affecting satellite-borne measurements. When comparing the measured LAI values with MODIS values of November (Fig. 23), it is visible that the

discrepancy is small for vegetation that is mostly concentrated on well defined, large areas like *Mopane shrubland*.

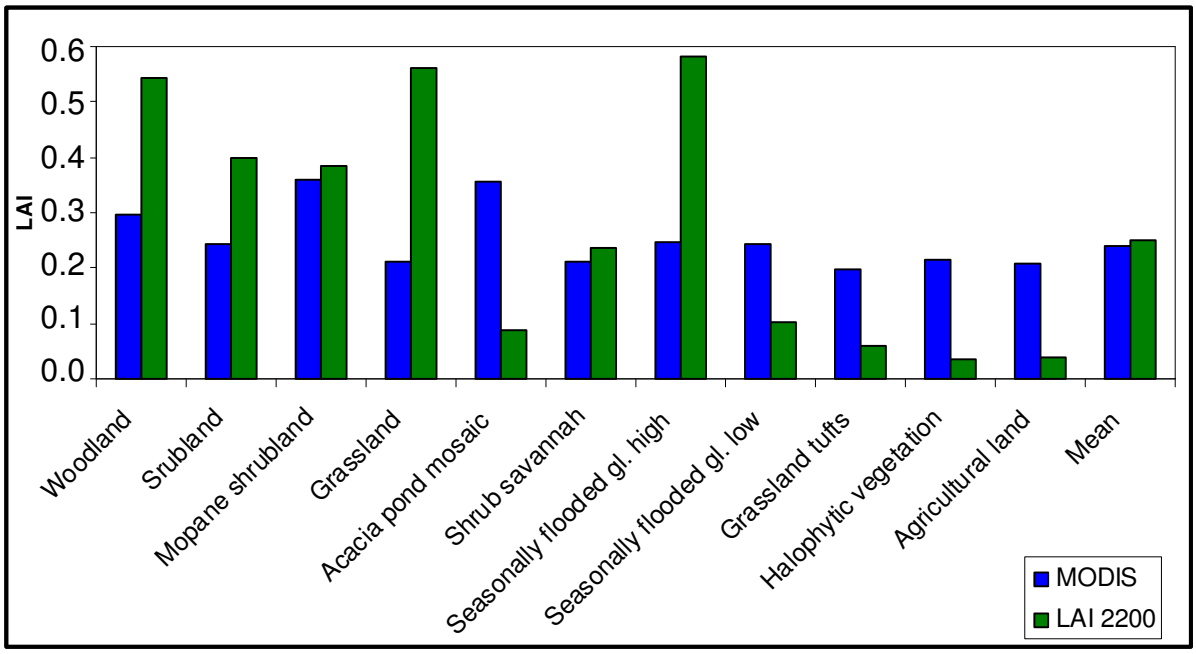

Figure 23: Comparison of mean measured and MODIS LAI values for each soil-vegetation unit in November (MODIS source: NASA LP DAAC 2011).

However, significant differences occur when means for many other units are compared as patches of different vegetation and non-vegetated areas are all averaged to one large MODIS-pixel. This becomes plausible when looking at the means for the whole research area (measured values for the entire map were assigned via classified vegetation units and averaged) in which the different LAI sources show very good agreement. Therefore, MODIS data seems to be an acceptable source for substitution of monthly LAI values averaged over larger areas. This matches with results from other studies which state good agreement between MODIS and field measured LAI data in savannah environments (SCHOLES et al. 2004). As no other data is available to compute LAI maximum values, the observed agreement over larger areas has to be sufficient to derive respective factors. Monthly means for the whole area were utilised for all areas except *Agricultural land* and *Halophytic vegetation*. For the latter one, higher factors had to be determined because nearly no standing plants were remaining at the end of the dry season, which results in extremely low LAI values. But as higher plants are present in the wet season, it is likely that those areas show a stronger increase compared to other units. The factors were calculated using MODIS pixels that contained a high proportion of

respective sites and showed larger contrast between minimum and maximum LAI. In conclusion, it is important to emphasise that a number of uncertainties are connected due to the lack of measured LAI values in the wet season. The method applied herein is an attempt to bridge those gaps with available existing data, but it is not considered as an ideal solution. However, MODIS data indicates very low LAI values for the wet season as well, which leads to small differences between the wet and the dry season. MODIS LAI map from 9th of November and seasonal LAI variation are illustrated in appendices 9 and 10.

Soil-vegetation unit	Mean calculation factor	Factor for Agricultural land	Factor for Halophytic vegetation
January	1.86	5.07	1.52
February	1.92	5.10	1.86
March	2.39	4.60	3.86
April	2.33	4.00	3.43
May	1.89	3.73	2.10
June	1.33	2.00	1.29
July	1.16	1.80	1.29
August	1.11	2.20	1.29
September	1.19	1.60	1.14
October	0.96	1.60	1.14
November	1.00	1.00	1.00
December	1.52	2.40	1.00

Table 6: MODIS derived factor for the computation of seasonal LAI variations

5.4.3 Interception Storage of Plants

A considerable amount of water is absorbed by leaves and twigs of plants during a precipitation event. This amount of rainfall drops down, runs off along the trunks as stem flow or is stored on the respective surfaces. The last-named process is called interception and this quantity of water can be evaporated before ever reaching the soil (HÄCKEL 1993). Therefore, detailed knowledge of interception storage and interception losses is a precondition for calculating the water balance (VON HOYNINGEN-HUENE 1983). To incorporate these processes in the model, related information of interception storage in mm and vegetation cover has to be provided for every vegetation class (UDLUFT AND DÜNKELOH 2009).

The maximum storage capacity is determined following the approach of VON HOYNINGEN-HUENE (1983) who analysed the relationship of the leaf area index (LAI), precipitation and the interception storage amount in different crops (Fig. 24).

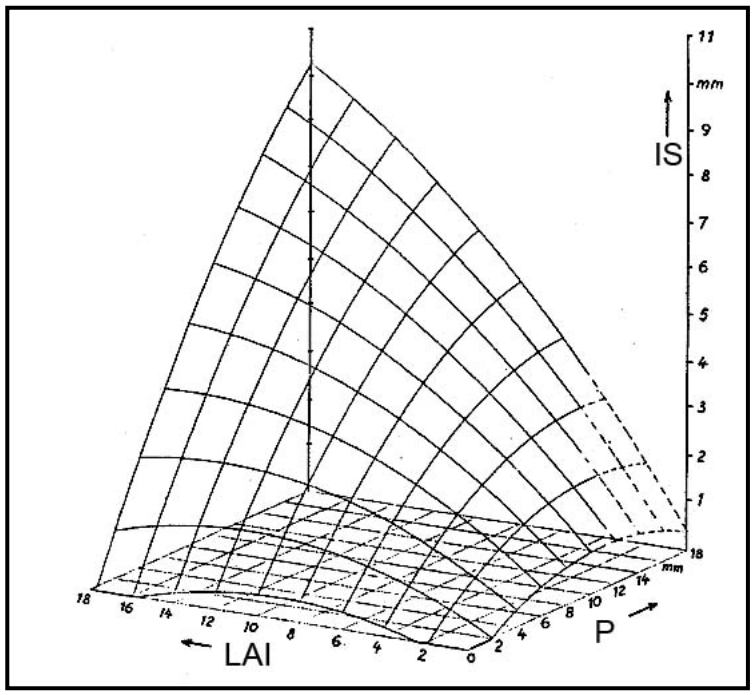

Figure 24: Interception storage IS and its dependency on leaf area index LAI and precipitation P (VON HOYNINGEN-HUENE 1983)

Also dead plant parts and branches were included in the experiment because they significantly contribute to maximum interception storage capacity (VON HOYNINGEN-HUENE 1983). The derived relationship can be expressed by the following regression equation (VON HOYNINGEN-HUENE 1983):

$$IS = 0.935 + 0.498*LAI - 0.00575*LAI^2$$

where

IS = maximum interception storage (mm)

LAI = leaf area index

The calculated maximum interception storage amount is highest in March at the end of the rainy season and varies between 1.6 mm for denser and 1 mm for sparse vegetation sites. In relation to interception values which were used in studies that

were carried out elsewhere in the Kalahari basin (about 4mm for shrubland and 1 to 3 mm for grassland, WANKE et al. 2008), the amounts calculated herein are generally lower, which may result from the scarce occurrence of dense or higher vegetation in the research area. An additional mm of interception storage is added to all units to consider evaporation from other surfaces which are not captured by LAI (e.g. dead plant parts on the ground).

5.4.4 Albedo

The proportion of incoming solar radiation that is reflected from a specific surface is called albedo (HÄCKEL 1993). This parameter is needed to calculate net radiation if the original Penman-Monteith is used for computing the ETpot (ALLEN et al. 1998). The values for each land use class were derived using an approach by MAUSER (1989). Reflectance values for each band from the RAPIDEYE (2011) satellite images were calculated with TNT mips and weighted with the respective exo-atmospheric irradiance values according to the following formula:

$$A = (\Sigma\ Ishorti * Ai) / Ishort$$

where

A = mean shortwave albedo
Ai = Albedo / reflectance band i
Ishorti = shortwave radiation / exo-atmospheric irradiance in band i
Ishort = entire shortwave radiation / exo-atmospheric irradiance

(according to MAUSER 1989)

Exo-atmospheric irradiance values were taken from the RAPIDEYE Satellite Imagery Product Specifications (2011) and are as follows:

Blue: 1997.8 W/m² µm
Green: 1863.5 W/m² µm
Red: 1560.4 W/m² µm
RE: 1395.0 W/m² µm
NIR: 1124.4 W/m² µm

Finally, albedo values were averaged for each land use class. As there was no cloud cover when the satellite image was recorded, the reflectance values for each band should be significant. A limitation of this approach is the fact actuality that the calculated albedo just represents the wavelengths of the RAPIDEYE bands and it has to be assumed that they are representative for the entire reflected solar radiation. Another approach which was not pursued in this study would be the interpolation or extrapolation of reflectance values beyond the range of the satellite bands (MAUSER 1989). The calculated albedo rates range from 0.28 to 0.35 for water and dark areas (e.g. Oshana black) to 0.52 for bright areas like grassland tufts.

5.5 Topographic Data

MODBIL requires elevation, slope and aspect information for interpolation of climatic variables and for the computation of interflow. Climatic interpolation is not crucial in the research area because the terrain is smoothly undulating with absolute elevation differences of only a few metres, leading to nearly equal environmental conditions as far as topographic influence is concerned. But the slope gradient influences interflow and without that information, this parameter is only controlled by soil conditions.

Initially, topographic information was supposed to be derived by using a freely available digital elevation model (DEM) of the region, but existing models were connected with major problems. Analysis showed that the DEM contained numerous and clearly pronounced elevation differences of several metres even over short distances (extremes of 30m, Fig. 25) and in water areas as well. This is in stark contrast to the natural topography of the research areas (e.g. Figs. 20, 21) with an assessed relief variation of maximal 3 m between the Oshanas at the deepest points and adjacent higher regions. Further errors were visible as stripes causing additional problems. From this it follows that the ASTER DEM cannot be used for this area because the errors change the appearance of the landscape from gently levelled to severely sloped (taking the region as a benchmark). Consequences in the modelling may be an immoderately high interflow and changes in radiation resulting in changed ETpot caused by aspect. Similar errors occur not only in the ASTER DEM but also in the SRTM, which is not discussed here as it is outlined elsewhere (HIPONDOKA 2005).

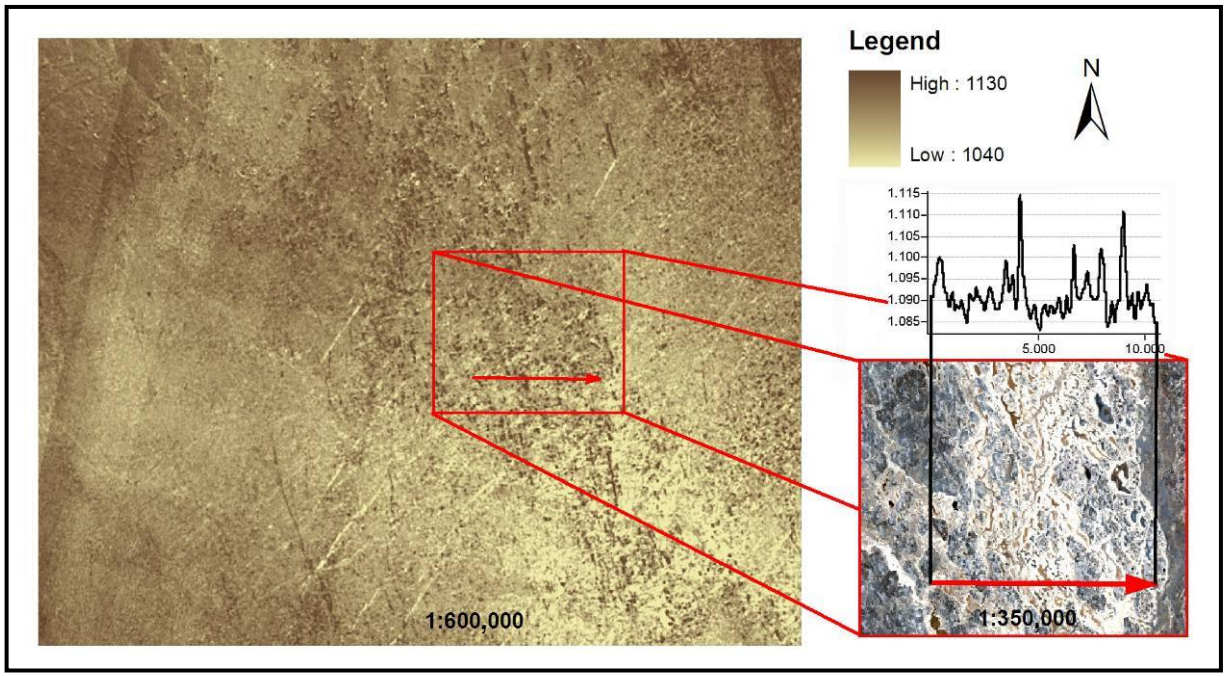

Figure 25: Raster image of the ASTER digital elevation model for the research area and elevation profile of a highlighted subsection. The highest point of the profile is situated in an Oshana. Immoderately high elevation differences and errors were observed in the entire region. Straight lines are visible in the western part which may be caused by the satellite's trajectory (data source: NASA LP DAAC 2009, RAPIDEYE 2011)

In summary, this lack of accurate and correct elevation data presents a serious problem for modelling. As an attempt to reduce and assess resulting uncertainties, two different approaches will be followed. One follows the assumption that the research may be represented best by a flat surface, because most existing slopes have a gradient of under 1°. Moreover, the soil parameters are most important for runoff and interflow in the region which can also be inferred from figure 20, where the sodic impermeable layer prevents infiltration which leads to standing water and the slope does not play a relevant role. So the basic modelling was carried out with a plane surface. But in order to assess the influence of a gently sloped terrain, one model run should be carried out with an improvised DEM. This was constructed due to qualitative field observations and some information given in the regional maps scale 1:50.000 (DSM 2001). The map indicated a mean elevation of about 1090m above sea level. This was assumed as highest part of the field and therefore assigned to all *Woodland*, *Shrub savannah*, *Shrubland*, *Mopane shrubland*, *Grassland* and *Agricultural areas*. *Seasonally flooded areas*, *Grassland tufts* and *Acacia pond mosaic sites* were usually situated below these areas and so received a value of 1089m. *Halophytic vegetation* and *Oshana bright* areas typically lie just

above the deepest areas and got a value of 1088 and as *dark Oshanas* and water bodies are situated at the lowest part of the field, the value of 1087 was assigned. Appendix 11 illustrates resulting improvised DEM. This is a rather simple way of deriving topographic information and it is connected with a number of uncertainties and abstractions but it should help to understand and quantify the influence of topography on the water balance of the research area.

6. Results

An extra spin up year containing climatic means of all years was introduced to generate balanced initial conditions at the start of the real modelling period from 2003 to 2010 (recommended by DÜNKELOH ARMIN, personal communication 2011). Naturally, all presented results herein are without data of that year. Derived land use parameters for all soil-vegetation units in the basic model run are illustrated in table 7. Modelling results are outlined in table 8.

Precipitation was exceptionally high during the modelling period, with mean precipitation of about 570 mm per year. According to Lloyd (1986), this would imply more rainfall than in typical semi-arid regions. The highest precipitation amounts were recorded in 2009 with 833 mm followed by 2008 with 691 mm. Both of them were also among the years with the lowest ETpot with values of 1399 mm (2009) and 1471 mm (2008), which can be explained by higher relative humidity caused by the presence of moist air masses. In contrast to this, just 299 mm of precipitation fell in 2007, presenting the driest year. The highest modelled ETpot values occurred in 2005 (1844 mm) and 2007 (1699 mm), also representing the years with the lowest relative humidity and highest temperatures. Derived average ETpot was 1577 mm. As outlined in chapter 5.2.2, the effects of variations in relative humidity were assessed with values of minus 10%. This resulted in mean ETpot values of 1729 mm per year, which is considerably higher than the basic model run. These results show the significant influence of relative humidity on ETpot. Yearly temperature variations were generally small with maxima ranging from 30° to 33°C and minima of about 16°C; therefore, they had little influence on the yearly variation of ETpot.

Soil-vegetation unit	Vegetation cover %	Mean rooting depth m	PAW mm	Albedo	Sealed surfaces %	Macro pore factor	Maximum interception storage
Woodland	55	1.5	61	0.44	0	5	2.57
Shrubland	54	1.0	41	0.45	0	5	2.40
Mopane shrubl.	54	0.6	24	0.40	0	5	2.39
Grassland	55	0.3	12	0.39	0	3	2.59
Acacia pond Mosaic	46	1.5	213	0.35	0.3	5	2.04
Shrub savannah	41	0.6	24	0.45	0	3	2.24
Seasonally flooded grassland high	45	0.3	64	0.39	0.25	1	2.62
Seasonally flooded grassland low	27	0.3	16	0.39	0.1	1	2.05
Grassland tufts	21	0.2	16	0.52	0.5	1	2.01
Halophytic vegetation	14	0.2	10	0.48	0.1	3	2.01
Oshana bright	0	0.0	0	0.50	0	1	1.00
Oshana dark	0	0.0	0	0.35	0.5	1	1.00
Water	0	0.0	0	0.28	0.5	1	1.00
Agricultural land	50	0.4	16	0.51	0	3	2.04

Table 7: Important modelling parameters for soil-vegetation units for the basic model run. PAW = plant available water in the root zone

ETpot just determines the upper limit of water transfer into the atmosphere and ETact is the variable that really influences the water balance. It can be partitioned in ET from interception and soil. In addition to this, ET from wet surfaces with permanent water supply and no limitations, called ETsec, contributes to ETact. This amount only relates to *Water* and *Acacia pond mosaic* areas and is mostly dependant on ETpot. As this evaporated proportion originates not only from local precipitation but also from lateral surface or subsurface influx, its quantity exceeds the input amounts. ETact refers to the amount without ETsec in the following, while ETsec will be discussed later. Mean ETact for the research area was 301 mm per year. Modelled seasonal variations ranged from 353 mm as a maximum in 2006 to a minimum of

224 mm in 2007, whereby 2006 showed the highest ET from the soil (224 mm) while latter marks the minimum values of both interception ET (56 mm) and soil ET (168 mm). 2006 showed considerably higher interception losses with a total of 116 mm, which is a 45% increase of the mean value (80 mm). Despite being the wettest year, 2009 showed the second lowest ETact of all years with 262 mm, which is mainly due to lower soil ET compared to the mean.

Again, these results are compared to values derived by changed modelling conditions to estimate the influence of humidity and different p-factors. Decreased humidity leads to a yearly averaged ETact of 305 mm while increased p-factors result in the mean value of 308 mm. Compared to the mean of 301 mm in the basic model run, the differences are very small and nearly negligible for the water balance. In contrast to that stands the model with increased field capacity which had a greater effect on ETact with a yearly average value of 329 mm. The maximal quantity was modelled in the run with an additional rooting depth of 30 cm with a yearly average of 350 mm.

Interflow is generally low with a yearly mean of 31 mm and occurs in relation to precipitation amounts. The highest quantity modelled was 49 mm in 2009 and the lowest generated in 2007 with 15 mm. As a flat surface was assumed in the basic model run, this parameter may change significantly with the improvised DEM. This is confirmed by the modelling results: mean interflow for all years was 65 mm higher with topographic information whereby the yearly variation follows the precipitation amount. Interflow increase ranged from 32 mm in the driest to 101 mm in the wettest year, showing the effects of sloping surfaces.

Groundwater recharge was generally high ranging from 63 mm (2007, 11% of mean annual precipitation/ 21% of annual precipitation) to 521 mm (2009, 91 % of mean annual precipitation / 63 of annual precipitation) per year in the basic model run. Mean groundwater recharge was 241 mm per year (42% of mean annual precipitation). Its variation generally followed rainfall but the ratio increased during years with higher quantities. The only exception was 2003 with a modelled recharge rate of 109 mm (22% of the annual precipitation) which is not much higher than the driest year despite considerably higher rainfall amounts.

Mean recharge rates of the basic model run were not much higher than calculations for increased p-factors (236 mm) or decreased relative humidity (236 mm). The effects of the improvised DEM and an increased FC were greater with 29 mm less recharge annually compared to the basic model whereby the DEM run showed stronger influence with an increasing annual precipitation. Again, the model run with amplified rooting depth showed the highest effect with about 53 mm less recharge than the basic model run.

ETsec is not directly connected to the water balance of a cell because it also consumes water that comes from sources which are not incorporated in the model. Water areas evaporate without limits and a high value of 1565 mm of ETsec is modelled. On *Acacia pond mosaic* sites, this effect is lower with a modelled ETsec of 516 mm. The mean value of those sites for the whole research area is 49 mm. ETsec from *Acacia pond mosaic* sites alone leads to an areal average value of 40 mm per year. As *Acacia pond mosaic* sites mostly tab the discontinuous perched aquifer, this amount may be depleted after recharge has taken place, reducing the total net recharge.

Vegetation units/ model run	Area %	Mean ETact mm (min/max)	Interflow mm (min/max)	Groundwater recharge mm (min/max)
Research area	100	301 (224/353)	31 (15/49)	241 (63/521)
Woodland	6	416	0	150
Shrubland	10	382	0	184
Mopane shrubl.	7	341	0	225
Grassland	11	285	0	282
Acacia pond Mosaic	8	437	43	82
Shrub savannah	4	316	0	250
Seasonally flooded grassland high	8	386	28	151
Seasonally flooded grassland low	6	306	4	260
Grassland tufts	17	215	126	246
Halophytic vegetation	15	255	4	313
Oshana bright	4	36	1	532
Oshana dark	1	179	137	282
Agricultural land	1	287	0	280
Water	2	183	137	276
Model -10% RH	100	305 (226/358)	31 (15/48)	236 (61/514)
Model p-fact	100	308 (224/363)	31 (15/48)	236 (63/509)
Model DEMimp.	100	285 (211/334)	96 (47/150)	212 (54/462)
Model FC +30	100	329 (239/391)	31 (15/48)	212 (48/499)
Model root +30	100	350 (259/419)	31 (15/47)	188 (26/485)

Table 8: Modelling results for selected water balance components and different model runs. Mean yearly precipitation was 571mm (min 299mm/ max 833mm) for all models. ETact values are without secondary ET. Surplus or deficit in the yearly water balance is due to storage changes. Model runs below are with 10% decreased relative humidity (-10% RH), increased p factors (p-fact), improvised DEM (DEMimp.), increased field capacity of 30 mm (FC +30) and additional 30 cm rooting depth (root +30).

6.1 Temporal Variation of Recharge

The temporal distribution of recharge in the basic and the increased FC model runs (Fig. 26) show low values at the beginning of the modelling period in 2003.

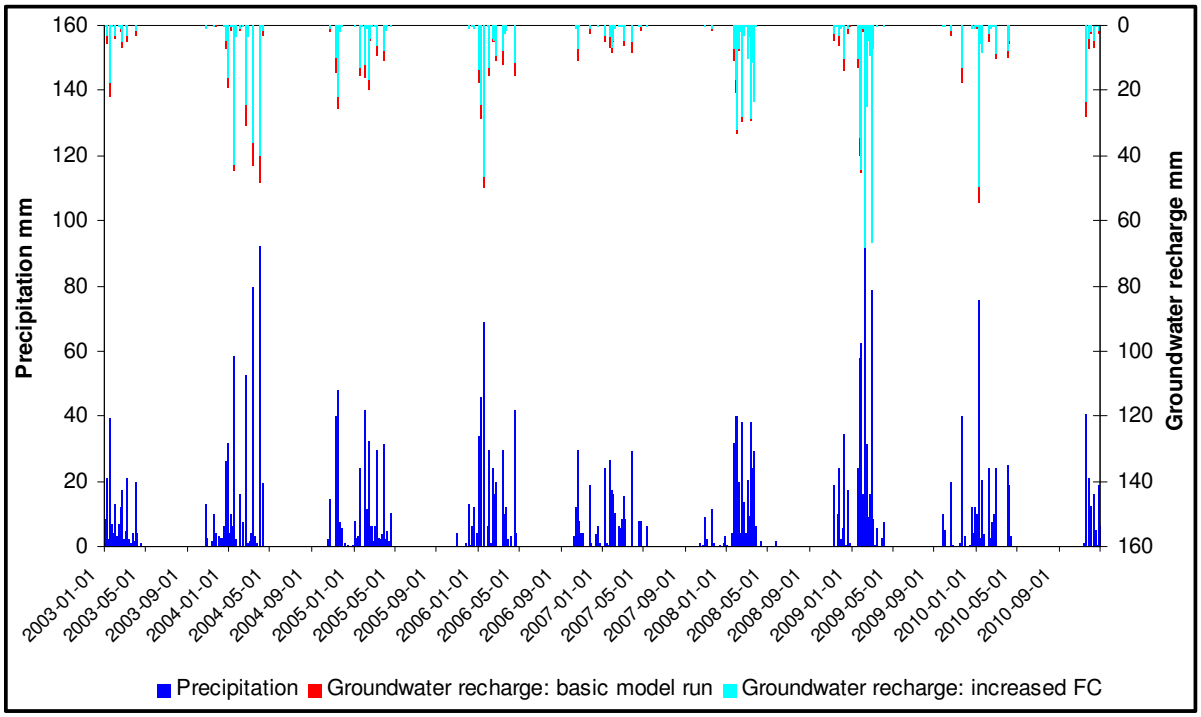

Figure 26: Daily sums of precipitation and calculated groundwater recharge rates in the basic model run compared to the model run with increased field capacity for the whole modelling period. When red colour is absent, both models show equal values. Precipitation during the rainy seasons (October to April) was 348 mm at the beginning of 2003, 613 mm in 2003/2004, 580 mm in 2004/2005, 557 mm in 2005/2006, 365 mm in 2006/2007, 581 mm in 2007/2008, 850 mm in 2008/2009, 449 mm in 2009/2010 and 204 mm at the end of 2010.

Only one strong precipitation event leads to a recharge of more than 10 mm. High rates are modelled in the following relatively wet rainy season of 2003-2004 especially after and during very intensive rainfall in January and March, whereby the basic model run shows noteworthy higher amounts. In the rainy season 2004/2005, precipitation was extensive but with less extreme values leading to lower recharge. In 2005/2006 rainfall somewhat decreased but one event with amounts of over 60 mm led to a mildly higher recharge amount than in the former season. The driest period occurred during 2006/2007 and resulted in extremely low recharge rates compared to other seasons. The precipitation pattern in 2007/2008 showed a concentration of rain in the first three months of 2008, which led to the generation of considerable

recharge amounts and no big differences between the two model runs. The rainy season of 2008/2009 was the wettest of the whole period and some of the highest daily precipitation amounts (96 mm and 79 mm) occurred in the beginning of 2009 as well. Therefore, this period was characterised by far the highest recharge rates and there were nearly no differences between the two model runs at the end of the respective episode. Precipitation presented itself with a more erratic distribution in 2009/2010, which led to high recharge amounts during extreme events only. The modelling period ended with strong rainfall amounts and relatively high recharge for the onset of a wet season.

Generally, lower recharge takes place during the first precipitation events when soil storage is depleted and high quantities are either modelled after intensive rains or when several moderate but successive precipitation events occur. When looking at the differences of both models, one can see higher discrepancies when rainfall happens sporadically with preceding dry periods. Both model runs generate equal recharge quantities when large consecutive precipitation events occur (mostly at the end of the wet season) which lead to the infilling of all available soil storage even if the field capacity is increased. Daily recharge plotted against precipitation illustrates the connection with rainfall intensities (Fig. 27). If rain is below 20 mm per day, most recharge values are clustered at the lowermost part of the Y-axis indicating no or marginal recharge. It is noticeable, however, that in some cases recharge is generated even during low or no precipitation events in the basic model run. This is caused by the oversaturation of the soil which leads to recharge in the following time step because interflow is generated only marginally on flat terrain. Differences due to sloping surfaces are visible when referring to the same plot with data generated by the model run with the improvised DEM. Therein, no or insignificant recharge is visible below 10 mm of precipitation and no pronounced accumulation of recharge values is present near the left end of the X-axis. Although some differences in the total amount exist, the distribution of both models is similar above 10 mm of precipitation. In several cases recharge is generated at relatively low precipitation intensities, which may be due to saturation of the soil, but the majority of the values is still clustered at the lower range of the Y-axis. Above 20 mm, an increasingly linear development of recharge with rising precipitation amounts is visible.

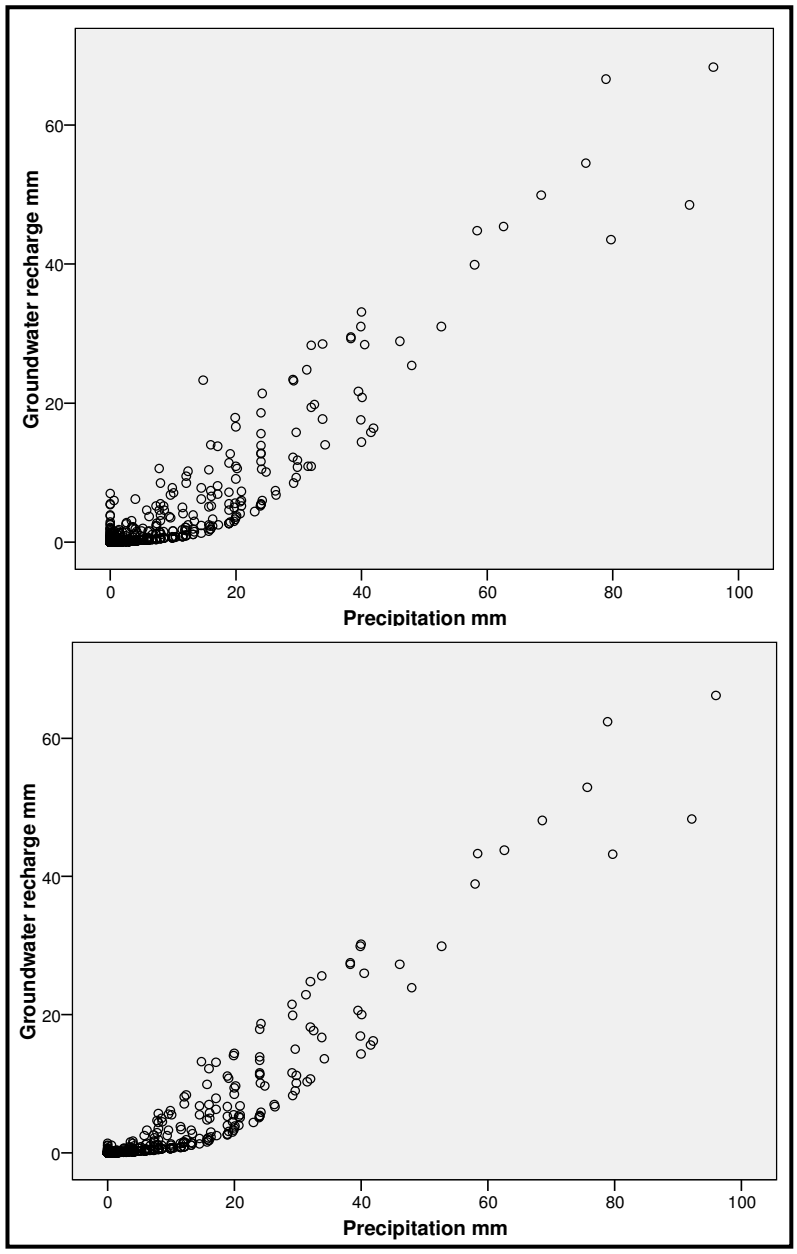

Figure 27: Plots of daily mean precipitation and modelled recharge in the basic model run (above) and the model run with the improvised DEM for comparison (below).

6.2 Spatial Variation of Water Balance Components

The figures mentioned are means for the whole research area without spatial variations taken into account. However, water balance components vary significantly across the region (Figs. 28 and 29). Interflow is concentrated on areas adjacent to the main channels of the *Cuvelai*, especially where their extent is wide like in the northern parts. Further runoff is modelled in the south-western and water areas. So

high interflow amounts are modelled where higher clay content and impermeable sodic layers characterise the soil, whereby many other areas do not show interflow. This applies for all soil-vegetation units on Arenosol I, leading to no interflow between the channels and to a greater extent in the central and western parts. The water balance of these units is therefore solely regulated by plant activities and soil storage, which is represented by ETact (Fig 29). ETact is high on the densely vegetated or deep-rooted parts which are concentrated on the margins of the study area. In the centre, high ETact amounts occur in a more scattered way and to a smaller extent, which represents the patchy distribution of deep rooted vegetation. In the broader *Omadhiya Lake* region and the area of the main Oshanas, very low ETact values are modelled, which represents the absence of (deep rooting) plants. As respective areas are characterised by open water surfaces, ETsec may be responsible for the largest part of ET here (not shown). When comparing ETact and groundwater recharge in figure 29, a clear inverse connection is visible. All areas in or adjacent to the channels or open water surfaces show high recharge values. Mostly, these are regions with the water table close to the surface. In the central areas, where grassland and sandy soils are predominant, high recharge rates are modelled as well. The opposite is true for woody or deep rooting vegetation, with patchy distribution in central parts and larger extent in the western, northern and eastern margins of the research area. Mean recharge values for specific soil-vegetation units range from 150 mm per year in *Woodland* to 282 mm per year on *Grassland* areas with a mean of 229 for all vegetation units on Arenosol I. Arenosol II areas with increased sodicity are within the same range but with marginal interflow (4 mm). Relatively low groundwater recharge rates occur on *Acacia pond mosaic* sites (82 mm). *Grassland tuft* and *Oshana dark* units show very high recharge rates despite partly sealed surfaces. Saline and sandy soil-vegetation units show the highest recharge rates, especially *Oshana bright* sites without plants. As the lower parts of the field are characterised by increased salinity and saline layers have to be expected in some depth, these areas seem unlikely to generate freshwater sources. Therefore, usable groundwater recharge may be restricted to the other areas (taken as areas with soil EC < 4 ds/m herein, map: appendix 12) and the areal mean value for those would be 200 mm per year. Another reason for considering this value is the fact that respective units are less prone to the influence of water sources originating from outside the research area, which would modify the local water balance.

When looking at the effects of changed modelling conditions according to soil-vegetation units, various results can be identified. In the model run with the improvised DEM, significant changes are connected to the modelled interflow amounts (Fig. 28). Generally, it is visible that the most intensive interflow amounts occur at the margins of Oshanas and water areas. This great enhancement is a result of relatively steep slopes at the edges of low lying parts. Interflow increase ranged from 100 to 200 mm on areas most affected by impermeable layers (*Seasonally flooded grassland high, Grassland tufts*) to 40 mm on slightly sodic areas (*Halophytic vegetation*). Most sandy areas showed additional interflow of about 1-3 mm. Groundwater recharge showed a similar pattern in the improvised DEM run. Arenosols showedmarginally reduced recharge (about 2 mm) but soil-vegetation units with water logging surfaces are characterised by significantly lower recharge rates with a decrease of about 30 mm on *Halophytic* and *Seasonally flooded grassland low* sites to a decline of more than 70 mm on *Grassland tufts* and *Oshana dark* units.

In contrast to that stands the model run with increased FC. ETact increased substantially with a parallel decrease in recharge. All sandy areas show considerably lower recharge rates than the basic model run. Greatest reductions of about 50mm per year occur on *Mopane, Grassland, Shrub savannah* and *Agricultural* areas while areas with sealed surfaces, clayey soils or no plants show very small changes (0-11 mm). As values of many soils are increasingly modified in this model run and field observations suggest higher FC, the mean value for areas assumed to be unaffected by salinity should be considered. These areas show an average recharge rate of 163 mm per year.

The model run with additional 30 cm rooting depth showed some similarities to the run with increased FC. Lower recharge rates occurred on all sandy areas, whereby the magnitude of change was lower on units who already had relatively deep roots (minus 10-20 mm recharge) and higher on sites with shallow roots in the basic model run (minus 40-70 mm recharge). Considerable changes were calculated for areas without defined rooting depth in the basic model, with reductions of 83 mm on *Oshana dark* and 235 mm on *Oshana bright* units whereby it should be emphasised, that no plants are present on both of these areas in reality. The average recharge

value for non-saline areas was the same as in the model run with increased FC of 163 mm.

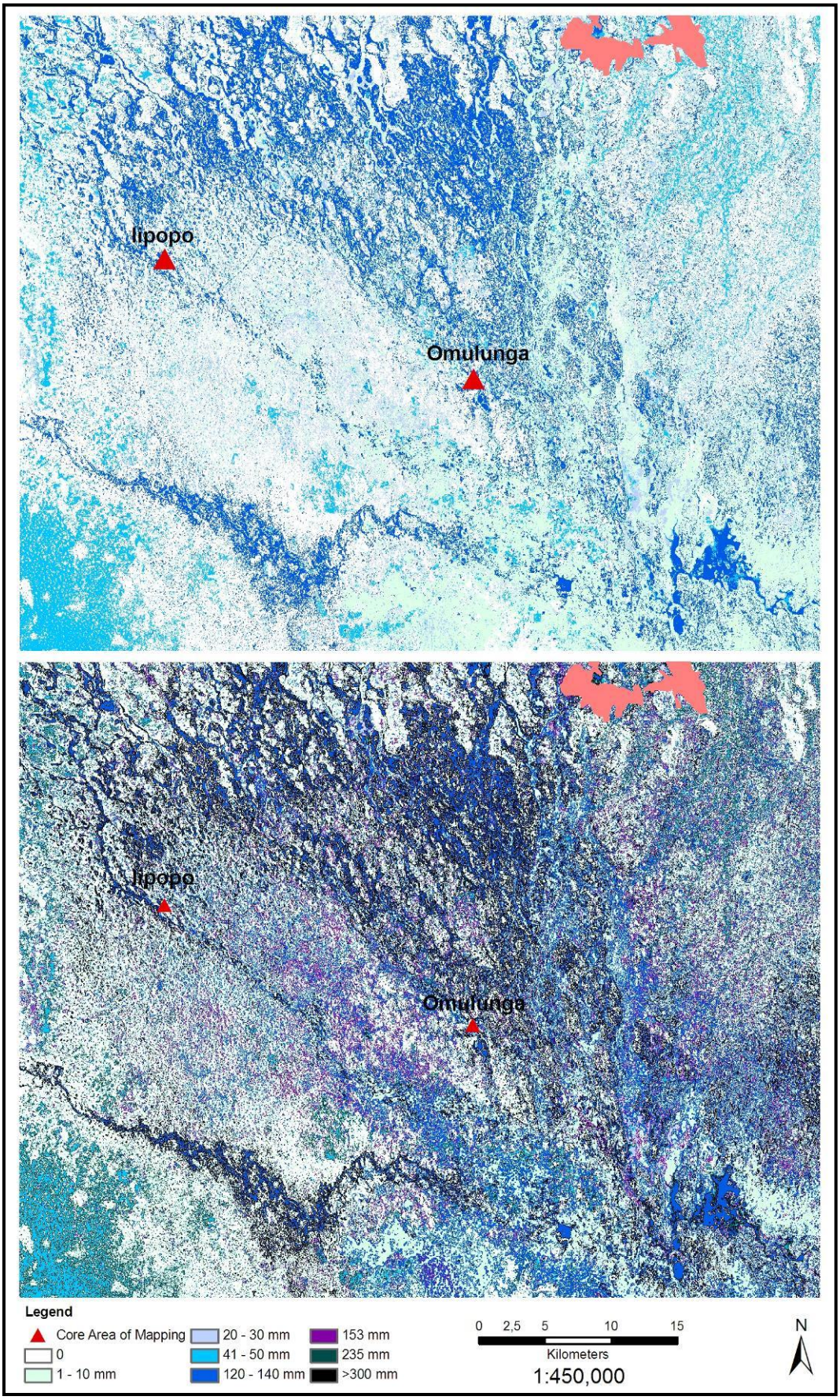

Figure 28: Modelled mean annual interflow in mm for the basic model run (above) and the model run with the improvised DEM (below). Red area in the Northeast represents urban districts (not modelled).

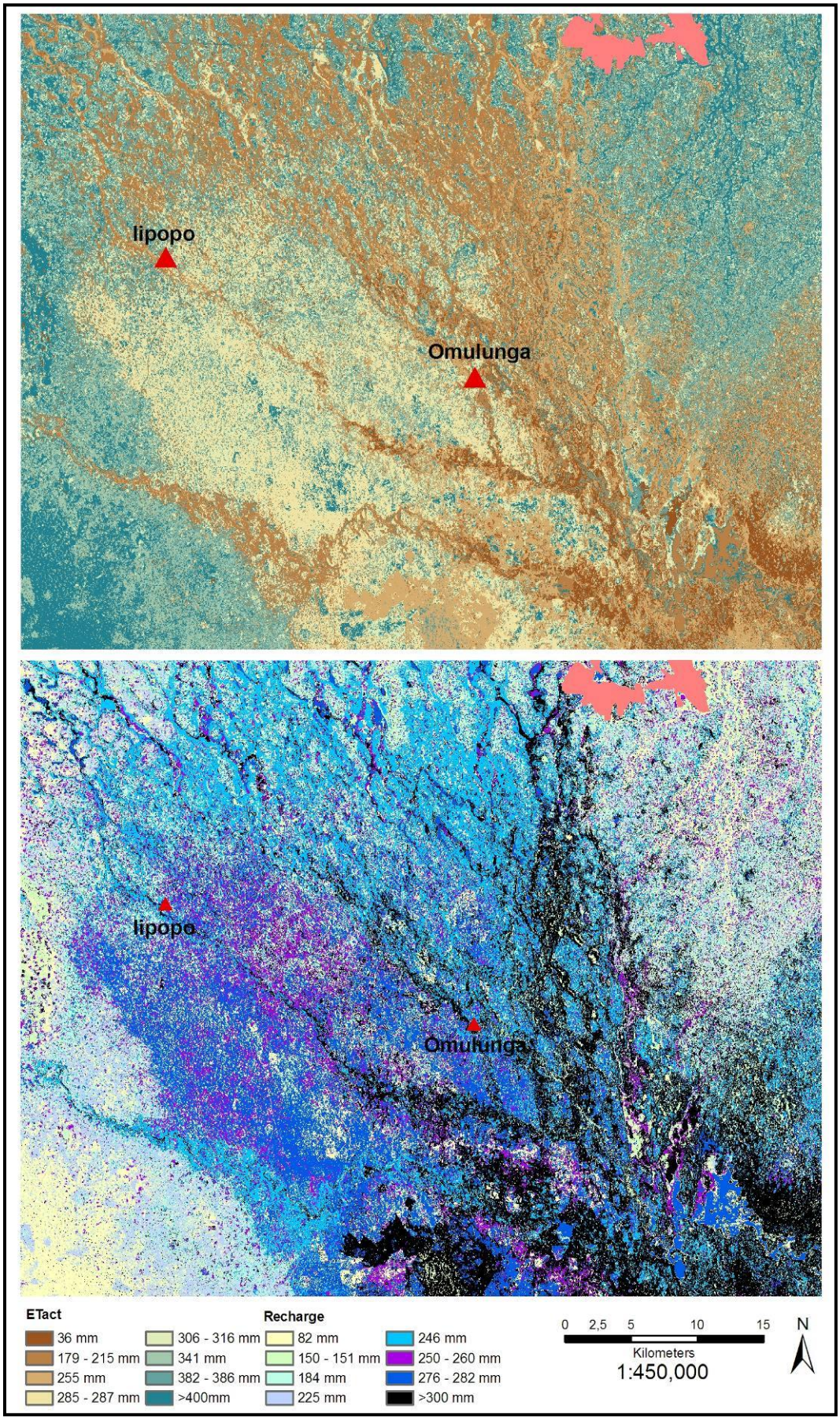

Figure 29: Modelled mean annual actual evapotranspiration (ETact, above) and potential groundwater recharge (below) in mm for the basic model run. ETact is without ETsec. Red area in the Northeast represents urban districts (not modelled).

6.3 Modelling Results Compared to Field Observations

The first strong precipitation events on 17th November in the rainy season of 2009/2010 led to an average groundwater recharge of 12 mm for the whole area. On this day, the depths of the wetting front were noted at some control plots in the field. Results showed that the main part of infiltrating water reached depths of approximately 17 – 20 cm on *Woodland*, *Shrubland* and *Grassland* sites (Fig. 30). A continuous, deep reaching infiltration was detected in the Omulunga region at low lying saline areas like *Halophytic vegetation* and *Oshana bright* areas. *Oshana dark* areas were water-filled in this area but not near Iipopo. *Grassland tufts* showed no deeper reaching infiltration because of water logging. Modelling results generated nearly no recharge at *Woodland* and *Shrubland* sites for the respective day, which was confirmed by field observations. On *Acacia pond mosaic* and *Seasonally flooded grassland high* units, no recharge was modelled either. Recharge was modelled for *Halophytic vegetation* and *Oshana bright* areas, which is in agreement with the detected deep infiltration on those test plots.

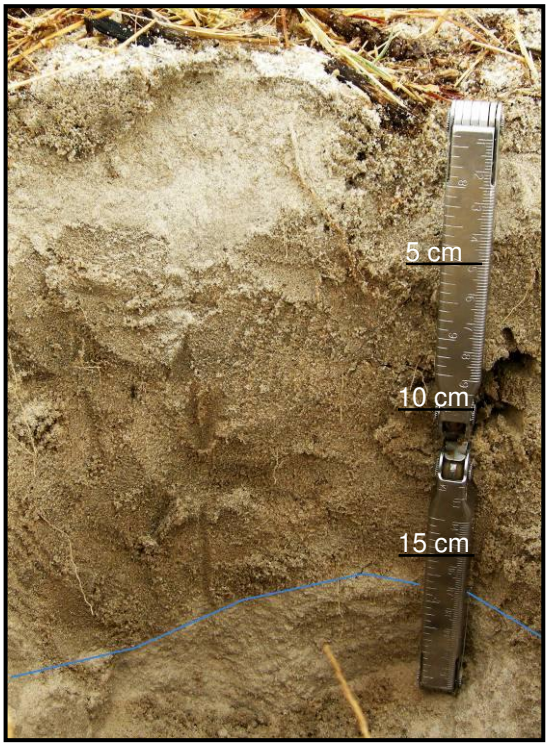

Figure 30: Infiltration depth indicated by blue line on 17th November 2010, Shrubland.

Contradictory results from field observations are modelled on *Grassland* with an amount of roughly 20 mm and *Grassland tuft* units with 12 mm of recharge. Yet, *Grassland* showed deeper reaching infiltration of approximately 30 cm on some plots. Other soil-vegetation units were not tested. However, it is not clear if precipitation amounts in the region of observations were exactly the same as those recorded in Ondangwa. As infiltration depth was noted during the day, a part of the precipitation amount may have been generated in the following night and resulting infiltration could not be observed hence. Furthermore, spatial variation of precipitation seemed to be very high during the first rainfall events. This is inferred from field based observation of the wetting front, which showed a different development on plots of the same soil-vegetation unit over relatively small distances.

7. Discussion

An assessment of the near surface groundwater recharge rate for the shallow discontinuous perched aquifer was the main purpose of this study. Results indicate a high amount of potential direct recharge for most soil-vegetation units with a mean value of 241 mm per year that may be reduced by about 30 mm to a maximum of 50 mm if some sensitive modelling parameters are varied. Thereby, the decrease induced by higher FC seems very likely according to moisture measurements. When recharge amounts are restricted to areas which are supposed to be unaffected by high salinity, additional reductions of about 30 mm apply. Finally, all this values refer to potential recharge and a number of processes are able to reduce this amount. High recharge may alter the water table and so expose it to ET. To take this effect into account, *Water* areas were allowed to evaporate unrestrictedly. The modelled total amount that is withdrawn this way is small, with an average value of 9 mm for the whole research area. Given that many of these areas are subject to flooding as well and a greater amount of water is likely to be supplied this way, it is difficult to include them into the total water balance. A variable extent of respective sites during the year makes the situation even more complicated. Another effect is ET from plants that have access to the shallow water table. This is represented by ETsec on *Acacia pond mosaic* sites, which show green vegetation which indicates adequate water supply. Their ET never falls below a threshold value of an estimated half ETpot. This would imply a further reduction of the discontinuous perched aquifer of 40 mm on average, but as this is not a connected structure, high spatial variations of water depletion may occur.

Results of this study differ significantly from other comparable studies. WANKE et al. (2008) use the same model and state a mean annual recharge of 8 mm at a mean annual precipitation of 409 mm in the Kalahari of Northeastern Namibia and Northwestern Botswana with spatially restricted maxima of 170 mm. Even lower recharge rates are modelled by KÜLLS (2000) in the Upper Omatako Basin in Northeastern Namibia. Other studies which applied different methods for recharge estimations were carried out elsewhere in Southern Africa. Higher recharge rates are outlined by BRUNNER et al. (2004) for the Chobe and Ngamiland regions in Botswana using surface water balance and chloride methods. This approach results

in recharge rates of 0 – 150 mm while water balance calculations lead to values of 0 to over 200 mm in the Chobe area with precipitation amounts of roughly 540 mm. Generally, recharge rates determined in different regions in Southern Africa vary drastically, even when precipitation amounts are similar (Fig. 31).

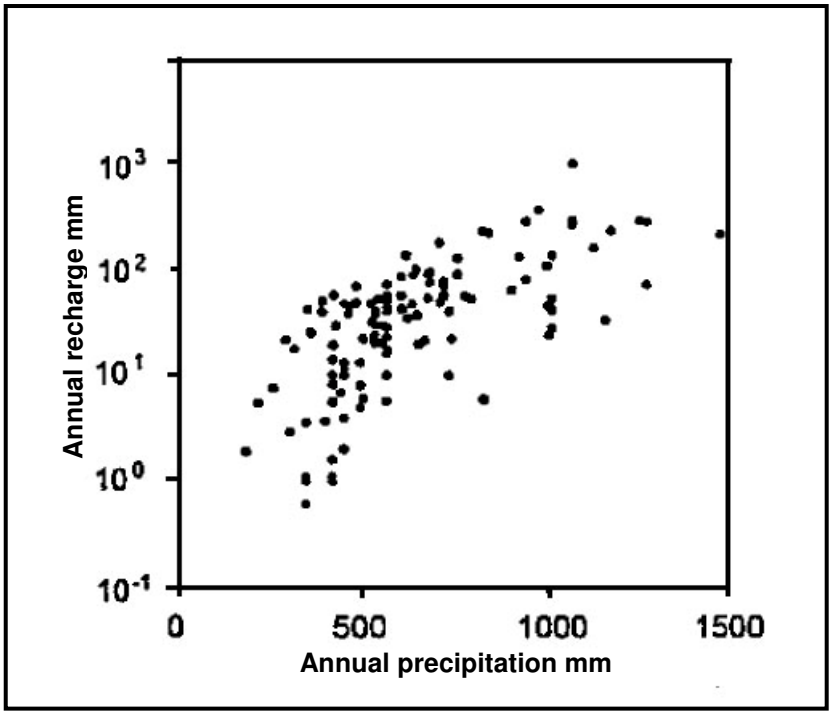

Figure 31: Annual Recharge compared to precipitation from several data sources in South Africa, Botswana and Zimbabwe (SELAOLO 1998 in DE VRIES and SIMMERS 2002).

Highest variations occur below 500 mm of rainfall. Above 500 mm, which is closer to the mean annual precipitation in the modelling period of this study, recharge rates still show a great distribution but generally range from 10 mm to about 100 mm with some higher values. The large variation is a result of different environmental conditions like hydrology, soils or morphology (DE VRIES and SIMMERS 2002).

In conclusion, modelled potential recharge leads to amounts that are situated above or on the uppermost end of observed quantities in semi-arid Southern Africa. This may be due to several reasons: First of all, precipitation during the modelling period was exceptionally high and above amounts that occurred in similar studies. In addition, most precipitation occurs in a very short time interval of about 3 months and high intensities or steady moderate rains amplify recharge. Nevertheless, the

amounts were higher than stated by many other recharge surveys even during years of low precipitation.

Another explanation that seems plausible is the difference of the hydrological situation. Extensive sedimentary layers or alluvial soils present a significant barrier for the percolation to a generally deep-seated water table in many areas of the Kalahari (DE VRIES and SIMMERS 2002). The discontinuous perched aquifer presents a stark contrast to that situation because it is mostly found within 1 m or 2 m below the surface (Fig. 32). Therefore, thresholds for recharge are much smaller within the research area. The effect of alluvial layers is also outlined in other studies, whereby high recharge rates are estimated for areas with an alluvial cover below 50 cm and marginal or no recharge when alluvial layers are above that value (STOTHOFF 1997 in SCANLON et al. 2002).

Figure 32: Excavation showing the depth of the water table at about 2m below the surface.

A further considerable difference between the research area and many other parts of the greater Kalahari basin is its vegetation. Apart from smaller, spatially restricted patches and the broader zone at the boundary of the research area, the dominant vegetation is grassland or plants with shallow roots. Many other regions in Namibia, especially those examined in studies mentioned before, are dominated by dense shrubby vegetation with deep reaching roots. On areas where bush encroachment is most severe (e.g. greater Tsumeb region), more than 4000 larger shrubs per ha are found (MENDELSOHN et al. 2002). This leads to a continuous and deep depletion of water stored in the soil, which hampers groundwater recharge. Another effect of dense vegetation is increased interception, which decreases the amount of water reaching the soil.

In summary, there are some reasons that support high modelled recharge rates. All conditions for favourable recharge stated in DE VRIES and SIMMERS (2002) apply to the research area: poor vegetation cover, permeable soil and high intensity of rainfall. In addition, the discontinuous perched aquifer has been used by the rural population since the onset of settlements in the Cuvelai (MENDELSOHN et al. 2000), thus the landscape is still characterised by a large number of hand dug wells. Without a considerable amount of recharge from precipitation, this freshwater source would be unsuitable for sustaining water supply in dryer periods when no flooding occurs.

Field observations on the other hand contradict recharge modelling on some soil-vegetation units. One reason for this may be local variations of precipitation amounts or the exact timing of rainfall. But other reasons have to be taken into account as well, especially that some parameters are connected to major uncertainties, which leads to the presumption of overestimated recharge amounts.

7.1 Sensitivity of Modelling Parameters and Uncertainties

Several problems occurred during the derivation of model input parameters. To evaluate the results and the performance of the modelling, the involved parameters will be discussed separately in this section.

Meteorological Parameters

Meteorological parameters are the basis for the water balance. As they are connected with some uncertainties due to data gaps, the resulting effects must be assessed. ETpot is the first parameter that is dependent on meteorological data. The respective mean value appears quite accurate when compared to regional references. This statement is based on comparison of calculated ETpot with the value of 2500 mm per year given in MENDELSOHN et al. (2000). Assuming that this value was derived by standard measurements with the Class-A evaporation pan, it can be converted to reference evaporation using a pan coefficient. No information is available about detailed circumstances of measurement for the figures in MEDNELSOHN et al. (2000), but as the area is generally dry with a relative humidity of about 50% (mean of modelling period) and moderate wind of about 2 m/s, numbers for the respective environment were selected from tables in ALLEN at al. (1998, Case B: dry fallow area with side length 10 m to 100 m). Derived coefficients are 0.6 and 0.65 leading to translated reference ET values of 1500 to 1625 mm per year, which matches the average modelled value of 1577 mm quite well. Although former values are only approximate, they may indicate that ETpot was modelled correctly and that the completion of relative humidity values was appropriate. In contrast to that stands the 10% lower relative humidity run which shows a mean value of 1729 and is considerably higher. The high Etpot in the respective model run does not lead to large changes in other water balance components, mean recharge rates were just 2% lower than in the basic model run, which means that regional ETpot is so high that it is no restrictive factor during the modelling period. Furthermore, errors that possibly derive from data substitution may not alter results to a great extent. Temperature has an influence on ETpot as well, but as relatively uniform conditions persisted during the modelling period, effects of temperature are not very apparent in the modelling results.

Precipitation and its intensity has an influence on interception and soil storage and hence, on ETact. This one is highest in 2006, which may be caused by a more evenly distributed rainfall pattern and constant supply for soil and plants. A similar explanation applies for the comparably high evaporation losses from interception in 2003, which may result from the application of mean values in the first three months. The mean precipitation distribution leads to continuous refilling of the interception

storage and parallel depletion through ET. When rainfall events happen more selective like in “normal” months, the vegetation cannot intercept the same constant proportion, which leads to lower ETact. As outlined earlier, 2009 shows a relatively reduced value of ETact as well. One explanation for this may be the lowest ETpot of all years, but the model run with increased RH shows a 170 mm higher ETpot value, which results in a negligible increase of 6 mm in ETact. Therefore, the low ET 2009 can also be attributed to the rainfall pattern which is characterised by some of the most intensive precipitation events. But in contrast to 2003, reduced soil ET is mostly responsible for the decrease. This may be caused by the infilling of soil storage to its maximum due to continuous rain before precipitation extremes, allowing an unhampered infiltration through the soil column afterwards.

The discussion above shows that uncertainties in temperature or relative humidity may have minor influences on the modelling results. This is not the fact with precipitation because obviously, both amount and intensity have strong effects on the modelling results. Although they are small, the existing data gaps in precipitation are very likely to be the cause of some variations in the modelling results, especially for above average interception storage.

Vegetation Parameters

Interception itself is a factor that had to be computed indirectly and is therefore also connected to uncertainties. As an unproportional increase of the LAI among the soil-vegetation units in the wet season is probable, field measurements in the respective period would improve the related modelling steps substantially. Although an LAI below 1 is appropriate in the dry season, it is not applicable for computing surface resistance- or kcb-factors according to ALLEN et al. (1998). These values are more important during the climax of vegetation. Thereby, a missing maximum LAI prevents the application of alternative and often recommended methods in determining ET.

Another issue is connected to areal cover of vegetation as all observations were conducted in the season with minimum vegetation. Therefore, many plants were parched on the ground or in case of edible species which were not fenced off, consumed by livestock. This makes a reliable assessment of vegetation cover

difficult and a completely different picture may emerge during the wet season. So again, an observation period during this time of the year is very important.

The amount of water that plants can use before water stress occurs is difficult to obtain for non-agricultural vegetation. The model run with slightly increased p-factors was used to assess uncertainties connected to the application of mean values. With a 2% decrease of mean groundwater recharge, results indicate only small effects for the water balance. This may be explained by the high precipitation amounts during most years, which led to a good moisture supply and hence, maximum transpiration during the wet season. As regards variations in p-factors and relative humidity, other model runs showed higher effects.

Topography

The improvised DEM caused a strong increase in interflow on impermeable soils. Sandy soils still showed marginal interflow, which is comparable to other studies (WANKE et al. 2008). As the DEM was inferred from classification results which are a significant generalisation of natural conditions, it introduces severe uncertainties. This comes from the fact that sharp transitions are generated between classes of different height, which leads to slopes that may be steeper than the characteristic topography of the region. Therefore, the modelled 30 mm recharge decrease is assumed to represent the upper end of terrain influences and the application of the improvised DEM is restricted as a tool to assess the probable effects of sloping terrain. So the total anticipated maximum effect on groundwater recharge is a mean 12% decline if sloping surfaces are introduced. However, it has to be emphasised that the lack of accurate elevation data poses a severe constraint to modelling and future research related to hydrological (and other) topics would benefit substantially from the provision of a precise DEM in near future.

Sealed Surfaces

Another issue that is connected with interflow is the definition of sealed surfaces. This was done on the basis of field observations and soil classification. The value was not set to 100% on sodic soils because some recharge is likely to happen even on relatively impermeable layers; a total sealing therefore seems immoderate. However, as recharge was modelled during the first precipitation events in November

2010 on *Grassland tuft* units and field observations showed that all water was kept above 10 cm at the same time, an increase in sealed surfaces seems reasonable. This increase was not applied during the modelling because of the lack of observations but further research on this topic would help to adjust the water balance on areas affected by sodicity.

Soil Storage

The most sensitive and important modelling parameters are connected to the soil column. First of all, the concept of effective field capacity introduces the importance of rooting depth which defines the range where water can be extracted. This introduces some limitations. On areas without plants like *Oshana dark* and *Oshana bright*, no roots are present, therefore no storage is defined. This is reasonable when respective areas are directly connected to the water table, which is the case in many low lying parts of the research area. In the *Omulunga* region, most of those areas had a shallow water film on top – at least partly – or soils were saturated up to the surface. On some other areas, measured moisture content was above calculated FC and therefore oversaturated a few centimetres below the surface. This would justify the definition of ETsec on these units, but as mentioned already in regard to water areas, this approach would add complexity and would unsettle the local water balance so this approach is delicate. The effects would be an average ETsec of 74 mm for the whole area if no ET limits would apply and all areas would evaporate likewise (ETsec *Oshana bright:* 1234 mm / *Oshana dark*: 1393 mm). On the other hand, there are several areas which show decreased moisture content and in those cases, defining a rooting depth of some centimetres would be reasonable. Lastly, on the majority of *Oshana dark* and *Oshana bright* units, a transition can be found from standing water or saturated conditions on central areas and dry conditions at the margins. So the determination of rooting depth and thus soil storage is a question of generalization as is ETsec. A more sophisticated remote sensing approach with soil moisture as the research focus may enable a workaround for this problem. As no rooting depth was defined, recharge was high especially on the permeable *Oshana bright* units. A rooting depth of about 10 cm, which was about the maximum range of drying, would lead to an assessed recharge decrease of 28 mm on dark and 78 mm on bright Oshana units. Transferred to the whole area, a mean reduction of 4 mm recharge would apply. As this estimate is based on results for the 30 cm increased

rooting depth model run, this quantity may even be lower, because of the unproportional rise of recharge after saturation. ETsec, however, has a stronger effect on the net balance. So it is very likely that the direct recharge on those areas is lower in reality, as a number of areas show shallow surface moisture depletion and, accordingly, a small threshold for precipitation. But the high changes as modelled in the increased rooting depth model are unlikely to occur, because there are no plants present on respective sites and so depletion would solely depend on other processes. Finally, the mentioned areas are also those which are most affected by periodic flooding due to water which originates from the upper reaches of the *Cuvelai*. This may lead to a replenishment of all available storage capacity on respective units whereby its volume is defined by topography and subsurface conditions. This implicates that other processes which are not included in the modelling – like indirect recharge and other limitations originating from the geological framework – dominate hydrological processes on these areas.

On other soil-vegetation units, rooting depth significantly reduces soil moisture storage capacity as well. Especially sandy soils with shallow rooted *Grassland* lead to an extremely low PAW. Field observations indicate that rooting depths are not subject to high variations on those areas, at least not in the dry season. Plants, therefore, may be unable to extract water from deeper soil layers. But although nearly no roots were observed below 30 cm, they may develop in the wet season and some sources state moisture uptake by grasses in greater depths as well, at least in some areas (KNOOP and WALKER 1985). Furthermore, it is likely that other processes which are not captured by the model reduce moisture even to greater depths. Sandy soils contain large amounts of air volume and contained water vapour moves to the area of lowest potential in the soil, which is the surface when the soil dries out from above after a wet season. Another process that is able to increase vapour transport is the development of a temperature gradient, an effect observed in other regions of the Kalahari (DE VRIES and SIMMERS 2002). Water vapour efflux is balanced by increased evaporation and therefore reduces soil moisture (BLUME et al. 2010). This process is very slow and may be insignificant compared to plant ET, but the long dry season may lead a reduction of soil moisture even to greater depths. This effect does not apply to clayey soils, as crusting prevents soil ventilation, but other effects not connected to plant activity may reduce moisture storage. In those

areas, capillary rise is one process that may occur. It is known to extract water from considerable depths (DE VRIES and SIMMERS 2002). All those processes can result in moisture depletion which is not captured by effective rooting depth alone, leading to thresholds not incorporated in the modelling parameters and therefore resulting in higher recharge rates. The model with increased rooting depths was implemented to assess a range for these uncertainties. Results showed that especially grassy sites shifted to lower recharge quantities. As the 30 cm increase is a drastic change compared to the basic model, the 22% change of mean annual recharge is high but it may be seen as maximum impact of above mentioned uncertainties and a considerable part of it derives from changes in Oshana units.

Another parameter that is related to soil storage as well is FC. The uncertainties related to PTFs were already mentioned and modelling results underline the sensitivity of this factor, especially on soils where the factor is generally low, showing a 50 mm decreased recharge in the elevated FC run. Furthermore, these are also the soils with shallow roots, therefore minimizing the threshold for deep percolation which leads to some of the highest recharge rates in the model. Because of reasons mentioned above, the connected uncertainties may be greatest on respective sites. Especially *Grassland* areas are very likely to be the subject of overestimated recharge amounts as indicated by field observations. This shows very good agreement with information given in KÜLLS (2000), who related modelled recharge and associated PAW to observed groundwater fluctuations. Results showed that nearly no recharge was modelled above 65 mm PAW but groundwater fluctuations were present. Below 55 mm, high recharge rates were modelled but no related groundwater fluctuations were measured and the best agreement between modelling and observations was reached at a PAW of 65 mm (KÜLLS 2000). This leads to the conclusion that field observations during the peak of the rainy season would greatly enhance modelling input parameters, especially extensive moisture measurements that are expanded to a certain depth after precipitation events. The great advantage of that would be a better founded adaption of soil water characteristics derived by PTFs. Furthermore, field based verification through water table fluctuations would provide the possibility to adjust a number of parameters as demonstrated by KÜLLS (2000).

To sum up, modelled recharge rates are mainly the result of a combination of FC and rooting depths. Both factors are generally low in a region that is dominated by sandy soils and grassland. In addition, there are high hydraulic conductivities and low interception storage amounts. All these parameters are highly sensitive for modelling and show large differences to factors defined in comparable studies in other regions. In WANKE et al. (2008), roots reach depths of up to 70 cm and more, PAW is remarkably higher, often by values of 100 mm or more, interception is increased by about 2 mm and hydraulic conductivity is generally lower. All these factors contribute to an increased ETact, whose mean value is about 100 mm higher in the mentioned study. Only one area shows factors comparable to this study and respective modelled recharge shows a considerably higher correspondence to the modelled recharge herein.

The sensitivity of mentioned factors introduces uncertainties that have to be regarded, as there are a number of processes which may reduce recharge significantly which again may not be captured sufficiently by the modelling parameters. Furthermore, the hydrological situation of the research area is connected to domains which are not the subject of this thesis, but are important for groundwater fluctuations as well. These encompass all surface or subsurface flow processes in the region, especially the extensive amounts of water influx from Angola, which in case of a major flood may also affect units situated at higher relative elevation.

7.2 Implications of the Modelling Results

One attempt of the CuveWaters project to improve rural water supply where no suitable perched aquifers are present is the operation of several subsurface water storage reservoirs which are planned to be fed by overland flow in the catchment (EISOLD and BENZING 2010). The results of this thesis suggest that subsurface water storage fed by infiltrating precipitation water would be another option, whereby amounts are estimated to range from a maximum of 200 mm per year (basic model run) to a minimum of 160 mm per year (increased FC/rooting depth models), excluding the lower frequently flooded and saline parts of the research area.

Naturally, verification of modelling results is highly necessary, although considerable additional work and the fulfilment of some preconditions are necessary for this.

The discontinuous perched aquifer itself is still connected with some unanswered questions, as the volume and spatial distribution of the different parts of the aquifer are not yet observed or mapped. Therefore, a further step would be the closure of this research gap. A possible method realising this issue would be the application of geoelectric techniques, which have been already utilised in comparable regions affected by salinity (BAUER et al. 2006). This would allow the connection of calculated recharge amounts to single enclosed aquifers, which in turn would introduce the option of assessing limitations determined by the geological framework. Furthermore, parallel field observations of water table fluctuations would make a verification of modelled rates possible. This is regarded as extremely important in water balance modelling because many parameters are significant abstractions of natural conditions and therefore connected to uncertainties. In addition to verification, future work should concentrate on the adaption of model input variables to the temporal variations of the research area, as this thesis is mostly based on information related to a relatively small time span in the dry season. Therefore, major topics of related research are:

- extended climate measurements based on a locally installed station
- vegetation analysis during the peak of the rainy season and corresponding LAI measurements
- the same for soil moisture measurements, also extended to deeper zones
- corresponding analysis of remote sensing data acquired in the wet season

As mentioned earlier, the research area can be regarded as an open hydrological system; relations of local conditions to supra-regional processes are not covered by this study, although they present a significant contribution to the total water balance. Large scale runoff modelling would therefore pose an interesting approach to determine quantities of in- and outflow. Obviously, this method would again be dependent on accurate climate and topographic data. The latter is particularly connected to problems, which has already prevented accurate runoff modelling in this thesis. If the issue of missing DEM datasets is resolved and discharge is

measured at representative locations downstream of the catchment, further options of model calibration will be possible. This can also be done with an extension of the applied model (DÜNKELOH ARMIN, personal communication 2011).

8. Conclusions

Near surface groundwater recharge modelling presents a complex task in general and particularly in the research area with its shallow aquifers and related sensitivity to surface and subsurface conditions. Results signify high temporal and spatial variations, whereby the latter are mostly related to soil storage capacities of vegetation units. This leads to favourable recharge conditions in all areas where plant activity is low or restricted to a narrow zone beneath the surface. However, also sites with an increased threshold in regard to deep percolation generate amounts that may lead to a significant replenishment of the aquifer. As there are some reasons that indicate overestimated quantities on the most sensitive areas, some limitations apply to modelled values. One lies in the modelling itself which is always an abstraction and simplification of natural conditions. Therefore, no model is able to capture all relevant processes in an ecosystem. In general, this implies that models should always be questioned and verified. The latter is hardly possible in this study due to a lack of available information about the aquifer in question or connected groundwater fluctuations therein. This leads to another source of uncertainties: data gaps or measurements not covering the whole season pose a significant limitation to this study. Finally, the definition of boundaries in an open hydrological system is an issue that has to be considered, especially when quantities of inflow and outflow are unknown.

But even under modelling conditions that take some of the respective restrictions into account, considerable recharge quantities are modelled. The most profound change in modelling conditions, represented by an explicit increase in rooting depth, leads to a total average change of 22%; a good proportion of this is related to areas that are also prone to flood water inflow from neighbouring regions which substitute evaporative deficits. Other model runs with increased field capacity or the introduction of an improvised DEM, which represent the most probable modifications, result in a mean change of 12% and all other variations lead to a maximum change of 2%. On the one hand, this shows which parameters are most sensitive and what possible successive work should concentrate on. On the other hand, this also indicates that even major alterations still result in a refilling of the discontinuous perched aquifer which presents itself as a water source with a potential that should

not be overlooked. Thus, additional research and reductions of data restrains in the region are highly recommended for the near future. As the hydrological system of the research area is challenging and a complete adjustment of all modelling parameters lies outside the scope and possibilities of this thesis, the stated results may be seen as a basis and encouragement for related future studies.

9. References

ABBASI Y., GHANBARIAN-ALAVIJEH B., LIAGHAT A. M. and SHORAFA M., 2011: Evaluation of Pedotransfer Functions for Estimating Soil Water Retention Curve of Saline and Saline-Alkali Soils of Iran. In: Pedosphere 21, 2, pp. 230–237

ALLEN R. G., PEREIRA L. S., RAES D. and SMITH M., 1998: Crop evapotranspiration: guidelines for computing crop water requirements. FAO Irrigation and Drainage Paper 56. Rome

ALLEN R. G., PRUITT W. O., BUSINGER J. A., FRITSCHEN L. J., JENSEN M. E. and QUINN F. H., 1996: Chapter 4 "Evaporation and Transpiration" – ASCE Handbook of Hydrology. New York

BATJES N. H., 2004: SOTER-based soil parameter estimates for Southern Africa (ver. 1.0), Dataset and Report, ISRIC – World Soil Information, Wageningen http://www.isric.org/UK/About+Soils/Soil+data/Thematic+data/Soil+Geographic+Data/ retrieved March 2011

BAUER P., SUPPER R., ZIMMERMANN S. and KINZELBACH W., 2006: Geoelectrical imaging of groundwater salinization in the Okavango Delta, Botswana. In: Journal of Applied Geophysics 60, pp. 126-141

BLUME H.P., BRÜMMER G. W., HORN R., KANDELER E., KÖGEL-KNABNER I., KRETZSCHMAR R., STAHR K. and WILKE B.-M., 2010: Scheffer/Schachtschabel – Lehrbuch der Bodenkunde – 16. Auflage, Spektrum Akademischer Verlag, Heidelberg

BRAUN F. J., 2002: Mesoskalige Modellierung der Bodenhydrologie. Dissertation. Faculty of Physics, Karlsruhe University (TH), Forschungszentrum Karlsruhe in der Helmholtz-Gemeinschaft, Wissenschaftliche Berichte, FZKA 6784

BRUNNER P., BAUER P., EUGSTER M. and KINZELSBACH W., 2004: Using remote sensing to regionalize local precipitation recharge rates obtained from the Chloride Method. In: Journal of Hydrology 294, pp. 241-250

BUCCIGROSSI F., CALIANDRO A., RUBINO P. and MASTRO M. A., 2010: Testing Some Pedo-Transfer Functions (PTFs) in Apulia Region. Evaluation on the Basis of Soil Particle Size Distribution and Organic Matter Content for Estimating Field Capacity and Wilting Point. In: Italian Journal of Agronomy 4, pp. 367-381

BURKE A. 2006: Savanna trees in Namibia – Factors controlling their distribution at the arid end of the spectrum. In: Flora 201, pp. 189-201

CHENEY C.S., 1994: Feasibility study for drought relief drilling in S E Owambo, Namibia. British Geological Survey Report No. WO/94/8H, Keyworth, Nottinghamshire

CHRISTELIS G. and STRUCKMEIER W. (editors), 2011 (2001): Groundwater in Namibia: an explanation to the hydrological map. Unrevised second edition 2011, first edition 2001, Formset Printing, Cape Town

COETZEE, M. E., 2001: NAMSOTER, A SOTER database for Namibia, Agro-ecological Zoning Programme, Directorate of Agricultural and Training, Ministry of Agriculture, Water and Rural Development, Republic of Namibia

DEA – Directorate of Environmental Affairs, Ministry of Environment and Tourism, 2002: Atlas of Namibia project

DE VRIES J. J. and SIMMERS I., 2002: Groundwater recharge: an overview of processes and challenges. In: Hydrogeology Journal 10, pp. 5–17

DIJKSHOORN K. and VAN ENGELEN V., 2003: Soil and Terrain Database for Southern Africa (ver. 1.0) – SOTERSAF, Dataset: NAMSOTER, the SOTER map of Namibia and Report, ISRIC – World Soil Information, Wageningen http://www.isric.org/UK/About+Soils/Soil+data/Thematic+data/Soil+Geographic+Data/ retrieved March 2011

DONATELLI M. and ACUTIS M., 2001: Soilpar v2.00 beta: software to estimate soil hydrological parameters and functions, PANDA Project 1993-2001

DSM – Directorate of Survey and Mapping of Namibia, 2001: 1:50.000 maps of Onaanda, Oshakati, Ondangwa, Afoti, Engombe and Uukwiyu. Windhoek

EISOLD J. and BENZING C. (editors), 2010: From Concept to Tap – Integrated Water Resources Management in Northern Namibia http://www.isoe.de/ftp/cuve/brochure_cuvewaters.pdf retrieved May 2011

FAO – Food and Agriculture Organization of the United Nations, 2006: World reference base for soil resources 2006 – A framework for international classification, correlation and communication, Report, Rome

FAO – Food and Agriculture Organization of the United Nations, 2005: Report of the regional workshop on salt-affected soils from sea water intrusion: strategies for rehabilitation and management. In: Regional office for Asia and the Pacific publications 11, Bangkok

FOODY G. M., 1992: Remote Sensing Brief – On the Compensation for Chance Agreement in Image Classification Accuracy Assessment. In: Photogrammetric Engineering & Remote Sensing 58, No. 10, pp. 1459-1460

FRENKEN K. (Editor), 2005: Irrigation in Africa in figures – AQUASTAT Survey – 2005, FAO Water Report No 29, p. 407-419, ftp://ftp.fao.org/agl/aglw/docs/wr29_eng_including_countries.pdf, retrieved January 2011

GIVI J., PRASHER S. O. and PATEL R. M., 2004: Evaluation of pedotransfer functions in predicting the soil water contents at field capacity and wilting point. In: Agricultural Water Management 70, pp. 83–96

GRASS Development Team, 2010: Geographic Resources Analysis Support System (GRASS) Software, Version 6.4.0. Open Source Geospatial Foundation. http://grass.osgeo.org, retrieved August 2011

GRASS Development Team, 2007: GRASS 6.2 Users Manual. ITC-irst, Trento, Italy http://grass.osgeo.org/grass62/manuals/html62_user/, retrieved August 2011

HÄCKEL H., 1993: Meteorologie – 3. verbesserte Auflage, Verlag Eugen Ulmer, Stuttgart

HIPONDOKA M. H. T., 2005: The Development and Evolution of the Etosha Pan, Namibia. Doctorate Thesis, Julius-Maximilian University of Würzburg

HOWARD P.J.A., 1965: The Carbon-Organic Matter Factor in Various Soil Types. In: Oikos Vol. 15, No. 2, pp. 229-236

KLUGE T., LIEHR S., LUX A., MOSER P., NIEMANN S., UMLAUF N. and URBAN W., 2008: IWRM concept for the Cuvelai Basin in northern Namibia. In: Physics and Chemistry of the Earth 33

KLUGE T., LIEHR S., LUX A., NIEMANN S. and BRUNNER K., 2006: IWRM in Northern Namibia – Cuvelai Delta. Final Report of a Preliminary Study. Frankfurt a. M.

KNOOP W. T. and WALKER B. H., 1985: Interactions of woody and herbaceous vegetation in Southern African Savanna. In: Journal of Ecology 73, pp. 235-253

KÜLLS C., 2000: Groundwater of the North-Western Kalahari, Namibia – Estimation of Recharge and Quantification of the Flow Systems. Doctorate Thesis, Julius-Maximilian University of Würzburg

LLOYD J. W., 1986: A review of aridity and groundwater. in: Hydrological Processes 1, pp. 63-78

MAUSER W., 1989: Die Verwendung hochauflösender Satellitendaten in einem geographischen Informationssystem zur Modellierung von Flächenverdunstung und Bodenfeuchte. Unpublished habilitation treatise, Albert Ludwigs University, Freiburg

MAWRD – Ministry of Agriculture, Water and Rural Development, 2000: National Water Policy White Paper.

MAWF – Ministry of Agriculture, Water and Forestry, Directorate of Agricultural Research and Training, Subdivision: Analytical Services. GIS datasets on Namibia 1999 – 2000

MAWF – Ministry of Agriculture, Water and Forestry, 2006: Desk Study Report – Cuvelai-Etosha Groundwater Investigation, Version 1.1 http://www.the-eis.com/track.php?id=5206&action=download_file&url=data/literature/Cuvelai%20Desk%20Study%20Report_Version%201.1.pdf, retrieved July 2011

MAYR M., 2011: Deduction of vegetation parameters from remote sensing for the integration into a regional SVAT (soil-vegetation-atmosphere-transport) –model in central Northern Namibia. Diploma thesis in preparation. University of Vienna

MENDELSOHN J., JARVIS A., ROBERTS C. and ROBERTSON T., 2002: Atlas of Namibia – A Portrait of the Land and its People, David Philip Publishers, Cape Town

MENDELSOHN J., EL OBEID S. and ROBERTS C., 2000: A profile of north-central Namibia. Gamsberg Macmillan Publishers, Windhoek

MILLER R. MC. G., PICKFORD M. and SENUT B., 2010: The Geology, Palaeontology and Evolution of the Etosha Pan, Namibia: Implications for Terminal Kalahari deposition. In: South African Journal of Geology, Volume 113, pp. 307-334

NASA Land Processes Distributed Active Archive Center (LP DAAC), 2009: ASTER AST14DEM, ASTER GDEM is a product of METI and NASA, USGS/Earth Resources Observation and Science (EROS) Center, Sioux Falls, South Dakota

NASA Land Processes Distributed Active Archive Center (LP DAAC), 2011: MODIS MOD15A2 – Leaf Area Index 8-Day L4 Global 1km. USGS/Earth Resources Observation and Science (EROS) Center, Sioux Falls, South Dakota https://lpdaac.usgs.gov/lpdaac/products/modis_products_table/leaf_area_index_fraction_of_photosynthetically_active_radiation/8_day_l4_global_1km/mcd15a2, retrieved July 2011

NASA, 2011: Earth Observatory – Flooding in Northern Namibia. http://earthobservatory.nasa.gov/NaturalHazards/view.php?id=49842 retrieved July 2011

NCDC – National Climatic Data Center, NESDIS, NOAA, U.S. Department of Commerce, 2011: Global Surface Summary of the Day – GSOD, Asheville, NC. ftp://ftp.ncdc.noaa.gov/pub/data/gsod/ retrieved April 2011

NIEMANN S., 2002: Indigenous Water Resources Management and Water Utilisation in Northern Namibia (Former Ovamboland) – Can Tradition Help to Overcome Current Problems? In: Die Erde 133, pp. 183-199, Berlin

NMS – NAMIBIA METEOROLOGICAL SERVICE 2010: climatic dataset Ondangwa

ÖNORM L 1061-2: Physikalische Bodenuntersuchung – Bestimmung der Korngrößenverteilung des Mineralbodens – Teil 2: Feinboden, 2002

ÖNORM L 1079 1999 04 01: Chemische Bodenuntersuchungen – Bestimmung der organischen Substanz als Glühverlust

ÖNORM L 1092 2005 03 01: Chemische Bodenuntersuchungen – Extraktion wasserlöslicher Elemente und Verbindungen

RAPIDEYE, 2011: RapidEye Ortho – Level 3A Product acquired on 9th November 2010 and RAPIDEYE Satellite Imagery Product Specifications – Version 3.2. RapidEye AG, Brandenburg an der Havel. All rights reserved

RENGER M., STREBEL O. and GIESEL W., 1974: Beurteilung bodenkundlicher, kulturtechnischer und hydrologischer Fragen mit Hilfe von klimatischer Wasserbilanz und bodenphysikalischen Kennwerten. In: Zeitschrift Kulturtechnik Flurbereinigung 15, pp.148-160

RHOADES J. D., CHANDUVI F. and LESCH S., 1999: Soil salinity assessment – Methods and interpretation of electrical conductivity measurements. FAO Irrigation and Drainage Paper 57, Rome

RIGOURD C. and SAPPE T., 1999: Investigating into soil fertility in the North Central Region. In: Kaumbutho, P. G., Simalenga, T. E. (Eds.), Conservation Tillage with Animal Traction. Rundu, Namibia

SANFORD W., 2002: Recharge and groundwater models: an overview. In: Hydrogeology Journal 10, pp. 110–120. Springer

SAXTON K. E., RAWLS W. J., ROMBERGER J. S. and PAPENDICK R. I., 1986: Estimating generalized soil-water characteristics from texture. In: Soil Sci. Soc. Amer. J. 50

SAXTON K. E. and RAWLS W. J., 2007 (revised): Soil Water Characteristics – Hydraulic Properties Calculator – Version 6.02.74, available online: http://hrsl.arsusda.gov/SPAW/SPAWDownload.html, retrieved April 2011

SAXTON K. E. and RAWLS W. J., 2006: Soil Water Characteristic Estimates by Texture and Organic Matter for Hydrologic Solutions. In: Soil Sci. Soc. Amer. J. 70, p. 1569 – 1578, Madison

SCANLON B. R., HEALY R. W. and COOK P.G., 2002: Choosing appropriate techniques for quantifying groundwater recharge. In: Hydrogeology Journal 10, pp. 18–39. Springer

SCHOLES R. J., FROST P. G. H. and TIAN Y., 2004: Canopy structure in savannas along a moisture gradient on Kalahari sands. In: Global Change Biology 10, pp. 292–302

SHORROCKS B., 2007: The Biology of African Savannahs. Oxford University Press, Oxford

SKAPRE C., 1996: Plant functional types and climate in a southern African savanna. In: Journal of Vegetation Science 7, pp. 397-404

SONMEZ S, BUYUKTAS D., OKTUREN F. and CITAK S., 2008: Assessment of different soil to water ratios (1:1, 1:2.5, 1:5) in soil salinity studies. In: Geoderma 144, pp. 361–369

STROHBACH B. J., 2000: Vegetation degradation trends in the northern Oshikoto Region: I. The Hyphaene petersiana plains. In: Dinteria 26, pp. 45-62, Windhoek

TIETJE O. and HENNINGS V., 1996: Accuracy of the saturated hydraulic conductivity prediction by pedo-transfer functions compared to the variability within FAO textural classes. In: Geoderma 69, pp. 71-84

TRMM – Tropical Rainfall Measurement Mission Project, 2010: Daily TRMM and Others Rainfall Estimate (3B42 V6 derived) – Version 6. NASA Goddard Space Flight Center, ftp://disc3.nascom.nasa.gov/data/s4pa/TRMM_L3/TRMM_3B42_daily/, retrieved July 2011

UDLUFT P and DÜNKELOH A., 2009: MODBIL – a numerical water balance model. Unpublished program and manual – V49 - 2009, Würzburg

US SALINITY LABORATORY STAFF, 1954: Diagnosis and improvement of saline and alkali soils – Agriculture Handbook 60, USDA, U.S. Government Printing Office, Washington, D. C.

VON HOYNINGEN-HUENE J., 1983: Die Interzeption des Niederschlags in landwirtschaftlichen Pflanzenbeständen. In: Schriftenreihe des Deutschen Verbandes für Wasserwirtschaft und Kulturbau e.V., Einfluss der Landnutzung auf den Gebietswasserhaushalt, DVWK Heft 57, Braunschweig

WANKE H, DÜNKELOH A. and UDLUFT P., 2008: Groundwater Recharge Assessment for the Kalahari Catchment of North-eastern Namibia and North-western Botswana with a Regional-scale Water Balance Model. In: Water Resource Management 22, pp. 1143-1158

WILLIAMS C. A. and ALBERTSON J. D., 2004: Soil moisture controls on canopy-scale water and carbon fluxes in an African savanna. In: Water Resources Research Vol. 40

WMO – World Meteorological Organization, 2009: Handbook on CLIMAT and CLIMAT TEMP Reporting. World Weather Watch Technical Report, WMO/TD-No. 1188, Geneva

XU Y. and BEEKMAN H. E. (editors), 2003: Groundwater recharge estimation in Southern Africa. In: UNESCO IHP Series No. 64, Paris

10. Index of Figures

Figure 1: Central Owamboland with the research area highlighted by a blue rectangle and the satellite image 10

Figure 2: Homestead with surrounding cropping area before cultivation and *iigandhi* granary for cereal storage.....13

Figure 3: Geological profile from Ruacana to Tsumeb 15

Figure 4: Characteristic pattern of soil and land use distribution in the research area 18

Figure 5: Simplified illustration of the ITCZ and its seasonal variation.....19

Figure 6: Monthly mean precipitation, period 1960 – 1989 at Ondangwa.....20

Figure 7: Box plot of monthly precipitation at Ondangwa 1960 – 1989 21

Figure 8: Cuvelai drainage system, Namibian part of its catchment and position of the Cuvelai Iishana Subbasin 22

Figure 9: MODIS image from 20th March 2011 showing a large flood (*efundja*) in the research area.....23

Figure 10: Simplified schematic illustration of the geological formations of the Kalahari Sequence and existing or assumed aquifers.....25

Figure 11: Shallow hand dug well (omithima), not fenced off and therefore used for livestock watering.....26

Figure 12: Simplified scheme of groundwater recharge in semi arid areas.....28

Figure 13: Abstract flowchart of the water balance model MODBIL 32

Figure 14: Relationship of water content and water stress coefficient 39

Figure 15: RAPIDEYE (2011) RGB image (above), derived land use/cover classes and outlines of general vegetation units as given by MAWF (2000) for comparison 45

Figure 16: Overview of classified soil-vegetation units 46

Figure 17: Climate time series comparison of field measured, NMS- and GSOD data 48

Figure 18: Scatterplots with regression line of maximum Temperature and minimum Temperature between the NMS- and the GSOD datasets 51

Figure 19: Scatterplots with regression line of maximum and minimum relative humidity 2003 - 2005 and 2007 - 2010 between the NMS- and the GSOD datasets 53

Figure 20: Water logging on grassland tuft area after first precipitation event in November 2010 61

Figure 21: Excavation on halophytic vegetation site 62

Figure 22: A typical Vertisol in one of the Oshana Dark areas.....63

Figure 23: Comparison of mean measured- and MODIS LAI values for each soil-vegetation unit in November 73

Figure 24: Interception storage IS and its dependency of leaf area index and precipitation 75

Figure 25: Raster image of the ASTER digital elevation model for the research area and elevation profile of a highlighted subsection.....78

Figure 26: Daily sums of precipitation and calculated groundwater recharge rates in the basic model run compared to the model run with increased field capacity for the whole modelling period 85

Figure 27: Plots of daily mean precipitation and modelled recharge in the basic model run and the model run with the improvised DEM for comparison.....87

Figure 28: Modelled mean annual interflow in mm for the basic model run and the model run with the improvised DEM 91

Figure 29: Modelled mean annual actual evapotranspiration and potential groundwater recharge in mm for the basic model run.....92

Figure 30: Infiltration depth indicated by blue line on 17th November 2010, Shrubland.....93

Figure 31: Annual Recharge compared to precipitation from several data sources in South Africa, Botswana and Zimbabwe.....96

Figure 32: Excavation showing the depth of the water table at about 2 m below the surface 97

11. Index of Tables

Table 1: Accuracy assessment values for the supervised classification 42

Table 2: Regression terms for substitution of missing temperature values in the NMS data set 51

Table 3: Regression terms for substitution of relative humidity in the NMS data set 53

Table 4: WRB classification of vegetation units and assignment of averaged soil properties 65

Table 5: Soil water characteristics calculated with the software by SAXTON and RAWLS (2007) and mean measured moisture content previous to the first precipitation event 68

Table 6: MODIS derived factor for the computation of seasonal LAI variations

Table 7: Important modelling parameters for soil-vegetation units for the basic model run 74

Table 8: Modelling results for selected water balance components and different model runs 84

12. Appendix

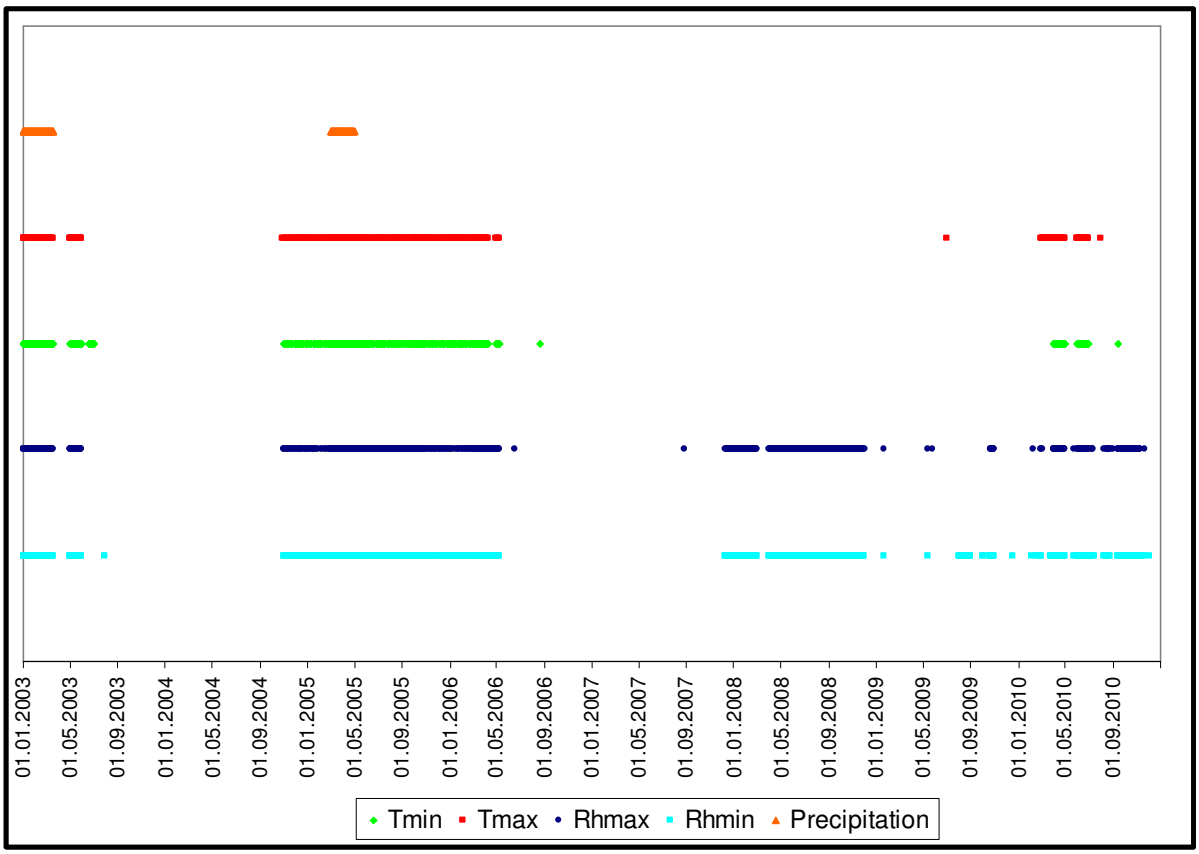

Appendix 1: Overview of missing climatic data. Signs mark missing values. Total number of missing days: Tmin 499, Tmax 516, RHmax 1004, RHmin 926, Precipitation 139

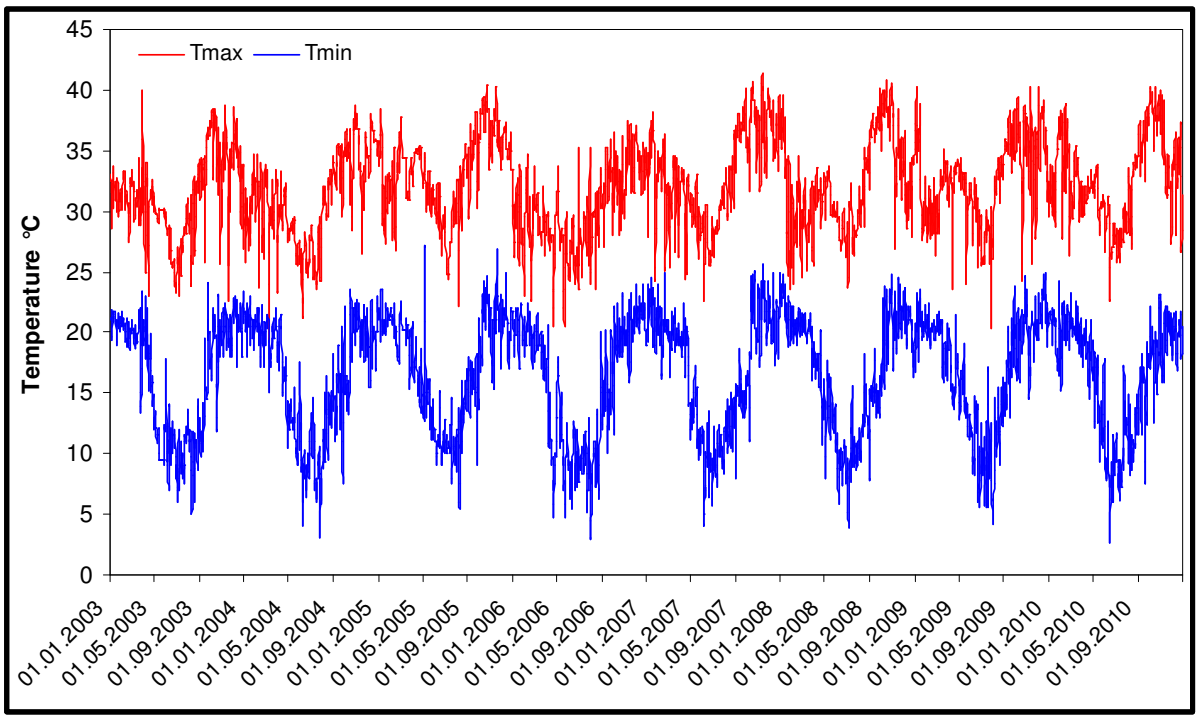

Appendix 2: Completed temperature time series 2003 – 2010.

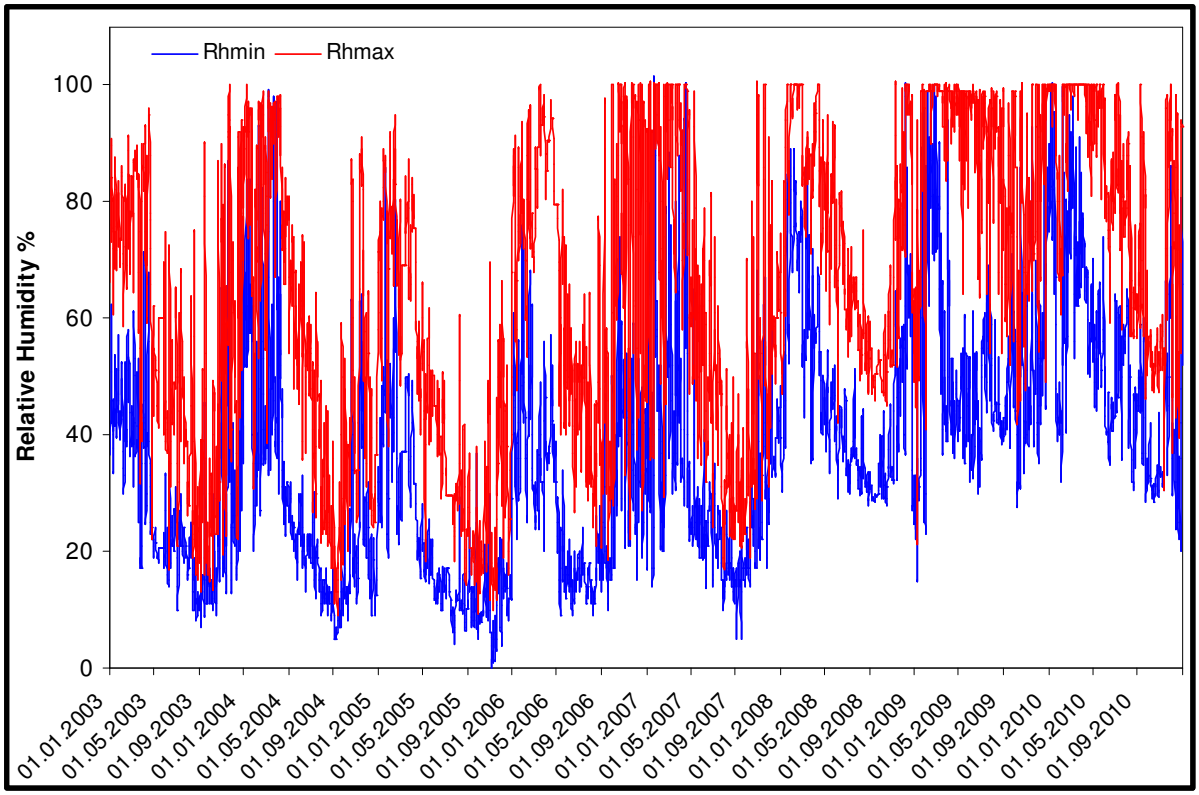

Appendix 3: Completed relative humidity time series 2003 – 2010.

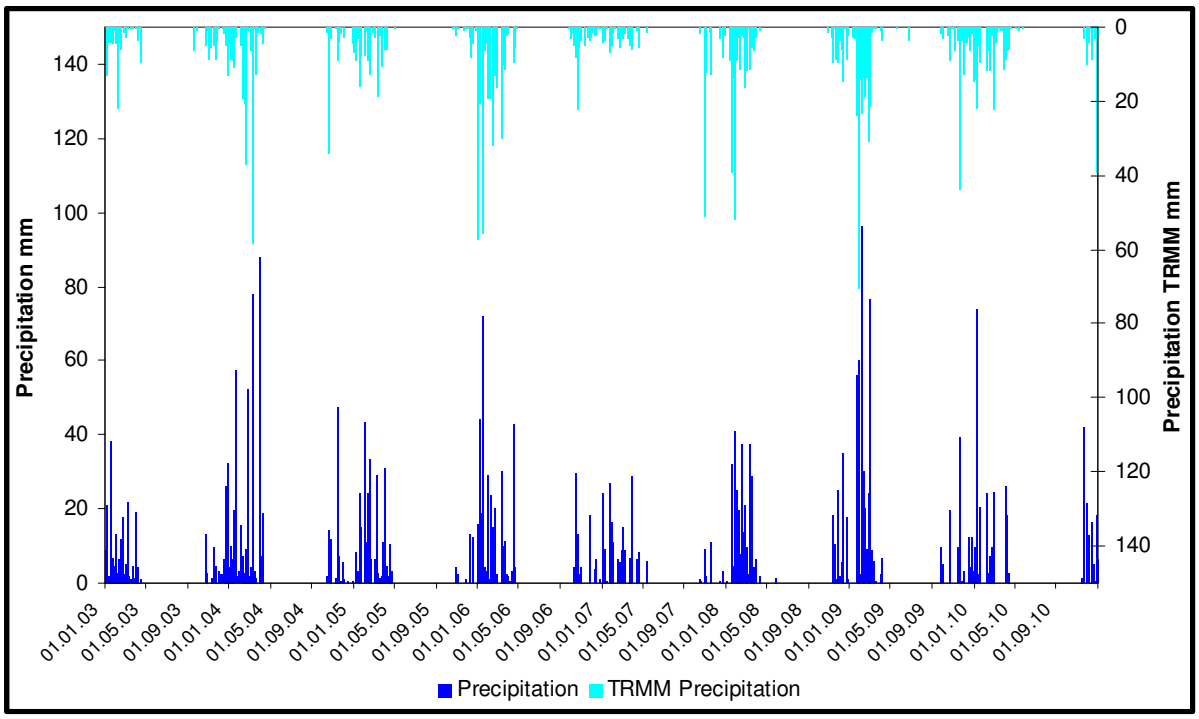

Appendix 4: Comparison of the completed NMS (2010) precipitation dataset with the TRMM (2010) precipitation time series

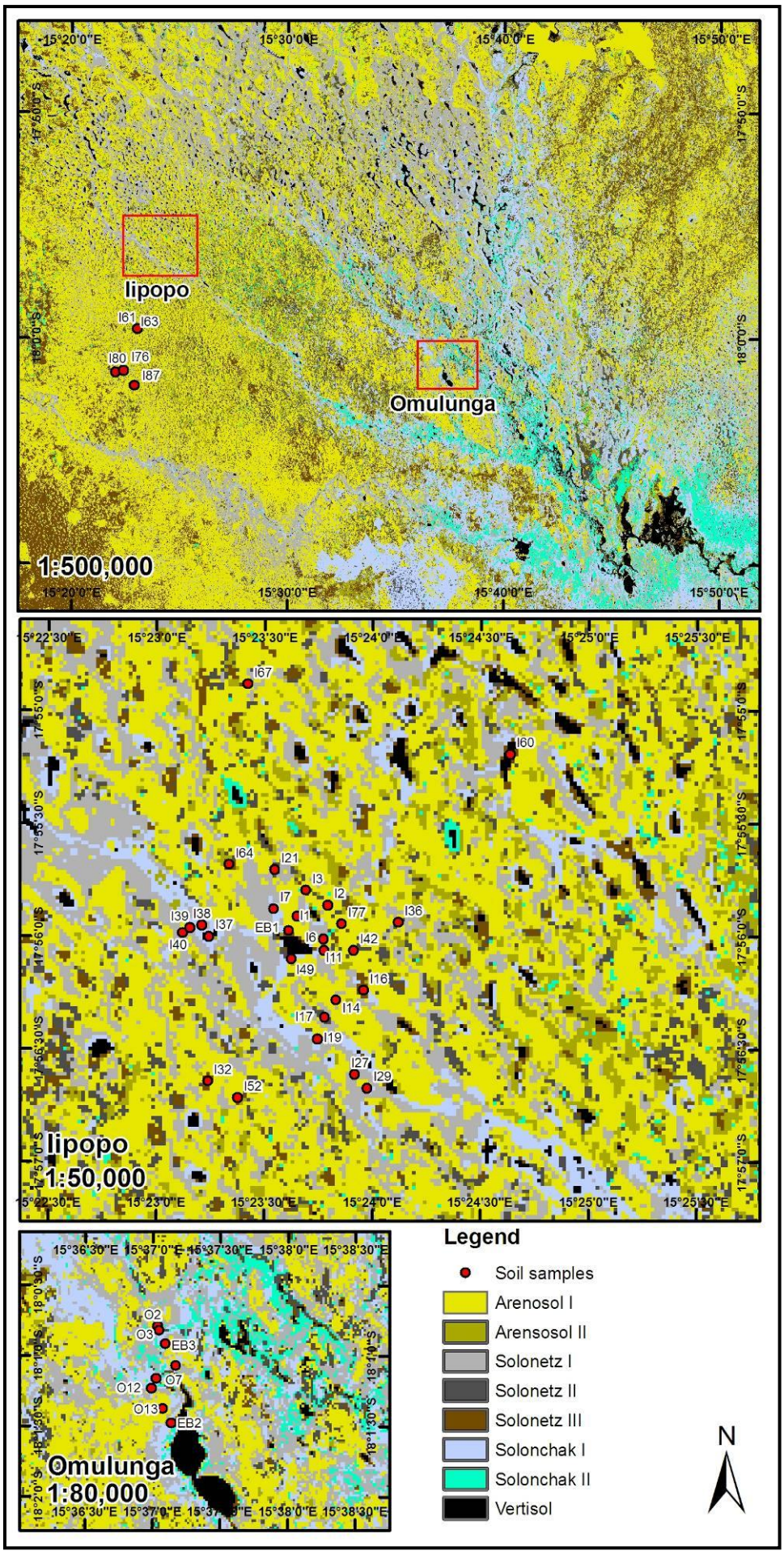

Appendix 5: Classification derived soil units and soil sampling sites

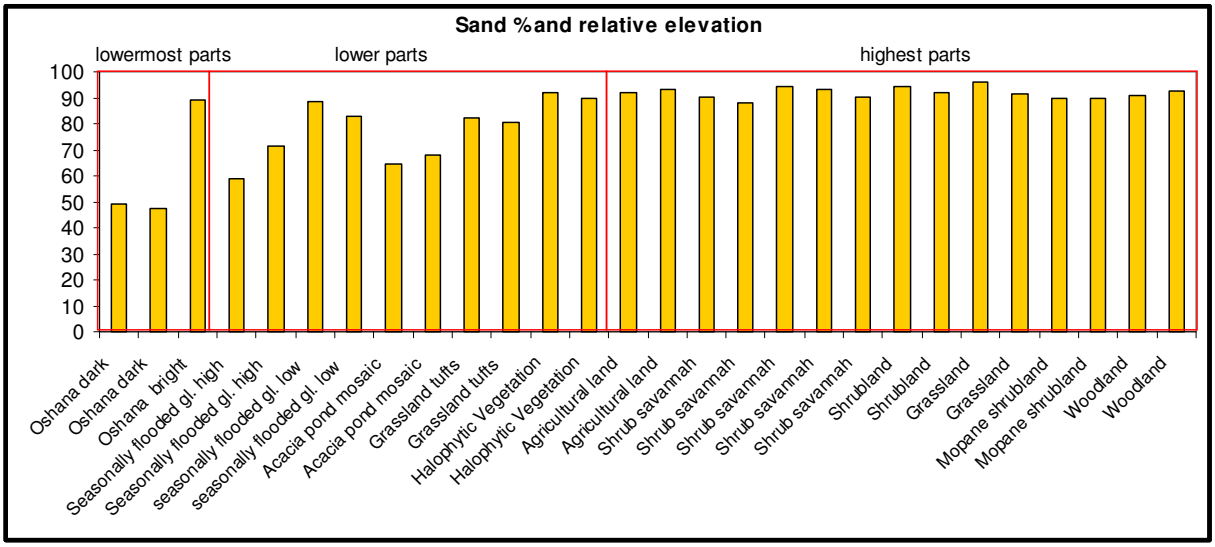

Appendix 6: Sand content of analysed samples showing variations according to relative elevation and small differences between soil-vegetation units.

Field plot nr	Sand %	Silt %	Clay %	Corg mass %	EC ds/m	Bulk density
Arenosol I						
i1	94.3	3.4	2.3	0.4	381.1	1.6
i2	94.0	3.4	2.6			1.5
i3	90.9	3.8	5.2	0.5	488.5	1.4
i11	93.8	3.2*	3.0*		346.5	1.5
i14	90.4	4.9*	4.7*		779.4	1.5
i40	87.9	6.2*	5.9*	0.3	388.0	1.6
i42	96.8	1.7*	1.6*	0.2	533.5	1.6
i61	92.7	3.7*	3.6*		299.7	1.6
i67	91.9	4.2*	4.0*		298.0	1.6
i77	91.7	4.2*	4.0*	0.3	556.1	1.5
i80	89.7	5.3*	5.0*	0.5	472.9	1.5
i87	89.8	5.2*	5.0*		450.4	1.5
o13	90.4	5.0*	4.7*	0.2	433.1	1.5
o14	91.5	4.4*	4.1*	0.2	519.7	1.5
Mean	91.8	4.2	4.0	0.3	457.4	1.5
FAO class	92.1	4.0	4.0			
Arenosol II						
i36	88.7	5.3*	6.0*		875.9	1.6
i76	83.1	7.9	9.0	0.7	938.3	1.7
i7					1388.2	1.8
i49					1336.2	1.5
Mean	85.9	6.6	7.5	0.7	1134.7	1.7
FAO class	86.3	6.3	7.5			
Solonetz I						
i27	80.4	5.8	13.7		6456.3	1.6
i39	82.4	6.2	11.5	0.8	6099.2	1.5

i6					1701.1	1.5
Mean	81.4	6.0	12.6	0.8	4752.2	1.5
FAO class	81.7	5.7	12.6			
o2 (above hard layer)					429.6	
Solonetz II						
i17	58.9	15.8	25.3	1.6	1240.6	1.5
i29	71.5	11.0*	17.6*		2001.5	1.4
i21					479.7	1.5
i63					818.8	1.4
Mean	65.2	13.4	21.4	1.6	1135.2	1.4
FAO class	65.9	12.7	21.4			
Solonetz III						
i16	64.5	3.3*	32.2*	2.6	1018.8	1.4
i32	68.1	3.0	28.9		3669.0	1.4
i52					537.6	1.5
i64					855.0	1.4
Mean	66.3	3.1	30.5	2.6	1520.1	1.4
FAO class	66.5	3.0	30.5			
Solonchak I						
o7	90.0	3.2*	6.8*	0.2	7481.1	1.6
i38	91.9	2.6*	5.5*		554.3	1.5
o3					15480.4	1.5
i19					556.1	1.6
Mean	91.0	2.9	6.1		6018.0	1.5
FAO class	91.1	2.8	6.1			
Solonchak II						
o12	89.4	6.3	4.3	0.3	19510.0	1.5
eb1					15519.6	1.6
eb2					21023.3	1.5
eb3					22123.7	1.5
Mean					19544.2	1.5
FAO class	89.7	6.0	4.3			
Vertisol						
i37	49.1	7.2*	43.7*	2.3	4885.3	1.3
i60	47.4	7.4	45.2	2.3	4385.8	1.3
MEAN	48.3	7.3	44.4	2.3	4635.6	1.3
FAO class	48.7	6.9	44.4			

Appendix 7: Results of laboratory analysis. Texture is in the Austrian classification system with respective FAO mean values below. Latter was calculated using Soilpar v2.00 software by DONATELLI and ACUTIS (2001). Asterisks signify silt and clay values that were derived using the ratio of analysed samples. EC values were transferred to saturated paste equivalents using the method of SONMEZ et al. 2008. Soil samples of abandoned field classes not shown.

Field plot nr	Date	Soil moisture mm/m	Date	Soil moisture after rain mm/m
Arenosol I				
i1	13.10.2010	16.0	17.11.2010	90
i10	18.10.2010	20.0		
i11	18.10.2010	21.0		
i13	18.10.2010	22.5		
i14	19.10.2010	17.0		
i18	01.11.2010	21.5		
i2	14.10.2010	10.0		
i20	02.11.2010	18.5		
i22	02.11.2010	15.5		
i23	02.11.2010	16.0		
i24	02.11.2010	17.5		
i25	02.11.2010	20.0		
i26	02.11.2010	23.5		
i3	14.10.2010	25.0	17.11.2010	82.5
i30	03.11.2010	61.5		
i31	03.11.2010	20.5		
i33	03.11.2010	46.5		
i34	03.11.2010	19.5		
i4	14.10.2010	16.0		
i40	04.11.2010	23.0		
i41	04.11.2010	25.0		
i42	04.11.2010	18.5	17.11.2010	107
i43	04.11.2010	24.0		
i47	05.11.2010	20.5		
i48	05.11.2010	20.5		
i50	08.11.2010	18.5		
i51	08.11.2010	17.5		
i53	08.11.2010	15.5		
i54	08.11.2010	22.5		
i55	08.11.2010	18.5		
i57	08.11.2010	24.5		
i58	09.11.2010	19.0		
i61	09.11.2010	42.5		
i62	09.11.2010	11.0		
i65	09.11.2010	17.5		
i66	10.11.2010	18.5		
i67	10.11.2010	21.0		
i68	10.11.2010	21.0		
i69	10.11.2010	20.5		
i74	11.11.2010	20.5		
i75	11.11.2010	23.5		
i77	11.11.2010	35.0		
i78	11.11.2010	24.5		
i79	12.11.2010	23.0		
i80	12.11.2010	30.5		
i81	12.11.2010	33.0		
i82	12.11.2010	32.5		
o1	12.10.2010	8.5		
o10	22.10.2010	41.5	17.11.2010	100
o13	25.10.2010	14.5	17.11.2010	80.5
o14	25.10.2010	17.5	17.11.2010	101
o4	21.10.2010	15.5	17.11.2010	105
i96			17.11.2010	127.5

Mean		22.5		99.1875
Arenosol II				
i36	03.11.2010	26.5		
i49	08.11.2010	28.0		
i56	08.11.2010	26.5		
i59	09.11.2010	31.5		
i76	11.11.2010	33.5		
Mean		29.2		
Solonetz I				
o2	12.10.2010	47.5		
i5	14.10.2010	70.5	17.11.2010	243
i6	14.10.2010	59.5		
o6	21.10.2010	92.0	17.11.2010	327.5
i27	02.11.2010	54.0		
i39	04.11.2010	77.0		
i45	05.11.2010	39.5		
MEAN		62.9		285.25
Solonetz II				
i17	20.10.2010	29.0		
i21	02.11.2010	27.0		
i29	03.11.2010	51.0		
i44	05.11.2010	29.5		
i63	09.11.2010	17.5		
i73	10.11.2010	30.5		
Mean		30.8		
Solonetz III				
i16	19.10.2010	120.0		
i32	03.11.2010	274.0		
i52	08.11.2010	152.5		
i64	09.11.2010	240.0		
i72	10.11.2010	78.0		
Mean		172.9		
Solonchak I				
o3	12.10.2010	375.0	excluded: wet	
i8	18.10.2010	19.0		
o7	22.10.2010	15.5	17.11.2010	112
o15	26.10.2010	11.5	17.11.2010	89
i19	01.11.2010	28.5		
i38	04.11.2010	43.5	16.11.2010	55.5
i70	10.11.2010	19.0		
o16			17.11.2010	41.1
Mean		22.8		85.5
Solonchak II				
o12	25.10.2010	262.5	excluded: wet	
eb1	13.10.2010	24.5		
eb2	22.10.2010	22.0		
eb3	26.10.2010	397.0	excluded: wet	
MEAN		23.3		
Vertisol				
i37	04.11.2010	310.5	16.11.2010	330
i60	09.11.2010	417.5	excluded: wet	
eb	13.10.2010	287.0		
mm	21.10.2010	380.0	excluded: wet	
Mean		298.8		330

Appendix 8: Results of field based soil moisture measurements before and after the first precipitation events. All values are means of two measurements.

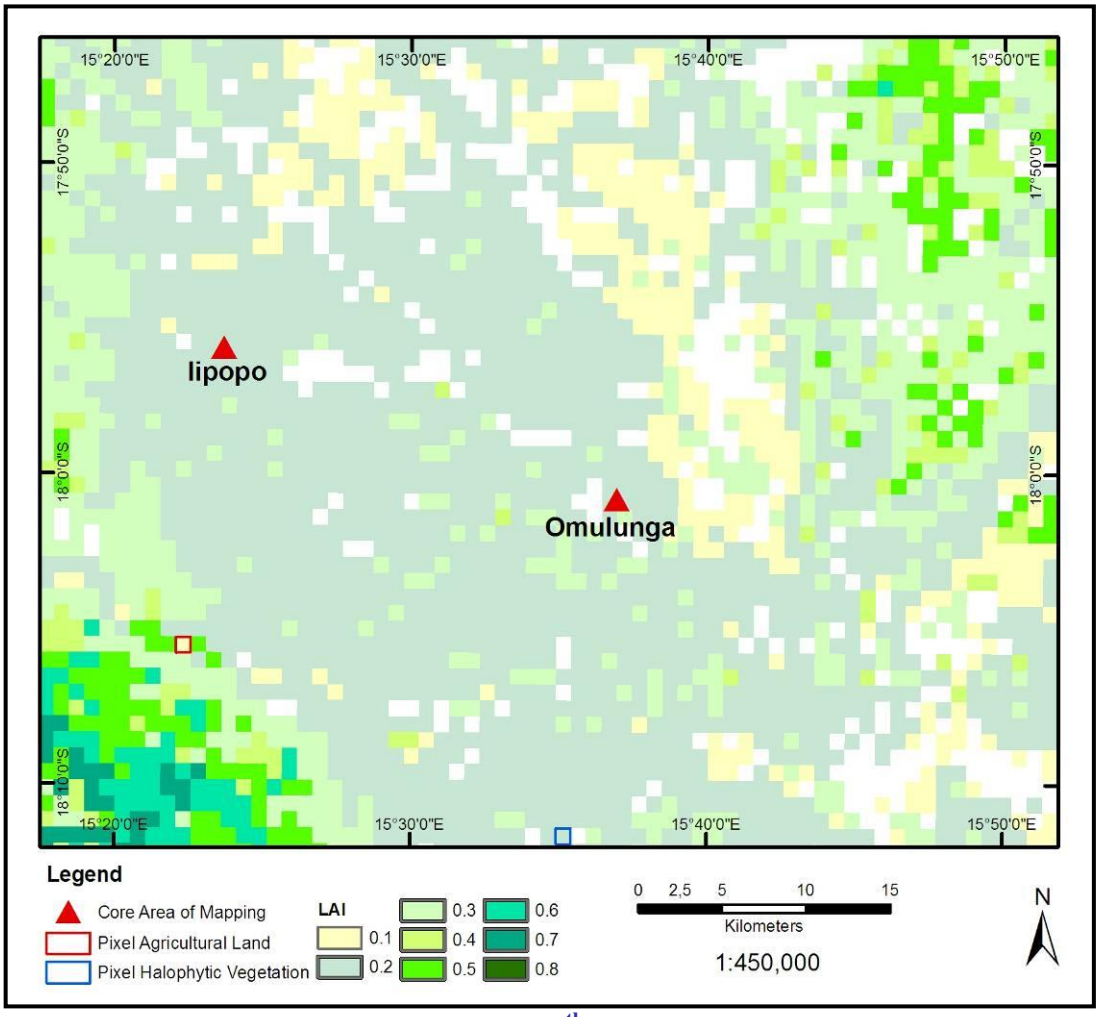

Appendix 9: MODIS LAI values from 9th of November and position of pixels for extra LAI factors. White areas = no data

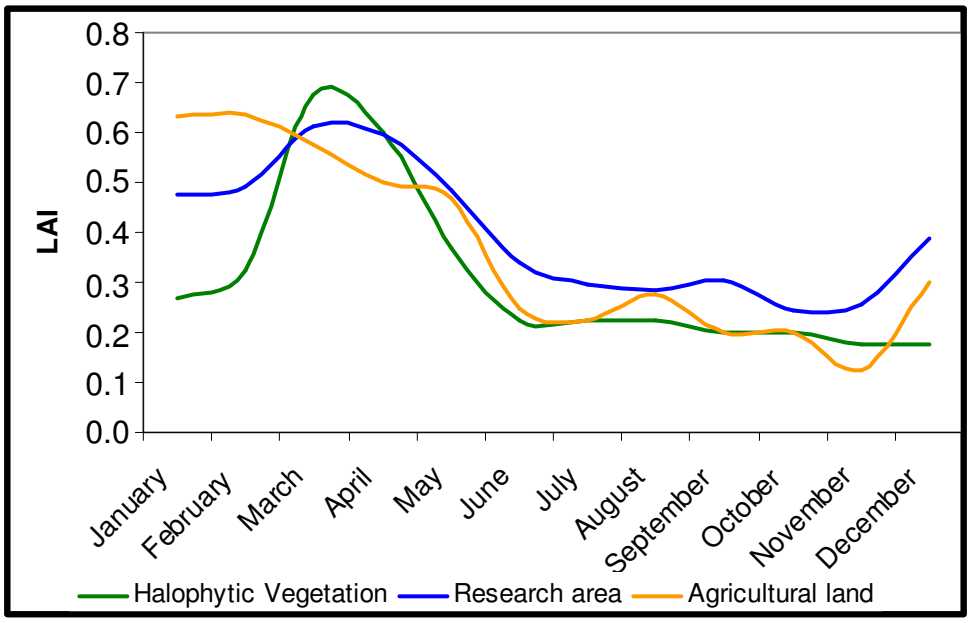

Appendix 10: MODIS LAI time series for Agricultural land-pixel, Halophytic Vegetation pixel and mean of the whole research area,

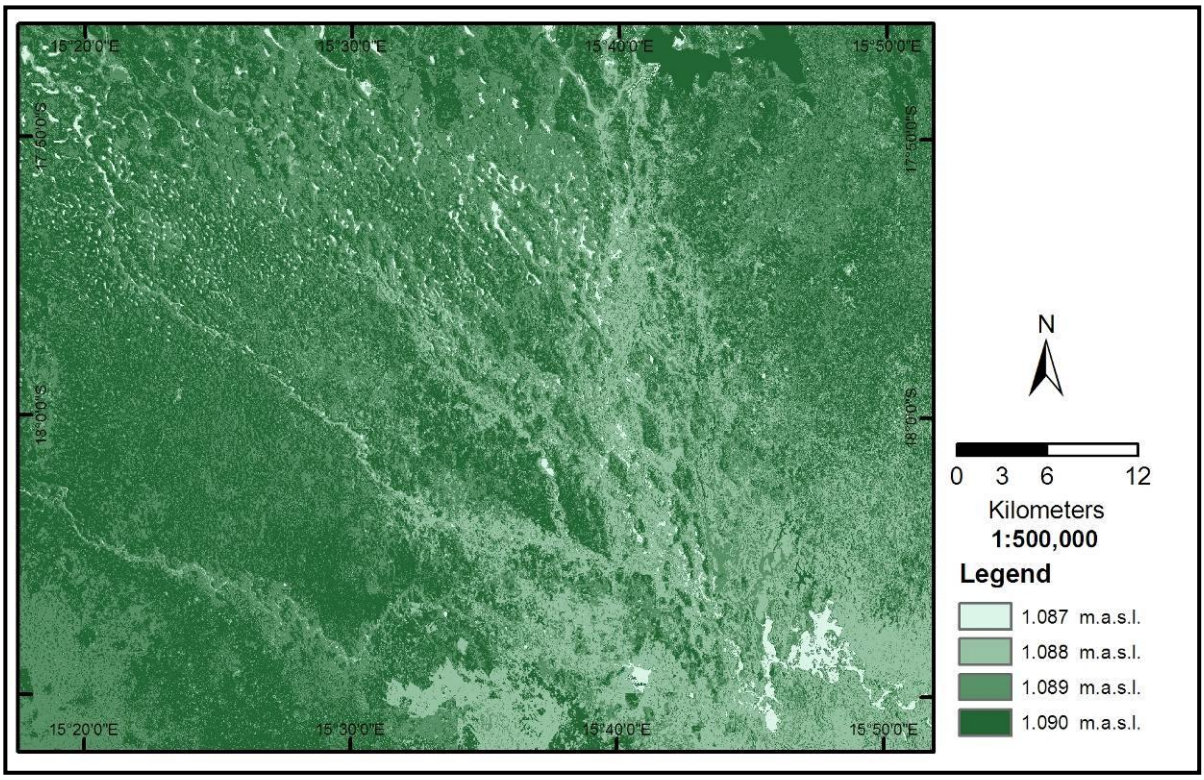

Appendix 11: Improvised DEM from classified units

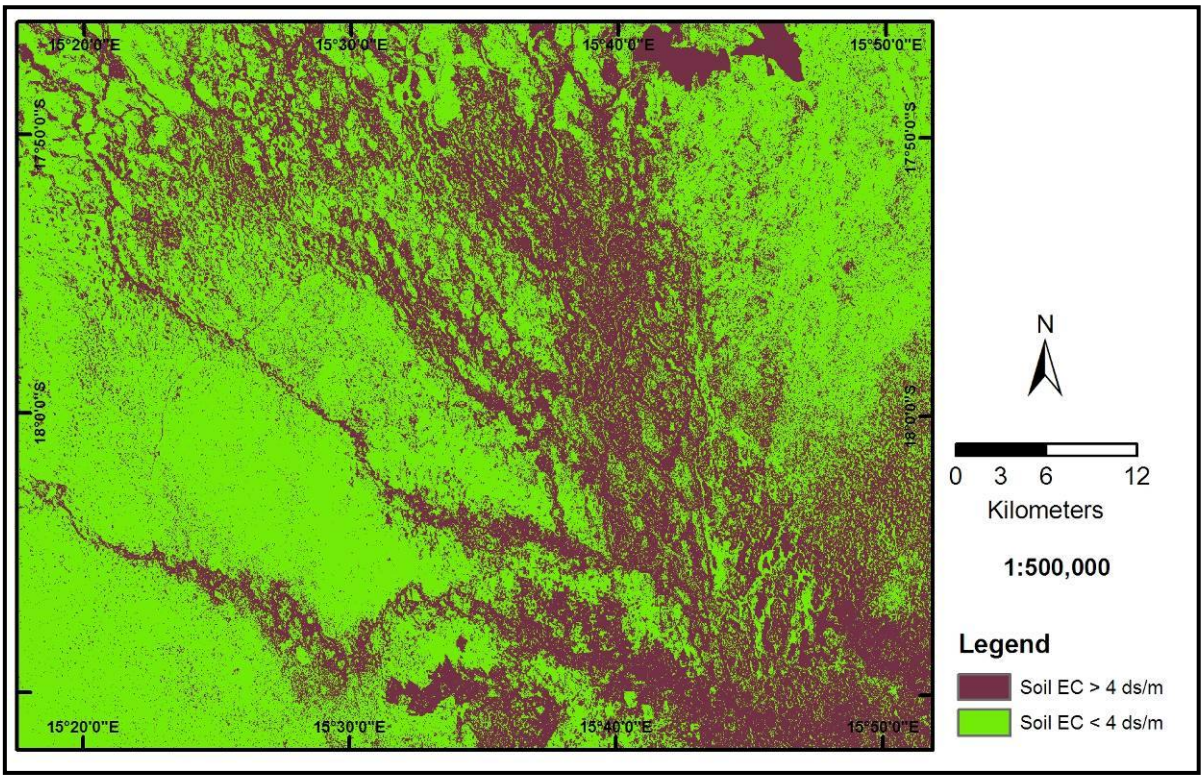

Appendix 12: Areas most likely affected by salinity. Assessment is based on classification results and assignment of laboratory derived electrical conductivity (EC).

Curriculum Vitae

Personal data

First name, Surname: Harald, Zandler

Adress: Unterfeldstr. 8, 6923 Lauterach

Date of birth: 24.09.1984

Place of birth: Feldkirch

Nationality: Austrian

Education

Since October 2005	Diploma studies at the University of Vienna, Theoretical and Applied Geography Major: Geoecology; Minors: Global Environmental Change, Geoinformation and Visualisation
1995 – 2003	Secondary School (High School) BG Bregenz-Blumenstr
1991 – 1995	Primary School Lauterach

Work experience

Summer 2010	Internship for ‘‘Austrian Service for Torrent and Avalanche Control”, Department Bludenz
Summer 2008 – 2010	Tutor for “Field Class in Physical Geography”, University of Vienna
Summer 2006 – 2007	Internship for the Federal State Vorarlberg, Topographical survey, department of road construction
2004 – 2005	Civilian service for “Lebenshilfe Vorarlberg” in Hard
2003	Part time job for „Österreichischer Wachdienst“
2003	Internship for „Alpenschutzverein für Vorarlberg“

Language Skills

German (mother tongue)
English (fluent, spoken and written)
French (school knowledge)

Computer Skills

Microsoft Office
ArcGIS
SPSS / PASW
R (basic)
Adobe Photoshop
Cinema 4D (basic)